Cyclophilin D as a potential therapeutic target for Alzheimer's disease

By

Erika D. Nolte

PhD, Pharmacology and Toxicology, 2019

B.S., Neurobiology, University of Kansas, 2015

Submitted to the graduate degree program in the Department of Pharmacology and Toxicology and the Graduate Faculty of the University of Kansas in partial fulfillment of the requirements for the degree of Doctor of Philosophy.

_____

Chair: Dr. Shirley ShiDu Yan

_____

Dr. Nancy Muma

_____

Dr. Rick Dobrowsky

_____

Dr. Honglian Shi

_____

Dr. Adam Smith

_____

Dr. T. Chris Gamblin

Date Defended: May 2, 2019

The dissertation committee for Erika D. Nolte certifies that this is the approved version of the following dissertation:

Cyclophilin D overexpression as a mechanism of mitochondrial dysfunction in aging and Alzheimer's disease with implications for therapeutic interventions

_____

Chair: Dr. Shirley ShiDu Yan

Date Approved: May 2, 2019

Abstract

Alzheimer's disease (AD) is the sixth leading cause of death in United States, affecting more than five million people every year. Despite substantial research into the topic, including over a hundred thousand research papers on the topic and nearly a billion dollars per year in funding, no drugs have been approved by the FDA to prevent, slow, or cure AD. Upon discovering that patients with Alzheimer's disease had increased Cyclophilin D (CypD), a key mitochondrial matrix protein responsible for the initiation of mitochondrial apoptosis, we generated models of tau-induced AD with altered CypD expression. CypD overexpression (OE) mice were successfully used to model more severe AD pathology. These mice showed increased levels of hyperphosphorylated tau (HPT). Additionally, these mice showed mitochondrial failure in an age dependent manner. Synaptic and neuronal loss were also identified in an age dependent manner. Finally, cognitive impairments were detected using an open field study and a daily task performance study. CypD knock out (KO) mice were used to model the potential therapeutic effects of lowering CypD in an AD model. These mice showed an amelioration of every AD biomarker tested. CypD KO mice showed lower HPT loads and normalized mitochondrial function. There was no detectable loss of synaptic terminals in the CypD KO line, and there was no loss of cognitive function in either open field or a daily task performance test.

A small molecule CypD inhibitor created in our lab was used in a tau-induced model of AD to attempt to create the significant improvements seen with genetic ablation of CypD. This compound was determined to be safe for use in mice after testing in cell cultures revealed that it was non-toxic and effective at preventing Aβ-induced cellular death. In mice, the CypD inhibitor reduced HPT accumulation, restored mitochondrial function, and prevented cognitive declines without inducing any apparent toxicity in the mice.

We identified that CypD played a similarly important role in non-transgenic aging mice. Non-transgenic mice show signs of decline with aging. By 24 months, mice show increases in anxiety and decreases in daily task performance. These can be explained by increased mitochondrial failure and reactive oxygen species production. CypD OE mice not crossed into any AD model show an advanced aging phenotype in which the previously identified biomarkers of aging mice present stronger and at an earlier time point. CypD KO mice not crossed into any AD model show an amelioration of all aging-related cognitive dysfunction and molecular failures measured.

Overall, these studies point to an important role of CypD in both aging- and AD-induced cognitive impairments through the restoration of mitochondrial function and the preservation of synapses. These studies also establish our small molecule CypD inhibitor as an effective method to reduce the phenotype of AD.

Acknowledgements

I would like to express my very great appreciation to Dr. Yan, for her patience and careful guidance in my research. Without her dedication to my development as an independent scientist, I would not be the researcher that I am today. I would also like to thank my entire committee, Dr. Nancy Muma, Dr. Rick Dobrowsky, Dr. Honglian Shi, Dr. Adam Smith, and Dr. Chris Gamblin, for the assistance with reviewing my dissertation.

Further, I would like to offer my special thanks to Dr. Eduardo Rosa-Molinar and Dr. Adam Smith for their thoughtful discussions and assistance with experimental designs and theories. I am particularly grateful for assistance given by Rachel Khaw, Abigail Berland, Claire Eggleston, and Zoe Lai who assisted with experiments. I am thankful for the staff of the Animal Care Unit, particularly Kendra Clark, for their assistance with my animal experiments and dedication to providing an environment conducive to my research.

My fellow students and post-doctoral researchers, while too many to name, have my utmost gratitude as I know that without their assistance and friendship this dissertation would not be possible.

Finally, I wish to acknowledge the support provided by my family and friends, particularly my husband Alex Nolte, without whom I most certainly would not be here.

Table of Contents

List of Figures

List of Tables

List of Schematics

Table 1: List of Abbreviations

Abbreviation	Full name
AD	Alzheimer's disease
ALS	Amyotrophic Lateral Sclerosis
ANT	Adenine nucleotide translocator
APP	Amyloid precursor protein
Aβ	Amyloid beta
Ca^{2+}	Calcium
CsA	Cyclosporin A
Cyp40	Cyclophilin 40
CypA	Cyclophilin A
CypB	Cyclophilin B
CypC	Cyclophilin C
CypD	Cyclophilin D
CypE	Cyclophilin E
Cyt C	Cytochrome C
DPL1	Dynamin like protein 1
ER	Endoplasmic reticulum
ETC	Electron transport chain
HD	Huntington's disease
HIV	Human immunodeficiency virus
HPT	Hyperphosphorylated tau
HSP70	Heat shock protein 70
HSP90	Heat shock protein 90
HTF	Hyperphosphorylated tau filaments
KO	Knock out
LTP	Long term potentiation
MND2	Motor neuron desecration 2
mPTP	Mitochondrial permeability transition pore
MTC	Methylthioninium chloride
NMDAR	N-methyl-D-aspartate receptor
OE	Overexpression
OSCP	Oligomycin sensitivity-conferring protein
PD	Parkinson's disease
PiC	Phosphate carrier
PPIase	Peptidyl prolyl cis/trans isomerases
ROS	Reactive oxygen species
SDS-PAGE	Polyacrylamide-gel electrophoresis
SOD	Superoxide dismutase
SPECT	Single Photon Emission Computed Tomography
Tg	Transgenic
UPD	Up-and-down
VDAC	Voltage-dependent anion channel

Chapter 1 Introduction

Alzheimer's disease

Alzheimer's disease (AD) is the most common cause of dementia [1], affecting one in six adults over the age of 65, and one in three over the age of 85. Sporadic AD makes up 90 to 98% of all AD cases, with early onset familial Alzheimer's disease as a result of genetic mutations in presenilins being less common [1]. More than 5 million Americans were living with AD in 2016, and that number is expected to grow to as many as 13.8 million people by 2050. AD is characterized by several common cognitive, behavioral, and psychological symptoms which include memory loss, confusion, difficulty with self-care, and depression. The socioeconomic cost of AD is enormously high, costing $236 billion in payments to American health care providers alone, representing 1.3% of the USA GDP [2]. In 2015, an additional $221.3 billion worth of care was provided by unpaid family caregivers. Despite this impact, AD remains the only top 10 cause of death with no treatment to cure or even delay disease progression [3].

Aging is the top risk factor for developing AD, as well as a high risk factor for the development of cancer [4-6], type 2 diabetes [7, 8], cardiovascular disease [9, 10], stroke [11, 12], and Parkinson's disease [13, 14]. Healthy aging in the absence of any diagnosable neurocognitive disease is associated with cognitive decline. In a longitudinal study of 1,721 adults tested for visual memory and crystallized intelligence (an example would be nice as this is not a common term), an increasing rate of decline correlated with age, particularly from 65-74 years of age [15]. The exact cause of these losses are unknown, but researchers have hypothesized neuronal loss and lowered neuronal conduction speeds may explain the deficits. However, while loss of cerebral volume is associated with aging, neuronal loss is not, disproving hypotheses attributing cognitive loss to neuronal death [16]. Research currently suggests that loss of synapses, rather than entire neurons, is responsible for the cortical thinning and the accompanying cognitive deficits seen with age. In

healthy aging, brain volumes can be reduced by 0.5%-1% each year. Synaptic loss is accompanied by changing dendritic strength and length, as well as reduced myelinated axon length [17]. It is likely then that the root cause of memory loss in healthy elderly populations is synaptic loss and reductions in signal strength due to demyelination.

Biochemically, AD is characterized by accumulations of amyloid-beta (Aβ) (Figure 1-1 A,D), increases in hyperphosphorylated tau (HPT) (Figure 1-1 B,E), and hypometabolism (Figure 1-2 A,B) [18], which have led to three major hypotheses of AD development that will be discussed here.

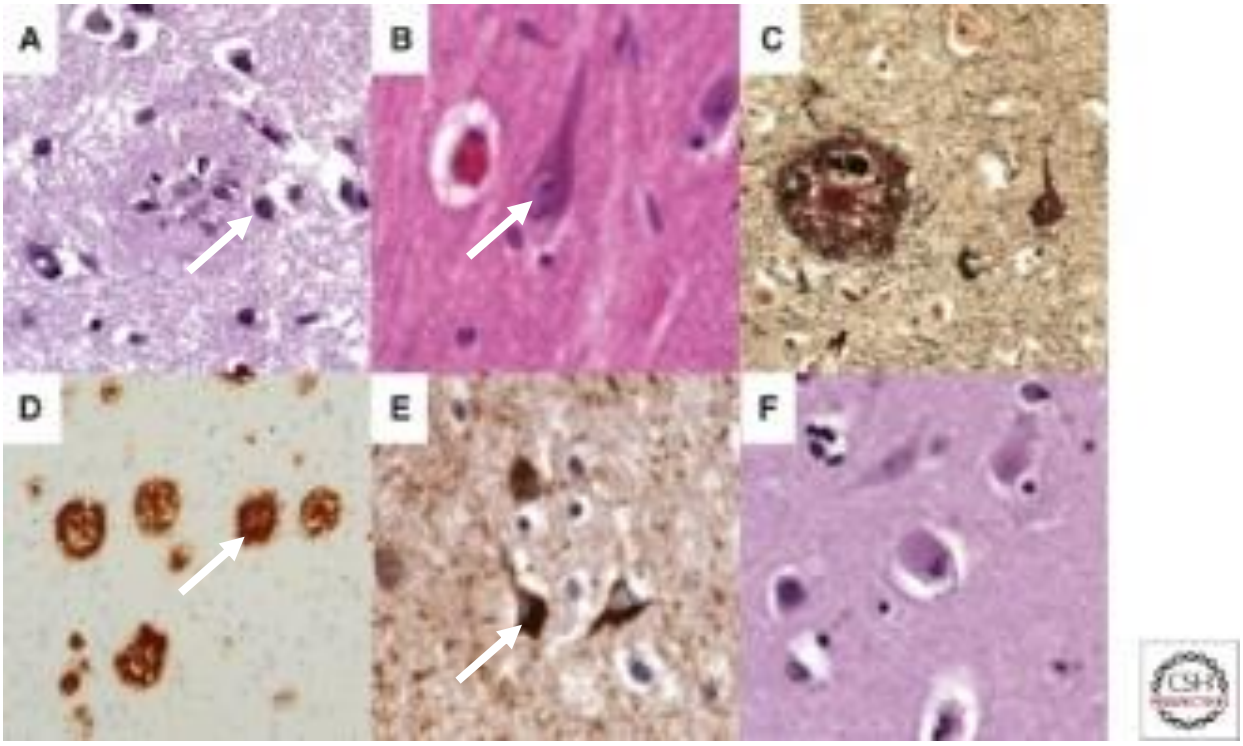

Figure 1-1: AD is marked by accumulation of Aβ plaques and tau tangles

A) Plaques in the frontal cortex are stained with Haemotoxylin and Eosin. B) Tangles are stained with H&E in the hippocampus. C) Silver staining can identify both Aβ plaques and tau tangles. D) Antibodies specific to Aβ mark plaques. E) Specific antibodies mark Tau tangles. F) Lewy bodies can be identified with H&E staining in the cortex. [19]

Amyloid Cascade Hypothesis

Amyloid precursor protein (APP) is a ubiquitously expressed membrane protein that appears to be involved in cell growth and neuronal process outgrowth, but researchers have failed to identify specific functions. Once embedded in the membrane, several processing pathways exist for APP based primarily on how the protein is localized. In the AD pathway, APP is cleaved sequentially by β-secretase and γ-secretase to produce Aβ fragments 1-40 and 1-42, with Aβ 1-42 considered more toxic [20]. Aβ fragments can exist as monomers, dimers, filaments/oligomers, or insoluble plaques. While it is the insoluble plaques that are necessary for diagnosing a patient with AD, smaller, soluble Aβ conformations are likely more toxic [21]. Aβ accumulations are difficult for the cell to degrade and often disrupt cytosolic degradation on a large scale, as well as disrupting cell signaling. The amyloid cascade hypothesis depends on the appearance of Aβ plaques that appear long before hyperphosphorylated tau filaments (HTF), described later in detail. In human tissue, animal models, and various cell lines, Aβ plaques have been proven to cause disruption of cellular membranes, induce mitochondrial DNA mutations, decrease metabolism of glucose, decrease electron transport chain (ETC) activity, increase reactive oxygen species (ROS), disrupt long term potentiation (LTP), and disrupt calcium homeostasis and calcium buffering [22-25]. These sweeping alterations to cell physiology have supported the amyloid hypothesis as they indicate a causative role.

The amyloid hypothesis is further buoyed by research into familial AD, which is always caused by mutations in genes related to APP and amyloid processing. Specifically, familial AD is caused by mutations in APP, Presenilin-1 (PS1), or Presenilin-2 (PS2), with PS1 mutations being the most common. PS1 and PS2 make up the core of the γ-secretase unit that cleaves APP. The genetic disruption of these proteins always leads to early onset, or familial, AD [26].

Many experiments have demonstrated that the addition of Aβ to cellular and animal systems results in AD-like phenotypes, giving credence to the amyloid cascade hypothesis [27-30]. However, over 50 drugs have been shown to modify Aβ deposition, accumulation, and the resulting neuronal damage, none have succeeded in passing through clinical trials [31]. Most often, these drugs have failed for lack of efficacy rather than due to safety concerns.

With the creation of the Pittsburg Compound B to stain Aβ plaques under positron emission tomography [32-36], it was determined that Aβ accumulations are found in a small percentage of brains of cognitively normal, adults of advanced age [37]. This suggested to some researchers that these plaques precede the cognitive symptoms of AD that are usually used for diagnosis [35, 36, 38-42], while others interpreted this as a negation of the amyloid cascade [43]. For the former scientists, the early deposition of Aβ indicated a need for earlier screening and treatment of patients. For the latter scientists, the early appearance of Aβ without symptoms suggested that other proteins may play a larger role in AD.

Tau hypothesis

Tau is a microtubule-associated protein that promotes neuronal process outgroWTh during development, giving neurons polarity. In developed neurons, tau binds to microtubules, providing stability [44-48]. Tau also supports membrane interactions and cellular trafficking [44], giving tau an important function in microtubule dynamics. Microtubule dynamics are integral in synapse formation and pruning, both are essential functions for learning [49]. Despite these important roles, genetic ablation of tau creates no overt phenotype; this is likely due to a striking upregulation of microtubule-associated protein 1A, which can assume the functional role of tau with only minimal reorganization of the microtubules [50]. A later study of the same model identified that axonal trafficking was slower and axonal groWTh was reduced in the tau knock-out (KO) model, although

these factors did not give rise to a behavioral or disease phenotype [51]. The role of tau in trafficking is of heightened importance in the brain, where proteins and organelles, including mitochondria, must be trafficked from the soma to the synaptic terminals.

Tau contains 79 serine and threonine residues [52, 53] and four tyrosine residues that provide sites capable of undergoing phosphorylation , meaning that 20% of the protein is made up of amino acids with potential for phosphorylation [54, 55]. Studying these phosphorylation sites has proved to be difficult owing to the need for specific antibodies to differentiate between phosphorylation sites that are often very similar in structure [55]. Additionally, because there are several different protein domains with phosphorylatable sites, researchers have assumed that phosphorylation in different regions cannot be considered to have the same effect [56]. However, despite these difficulties, repeated experiments have shown hyperphosphorylation of tau in pathological conditions [44, 45, 54, 57, 58].

Because HPT does not efficiently bind to microtubules, HPT impairs microtubule formation and induces destabilization after formation [58-60]. OutgroWTh of neuronal processes can be affected by HPT, but because AD is an aging disease, there is little effect on the outgroWTh of axons in this condition, since outgroWTh happens embryonically.

HPT, once dissociated from the microtubule, dimerizes to form paired helical fragments, which then group to form hyperphosphorylated tau filaments (HTF) [61, 62]. HTFs show phosphorylation at 45 of the possible sites, compared to 15 phosphorylated sites in control tau [63-66]. The driving force behind this rampant increase in phosphorylation is unknown, but researchers have observed that many of these sites may be transiently phosphorylated and then rapidly dephosphorylated in cognitively normal, human patients. Rapid dephosphorylation can be blocked by inhibitors of Ser/Thr phosphatases. Some researchers hypothesize that HPT is not the result of increased phosphorylation, but rather a decrease in dephosphorylation. Additionally, the build-up

of HPT favors dimerization and eventual HTF formation due to an inability to efficiently degrade the hyperphosphorylated form [52].

While Aβ appears before HTFs, concentration and location of HTFs appears to better correlate to disease progression, which in combination with the studies that identify Aβ in the absence of cognitive impairment, led some researchers to support the tau hypothesis over the amyloid cascade hypothesis. In animal models, mutation of tau can result in AD-like symptoms [67]. However, some studies have identified HTFs in asymptomatic patients [68].

Mitochondrial cascade hypothesis

In a healthy human, 20% of the ingested glucose is required for energy metabolism in the brain [69, 70]. This is due to the high energetic baseline to generate the ATP required for basic neuronal activity. Maintaining proper membrane polarization is particularly important in neurons, which are routinely depolarized and must be rapidly repolarized as the neuron fires, in addition to a series of housekeeping requirements [71]. Additional energy is also necessary to modulate the transport of biomolecules down extended axonal processes, as well as maintaining synaptic functioning [72-76]. Mitochondria must regularly change size and shape to meet these needs through a process known as mitochondrial dynamics, including fission and fusion, both of which are energetic processes [77-82].

Fusion and fission allow the mitochondria to meet the bioenergetic needs of the cell while also replacing mitochondria functioning at suboptimal capacity. This process is commonly referred to as mitochondrial dynamics and is thought to be a controlling factor in neuronal health and survival [83]. Mitochondrial dynamics are tightly controlled by multiple proteins, and evidence in several models demonstrates that disturbing the homeostasis of any of these protein-enzyme interactions results in neurodegeneration [84-87]. Disrupted mitochondrial dynamics is an

early sign of mitochondrial dysfunction in AD [77, 78, 88, 89]. To test whether traditional hallmarks of AD could disrupt mitochondrial dynamics, M17 neuroblastoma cells were cultured with APP, which could reliably induce altered mitochondrial morphology and distribution throughout the cell. This effect was ameliorated by the addition of a β-secretase inhibitor [90]. Lastly, Aβ has been identified to accumulate in mitochondria before cytosolic plaques have formed in human patients [91-93] and in mouse models [24, 94-96]. This data demonstrates the importance of proper fusion and fission to maintain neurons in a non-degenerative state, and also demonstrates that Aβ can be a causative factor in mitochondrial dysfunction.

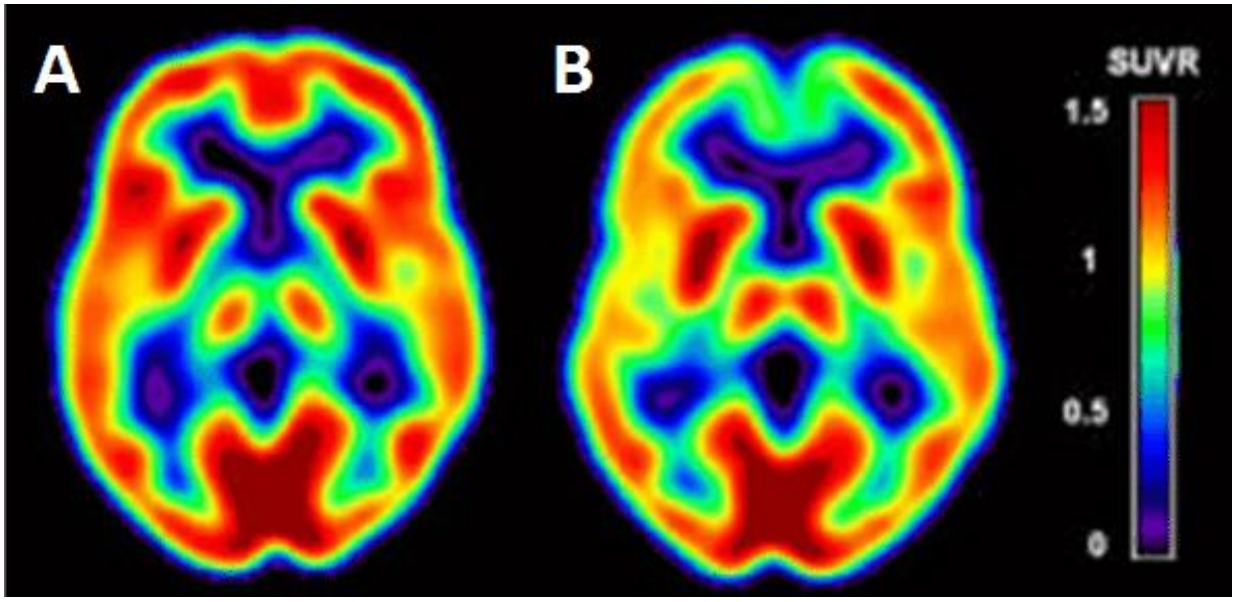

Figure 1-2: Hypometabolism in Alzheimer's disease [97].
A) A normal individual and B) B individual at high risk for AD [97].

Neither the amyloid cascade hypothesis nor the tau hypothesis generated the development of any FDA approved drugs in several decades of research, despite many drugs targeted at reduction of the accumulation of these proteins [98]. Better imaging technologies led to the development of the mitochondrial hypothesis. As shown in Figure 1-2, PET scans and fMRIs reveal that hypometabolism is established before Aβ plaques or HTFs [99], and hypometabolism predicts the appearance of Aβ and HPT. Hypometabolism in the brain was a better predictor of

cognitive dysfunction than the appearance of Aβ or HPT [100] since mitochondrial malfunction produces ROS, which increases the accumulation of both Aβ and HTFs.

Mitochondrial dysfunction is present in the most popular animal models of AD [101, 102]. The 3xTg-AD model was generated by creating mutations in the APP protein, PS1 protein, and tau protein [103], and is one of the most common mouse models to study AD [104-107], This model showed reduced mitochondrial respiration rates in 3-month-old female mice. Decreased mitochondrial function was assessed by measuring the expression of the pyruvate dehydrogenase complex and cytochrome c oxidation. This phenotype appeared four months before Aβ pathology appeared and ten months before tau pathology occurred. In this model, embryonic hippocampal neurons also displayed a significant decrease in mitochondrial respiration [108]. At three months, 3xTg-AD mice showed significantly more oxidative stress, as marked by increased lipid peroxidation and decreased levels of antioxidants glutathione and vitamin E [109]. These studies demonstrate that mitochondrial dysfunction is an early factor in models of AD pathology.

Synaptic mitochondria are particularly important in maintaining neuronal health, and several models have shown that impaired trafficking of mitochondria to the synapses results in neuronal death despite the mitochondria of the soma being fully functional [110]. For this reason, researchers began to study synaptic and non-synaptic mitochondria as separate pools which revealed pathology critical to AD. In mice overexpressing human APP, synaptic mitochondria showed impaired function by four months of age, compared to the non-synaptic mitochondria from the same animals and synaptic mitochondria from wild-type animals. Supporting this finding, Aβ accumulation occurred in synaptic mitochondria of transgenic (Tg) mice earlier than in non-synaptic mitochondria of Tg mice or synaptic mitochondria of non-Tg mice [111, 112]. This indicates that in AD pathology, synaptic mitochondria are among the first to be affected. Impaired synaptic mitochondrial function has been found to reduce synaptic plasticity in the earliest stages

of AD in several models [113, 114], providing a mechanism by which mitochondrial function may create the behavioral phenotype associated with AD.

In addition to synaptic mitochondria being more strongly affected and disrupted earlier in the progression of AD, several studies demonstrate that fewer mitochondria are targeted to the synapses [115]. In rodent models of AD expressing either human APP or tau, time-lapse imaging in primary neurons shows that mitochondria move more slowly and often have altered patterns of movement when compared to mitochondria in wild-type neurons [84, 116]. It would be over-simplistic to say that in healthy neurons, mitochondria move quickly along microtubule scaffolding while they do not move or move slowly in degenerating neurons. Rather, in healthy neurons, mitochondrial movements can be classified into five basic patterns based on combinations of starting, stopping, and moving distances of hundreds of microns, with all of these patterns being normal. In healthy neurons, mitochondria can move at a velocity of several microns per second and commonly change directions [117]. Current tracking technology does not allow for the tagging and monitoring of an individual mitochondrion; such technology would allow researchers to observe where a specific mitochondrion was moving, and from this data garner information about why mitochondria appear to be in nearly constant motion [118].

Despite not being able to track individual mitochondria, it has been possible to determine reasons for abnormal trafficking in AD models. Reduced expression of dynamin like protein 1 (DLP1), is seen in AD patients, and results in more mitochondria distributed into the soma, as well as higher productions of ROS. DLP1 depletion in a cell model results in mitochondrial trafficking disruptions and mitochondrial dysfunction, similar to that observed in traditional AD models. The addition of DLP1 to the system rescues mitochondrial distribution [119]. Treatments in AD that target the mitochondria will require understanding why and how fewer mitochondria are targeted to the synapse. Further, developing mitochondrial based therapeutics will be benefited by

understanding the mechanism by which synaptic mitochondria undergo more stress than somatic mitochondria.

Replicating what was seen in animal and cellular models, mitochondria numbers are significantly reduced in the affected brain regions of AD patients, such that it is unlikely that the neuron could support its bioenergetic needs [120]. Mitochondria that are present appear to be significantly damaged, with ruptured inner membranes, lipofuscin-filled vacuoles (a marker of "wear and tear" [121]), and variable mitochondrial DNA content [122]. Respiration in AD tissues shows a two-thirds reduction compared to age-matched controls [87]. Together, these human, animal, and cell studies suggest that mitochondrial deficits are key in AD pathology, but they are insufficient to determine a chain of events in AD pathology.

In determining how mitochondrial bioenergetics and ROS production affected amyloid load, a model of AD mice overexpressing APP was crossed with mice heterozygous for superoxide dismutase 2 (SOD2) KO [123]. SOD2 clears ROS produced by the electron transport chain [124]. Homozygotes for SOD2 KO in addition to the APP overexpression were embryonically lethal, while heterozygotes for SOD2 KO were not. When SOD2 heterozygotes were treated with antioxidants, several dose-dependent effects were seen. First, with the higher dose of antioxidant drug, lower Aβ loads were seen. Second, in the heterozygous mice receiving the low dose of antioxidants, significant tau phosphorylation was observed [123]. This study functionally and causally links mitochondrial health and ROS production to the common biomarkers of AD.

Interactions between Tau and Mitochondria

HPT has been shown to interact with mitochondria in several different conditions [125]. Based on molecular modeling, it was suspected that a motif on the N-terminus was responsible for this interaction [126]. A truncated form of tau containing only the N-terminus region was found

to localize to the mitochondrial matrix [127], where it impaired oxidative phosphorylation by blocking the adenine nucleotide translocator (ANT), resulting in mitochondrial fragmentation and elevated oxidative stress [125]. To more fully investigate this phenomenon, patient-derived Aβ oligomer extracts were cultured with rat embryonic hippocampal slices. Mitochondrial dysfunction and apoptosis were observed despite the concentration of Aβ being predicted to be too low to cause significant damage. HPT was found in these slices, leading researchers to determine that low-level Aβ was sufficient to drive the formation of HPT, which then imposed a significant negative effect on mitochondria, specifically the ANT, eventually triggering apoptosis [128].

In addition to impacting bioenergetics, tau and Aβ has been found to impact the mitochondrial proteome. In 6-month-old male 3xTg-AD mice, expression of 23 mitochondrial proteins differed significantly between transgenic and non-transgenic mice [129]. The affected proteins were involved in a variety of mitochondrial maintenance and energy production pathways. In a similar assay of hippocampal tissue from three other AD mouse models (P301L, APP(sw), and PS2-N1411), 24 proteins related to mitochondria were dysregulated. Eight of these proteins were related to complex I and complex IV. The P301L model of AD is driven by a single tau mutation [130]. This model showed increased dysfunction of complex I while the APP(sw) model showed increased dysfunction of complex IV [131] indicating that tau and Aβ have specific effects on the mitochondria. Further mechanistic understanding of how early stage APP and tau mutations cause dysregulation of the mitochondrial proteome may reveal a mechanism by which these AD-related mutations impair metabolism.

P301L tau mice were used to study the tau-dependent changes in axonal transport in a system free of Aβ plaques. The mutant tau was sufficient to form extensive HPT deposits, but did not form HTFs. Despite this, mitochondrial trafficking was impacted in 8-11 month old mice. In

these younger mice, the number of mitochondria moving in the anterograde direction (from the cell body to the synapse) was significantly increased. However, by 23-24 months, this effect was reversed and there were significantly less mitochondria moving to the synapse in the P301L mutant mice [132]. This study causatively shows that increased tau, specifically HPT, impairs mitochondrial transport to the synapse. As mitochondrial density at the synapse is reduced in AD, this link to tau is important in understanding how to increase bioenergetics at the synapse. The authors chose not to speculate on the increased anterograde transport of mitochondria in young mice, but when one considers this data in conjunction with previously proposed models of early mitochondrial deficits at the synapse, the inevitable hypothesis is that the increased transport of mitochondria to the synapse reflects a compensatory mechanism to prevent synaptic loss.

Current therapeutic targets in AD

Currently, there are five drugs approved for the treatment of AD which can be divided into two categories: cholinesterase inhibitors and N-methyl D-aspartate (NMDA) antagonists. All of these drugs target the symptoms of AD: memory loss and cognitive confusion.

The goal of medicating those with AD is not to attempt to cure the disease or extend the patients lifespan. More accurately, these drugs preserve some independent function for a short period of time and are typically e effective for less than a year.

Cholinesterase inhibitors

Cholinesterase is an enzyme that works by hydrolyzing the ester bond on acetylcholine, breaking the neurotransmitter down into choline and acetic acid. Acetylcholine is an excitatory neurotransmitter, and its degradation via cholinesterase allows neurons to return to resting states. Cholinesterase inhibitors prevent these actions, allowing for increased neuronal signaling [133].

Three cholinesterase inhibitors have been approved: Aricept, Exelon, and Razadyne. Aricept is approved for all stages of AD, while Exelon and Razadyne are approved only for mild to moderate AD. Cholinesterase inhibitors share a common list of side effects that tend to be very rare: nausea, vomiting, loss of appetite, and increased bowel movements. However, for most people these side effects are not severe [134].

Due to their shared mechanism of action regarding inhibition of cholinesterase, switching between these drugs does not provide further benefit for a patient, but patients may respond to one drug over another. What this means functionally, is that once the best drug for that patient has stopped having an effect, switching drugs will likely not cause any improvements in symptomology [134].

However, while all drugs inhibit cholinesterase as their main function, each drug does have slightly different mechanisms of action. Exelon prevents the breakdown of butyrylcholine, a synthetic compound similar to acetylcholine. Razadyne, in addition to inhibiting cholinesterase, stimulates nicotinic receptors to release more acetylcholine [134].

NMDA antagonists

Memantine is approved for moderate to severe AD. It is less frequently prescribed due to its more severe side effects, including headache, constipation, confusion, and dizziness. These side effects are slightly more severe than those from the cholinesterase inhibitors [134].

Inhibiting NMDA receptors reduces glutamate toxicity in AD. Glutamate can bind to multiple receptor types, including α-amino-3-hydroxy-5-methyl-4-isoxazolepropionic acid (AMPA) receptors. However, NMDA receptors were targeted in AD therapeutics due to the posited role of NMDA receptors in learning and memory. Glutamate binds to NMDA receptors and triggers an influx of calcium (Ca^{2+}) ions [135]. NMDA receptors are unique in their relatively large influx of Ca^{2+} ions [136].

NMDA receptors have a unique function in learning and memory due to the role of Magnesium (Mg^{2+}) gating. Simplistically, NMDA receptors are blocked by Mg^{2+} at the neuron's resting potential. Upon the activation of Long Term Potentiation (LTP), consistent glutamate release stimulates AMPA receptors, removing the Mg^{2+}. This allows the activation of NMDA receptors and the resulting Ca^{2+} cascade, including activation of $Ca2^{+}$/calmodulin-dependent protein kinase II (CaMKII) which modulates synaptic integrity. Thus, NMDA receptors have an established role in learning and memory [137].

Despite the importance of NMDA receptors in LTP, an excess of glutamate signaling can cause toxicity. Glutamate toxicity was initially termed excitotoxicity, a term still often found in AD literature [138-140]. Glutamate toxicity leads to a loss of post synaptic structures, and neurons appear to be more sensitive to glutamate-induced synaptic loss [141]. The presence of Aβ enhanced NMDA signaling [142], increased glutamate release from nearby microglia [142], and decreased clearing of glutamate [143]. Glutamate toxicity is thought to be mediated by high Ca^{2+} concentration in the cytosol [144-147]. Excessive calcium in the cytosol triggers apoptosis [148], disrupts the mitochondria [149], and perturbs cell signaling [150]. Therefore, Memantine works to suppress excessive NMDA activation that leads to high Ca^{2+} levels resulting in neuronal death.

Combination drugs

A drug trademarked Namzaric combines Aricept and Memantine to inhibit cholinesterase and NMDA receptors. Namzaric, like Memantine, is approved only for moderate to severe AD. However, it has significant side effects from both classes of drugs [134].

Molecular targets in the interaction of tau and mitochondria

Taking together the data presented herein, the link between HPT, mitochondrial dysfunction, and the AD phenotype is clear. However, despite over 20 years of research, these

interactions have not translated into clinically useful drugs. As drug development continues, there has been some progress in developing drug targets.

Mitochondrial dysfunction, in addition to leading to increased ROS levels and reducing the bioenergetic output, can induce apoptosis through opening of the mitochondrial permeability transition pore (mPTP) [151]. Several groups have sought to target this mechanism in hopes of preventing apoptosis. In order to understand how to pharmacologically intervene in this system, a brief description of the initiation of apoptosis is necessary (for a full review see reference [90]). While apoptosis can follow two basic pathways (extrinsic and intrinsic), it is the intrinsic pathway, also called the mitochondrial pathway, that poses an interesting drug target. Apoptosis is initiated through the binding of pro-apoptotic proteins to anti-apoptotic proteins to alleviate their self-inhibition. Mitochondria sequester these pro-apoptotic proteins to allow for careful control of this system while the anti-apoptotic proteins exist in the cytosol. A Ca^{2+} signal triggers the opening of the mPTP [152, 153], releasing cytochrome C (Cyt C) and multiple other pro-apoptotic proteins into the cytosol where Cyt C then binds to apoptotic protease activating factor 1 to induce the formation of the apoptosome, thereby activating caspase-9 and caspase-3/7. Caspases perform a variety of tasks in initiating apoptosis including the upregulation of DNA cleaving enzymes and cleaving proteins essential for DNA and nuclear stability, ultimately leading to cell death [154]. In addition to the pro-apoptotic proteins, mitochondria release a large amount of Ca^{2+}, which works to sensitize pro-apoptotic factors [155]. In order to fully understand the workings of the mPTP, a brief explanation of cyclophilins is required.

Cyclophilins

Cyclophilins are a class of proteins that were discovered and named from the identification of their peptidyl prolyl cis/trans isomerases (PPIase) enzyme activity [156, 157]. The role of a

PPIase enzyme is to stabilize the cis to trans conformational switch for proline residues. The cis/trans switch is necessary for the stability of many proteins [158]. Although structures vary between isoforms, all Cyclophilins have a conserved domain of 109 amino acids responsible for their PPIase activity [159-162]. Cyclophilins have been identified in mammals, plants, insects, fungi, and bacteria [161, 162]. Mammals have 7 cyclophilins that differ by structure, cellular location, and specific function.

Cyclophilin A (CypA) was the first identified cyclophilin [157]. It is cytosolic and found in all mammals [163]. Structurally, CypA is formed by an eight-stranded beta-barrel with two alpha-helices [164, 165].

Functionally, CypA has been identified as important for the folding of neuronal receptors [166]. CypA further regulates transcription factors, including Zpr1, likely through a stabilization method [167]. CypA has been indicated in T cell activation via regulation of interleukin 2 [168-170], which may be responsible for its role in infection of human immunodeficiency virus (HIV) [171-177].

CypA has the highest affinity for Cyclosporine A (CsA), which binds to a hydrophobic core of 7 amino acids [164, 165]. CsA works through the formation of a complex with CypA and binds to calcineurin, a calcium activated protein phosphatase. This complex blocks the translocation of nuclear factor of activated T cells from the cytosol to the nucleus, which prevents the transcription of interleukin-2 [178, 179]. The overall effect of this action is immune suppression, which allows CsA to be used as an immunosuppressant during organ transplantation. Further, CsA binds to calcineurin, creating a stable complex and reducing the effectiveness of cleavage by proteases. CypA-CsA-calcineurin has reduced phosphatase activity, altering calcium homeostasis in cells [178, 180-182].

Cyclophilin B (CypB) is very similar in structure to CypA [183], but is located in the endoplasmic reticulum (ER) [162, 163]. While less is known about CypB than CypA, CypB creates complexes with the peptide hormone prolactin to induce transcription [184]. CypB further governs the activation of interferon-regulatory factor 3, which induces interferon β upon translocation to the nucleus [185].

Cyclophilin C (CypC) is structurally homologous to CypA and CypB [186], and shares CypB's location in the ER [162, 163], where it regulates transcription factors.

Cyclophilin D (CypD) has more unique morphology and is the only cyclophilin located in the mitochondria [187, 188]. Due to its unique position and functions, more attention will be given to CypD later in the review.

Cyclophilin E (CypE) is an understudied cyclophilin located in the nucleus. Studies suggest that CypE helps to regulate DNA-binding proteins [189].

Cyclophilin 40 (Cyp40) has a similar structure to CypA, CypB, and CypC. However, Cyp40 has a series of tetratricopeptide repeats, similar to those seen in stress response proteins [190]. Cyp40 is located in the cytoplasm [190], where it forms complexes with steroid receptors [191, 192]. Cyp40 has been found to form a dimeric complex with heat shock protein 90 (HSP 90) [191, 192], which further supports hypotheses that Cyp40 is involved in the heat shock response pathway. Several studies identified Cyp40 as a regulator of the c-Myb gene via its PPIase activity [193, 194]. C-Myb binds to heat shock transcription factor 3, which induces the expression of heat shock protein 70 (HSP 70).

CypNK, the first identified cyclophilin in natural killer cells, is the largest cyclophilin [195, 196] and is located in the cytoplasm [195, 196].

Several cyclophilins exhibit catalytic degradation of DNA based on stimulation by calcium or magnesium [197]. CypA and CypB are best stimulated by a combination of both calcium and

magnesium, while CypC can be stimulated by magnesium alone [198]. Active CypA, CypB, and CypC degrade apoptotic DNA [187].

Cyclophilin D

Encoded by the *PPif* gene, CypD is sometimes referred to as Cyclophilin F. However, for the purpose of these studies, CypD will be used. CypD is a cyclophilin unique to mammals [199] that is sensitive to calcium fluctuations [200].

CypD is comprised of 178 amino acids [201] and forms up to four protein-protein hydrogen bonds. The structure is considered rigid and does not change a considerably upon binding to partners like CsA. CypD has 8 anti-parallel beta pleated sheets and two alpha helices formed against the sheets. A short alpha helical turn houses the active residue Trp121 [202]. The PPIase region is composed of catalytic arginine (Arg55) and hydrophobic, aromatic, and polar residues [202]. The back face of CypD exhibits protein-protein interactions [203].

The most important identified role for CypD is triggering the opening of the mPTP. Previous hypotheses identified the structure of the mPTP as the ANT in the mitochondrial inner membrane and the voltage-dependent anion channel (VDAC) in the outer membrane [204]. However, with the technology to create genetically modified experimental animals, these hypotheses lost credence. KO of ANT did not reduce mPTP formation [205]. KO of VDAC similarly did not affect mPTP formation [206]. Binding studies identified phosphate carrier (PiC) as a binding partner of CypD, which lead to hypotheses that PiC may be involved in forming the mPTP. However, PiC KO did not prevent mPTP opening. Interestingly, PiC KO did slightly change electrochemical dynamics of the mPTP opening, indicating that PiC may still have a regulatory role [207].

More recently, dimers of ATP synthase have been hypothesized to from the mPTP [208]. In isolated membrane fractions, dimers of ATP synthase form a pore of similar conductance to the mPTP. Additionally, the oligomycin sensitivity-conferring protein (OSCP) unit of ATP synthase has been identified as a binding partner of CypD [209]. With age and increases in CypD expression, binding becomes irregular and leads to mitochondrial damage [210-212].

Like other cyclophilins, CypD interacts with CsA with high affinity (K_D=13.4nM) [213]. CsA has a broad range of effects on cytosolic Cyclophilins. CsA binding to CypD prevents the opening of the mPTP [203]. Experimentally, CsA has become the gold standard positive control blocking the mPTP. CsA inhibits the PPIase activity of CypD [214], but it is unknown if this is functionally important to the opening of the mPTP. CsA binding improves the ability of mitochondria to buffer calcium *in vitro* and *ex vivo* [200].

CypD does not require PPIase activity to open the mPTP. Experimentally, sangliferin A can inhibit mPTP opening, but does not alter PPIase activity [215]. CypD has been classified as a redox sensor, which is intimately linked to the opening of the mPTP [216]. Under standard conditions, a disulfide bridge forms between Cys203 and Cys157, but this bridge can be disrupted by redox modulation. Cys203 is required for mPTP opening [217], which links functional redox sensing with mPTP opening. The disulfide bridge appears to block the binding site of CypD to the OSCP region in mitochondrial climates of low ROS. With high levels of ROS, the disulfide bridge is disrupted, allowing CypD to bind to the OSCP and open the mPTP. Further levels of precise control are offered by the S-nitrosylation of Cys203, which changes mPTP dynamics by making mitochondria more resistant to hydrogen peroxide induced opening [217].

Experimental models show that CypD triggers an opening of the mPTP in conditions of cellular or tissue stress, like high levels of calcium or ROS [217]. However, the precise molecular pathway by which this signaling occurs is still unknown. About 1% of active glycogen synthase

kinase 3 beta (GSK3β) is translocated to the mitochondria where it phosphorylates CypD at Ser38, Ser39, or Ser123. Phosphorylation at these sites leads to the induction of the mPTP [218]. Another route may be via p53, which can translocate to the mitochondrial matrix and has been detected after ischemia as a complex with CypD. The p53-CypD complexing is eliminated by CsA, indicating that CsA and p53 share a binding site. The p53-CypD complex is not affected by calcium induced mPTP opening [219].

Cyclophilin D in Alzheimer's disease

Aβ has been hypothesized to drive the formation of ROS through disruption of the ETC [220] and inhibition of ATP synthase [221, 222]. Aβ has been shown to prompt the opening of the mPTP [23, 223-227]. With the recent hypothesis that ATP synthase makes up the core of the mPTP, these observations link Aβ-induced ROS production directly to the mPTP, leading to research on the direct connections between Aβ and the mPTP.

In brain regions high in Aβ, CypD expression is elevated in both human patients (Figure 1-3) [23] and mouse models of AD [24]. In tissue from human patients and animal models of AD, Aβ was found to colocalize with CypD, and binding studies found that the two form a complex in the mitochondrial matrix [24]. This is specific to Aβ, as reverse sequence peptides do not colocalize with CypD or form a complex. In binding studies of CypD and the OSCP, Aβ enhances CypD binding [228].

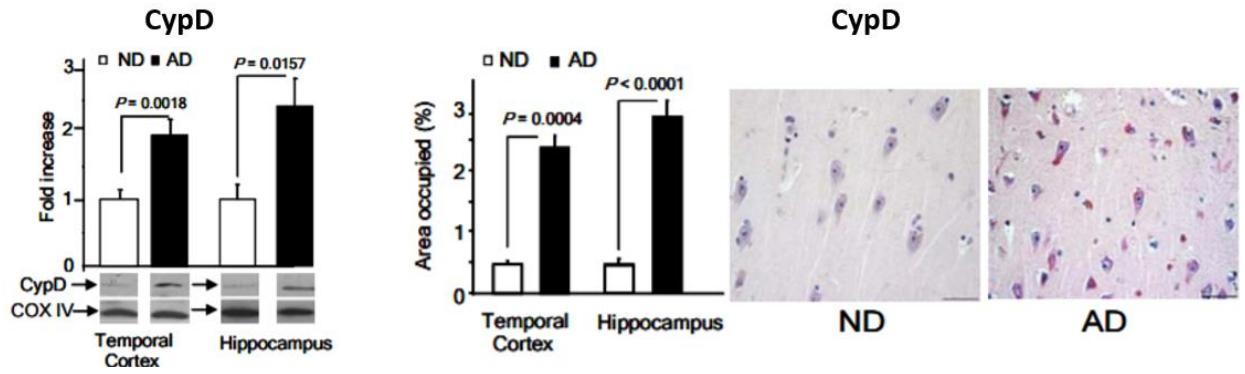

Figure 1-3: CypD expression in AD patients [229]

In a human-APP overexpression model of AD, CypD KO improved many metrics of the AD phenotype [23, 24], including calcium buffering capacity and calcium homeostasis, reduced mitochondrial swelling in response to calcium toxicity, improved mitochondrial membrane potential resistance, reduced super oxide production, ameliorated ATP levels and ETC activity, improved learning and memory dysfunction, normalized LTP, normalized neuronal trafficking [230], normalized ATP synthase activity[210], and improved intracellular signaling [231]. These promising results indicate that CypD should be targeted in AD therapies.

Inhibition of Cyclophilin D

Inhibition of CypD by CsA is not indicated in most neurodegenerative diseases due to the chronic nature of the disease that would create problems with CsA toxicity. Additionally, CsA cannot cross the blood brain barrier, which is necessary for the treatment of most neurodegenerative conditions. Thus, it has been necessary to design new small molecule compounds that are not toxic, have the ability to cross the blood brain barrier, and inhibit CypD in a specific manner.

A screening library of compounds that have been modeled based on the structure of CypD and satisfy Lepinsky's rule of five have been created for this purpose [232-234]. These compounds have all been modeled to cross the blood brain barrier. From this library, several compounds have

been successful in blocking mPTP opening without causing cellular toxicity. One has been tested in Aβ induced cell toxicity and can prevent cellular death. A pyrazinyl urea-based mPTP blocker has been found to be more efficient at preventing mPTP opening upon Aβ insult than CsA [235].

SS31, a cell membrane antioxidant, has been identified as an effective method of reducing CypD expression which reduced mPTP opening. SS31 treatment in AD models rescued learning and memory deficits and ameliorated the loss of synaptic proteins [236].

Several groups are attempting to develop drugs to prevent tau aggregation, which elucidates an earlier stage of tau-mitochondrial dysfunction. One such drug is thionine, and its more recently formulated derivative methylthioninium chloride (MTC), which inhibits tau-tau interactions [237, 238]. This drug has been criticized as being likely to inhibit microtubule assembly by blocking tau-microtubule binding [152, 239]. At 50 μM MTC, approximately 50% of microtubule assembly formation is inhibited, while the clinically necessary concentration to inhibit the formation of tau aggregates would be 0.2-0.4 μM. This data means that the chance of MTC inhibiting microtubule binding in a clinically relevant way is not significant [240].

A variant of MTC with better bioavailability (leuco-methylthioninium with a counter-ion, LMTX) is currently being tested in phase 3 clinical trials. Three hundred and twenty-one individuals participated in the phase 2 trials, for which a significant improvement over the placebo group was found in brain activity based on a Single Photon Emission Computed Tomography (SPECT) scan. A SPECT scan produces images similar to a PET scan, albeit at a lower resolution, for significantly less monetary investment; PET scan is the recommended functional imaging tool for diagnosis of AD [241]. Due to the decreased resolution and contrast, a subgroup of results was validated with PET scans. These results were significant at 50 weeks in both mild and moderate cognitive impairment [242]. Despite this promising ability to inhibit tau aggregates and improve phenotype, there are still off-target effects that would need to be addressed, including the increased

rate of β-oxidation in the mitochondria and inhibition of monoamine oxidase A, both of which could have severe phenotypic consequences regarding metabolism and mood alterations [240]. Overall, while there are several promising targets, more work is needed to ensure that there is a therapeutic option for AD that is effective with minimal side effects.

Animal Models Available for the Study of Alzheimer's disease

Most research in AD is done in rodent animal models, although some models have been created in *Drosophila*, *Caenorhabditis elegans*, and other mammals. 171 rodent models exist, 5 of which are rat models and 166 of which are mouse models. To create models of AD, 24 genes have been modified. These genes, along with summaries of the genetic modification of that gene, the number of models in which that gene is modified, and references for those models are summarized in Table 1. One hundred and thirteen AD models are single gene mutations and 52 are multi-gene mutations. One model, SAM-P8, generated through sister-brother mating is used as a model of sporadic AD [243]. Of the 24 genes modified in AD, 12 of the targeted genes are within the APP pathway and one is within the tau pathway with the remaining genes being associated across cellular trafficking, cell signaling, and axonal development.

Table 2: Genetic Modification in Models of Alzheimer's Disease

Gene	Most common modification	Number of Models	Reference
ABCA7	KO or modification of ABCA7 gene	2	https://www.jax.org/strain/030283 https://www.jax.org/strain/030320
APLP2	KO	1	[244]
APOE	Humanized knock in, humanized mutations	30	[245-252]
APP	Humanized mutations (Swedish, Florida, London)	75	[103, 253-259]
BACE1	KO	9	[260]
BACE2	KO	1	[261]
CEACAM1	KO	1	https://www.jax.org/strain/030673
CLASP2	knock-in L163P mutation	1	https://www.jax.org/strain/031944
CR1	Humanized	1	https://www.jax.org/strain/031668
CR2	Humanized	1	https://www.jax.org/strain/031668
1L1RAP	KO	1	https://www.jax.org/strain/030304
ITM2B	Humanized mutation	2	[262, 263]
KIF21B	knock-in T82T mutation	1	https://www.jax.org/strain/031938
MAPT	Humanized knock in, Humanized mutations (P30IL, P301S, A152T, L266V, G272V, R406W)	29	[103, 264-290]
MTHFR	A262V Knock in	1	https://www.jax.org/strain/030922
NOS2	KO	1	[291, 292]
PDGFRB	KO	1	[293]
PLCG2	KO, M28L knock in	2	https://www.jax.org/strain/030674 https://www.jax.org/strain/029910
PSEN1	Knock in (PS1M146V, Humanized mutation (R278I, M233T, L235P, L166P), humanized knock in	38	[103, 250, 253, 255, 271, 294-300]
PSEN2	Humanized, KO, Humanized mutation (N141I)	7	[282, 301-303]
RAGE	Humanized, Truncation mutation	2	[304]
SNX1	D465N mutation	1	https://www.jax.org/strain/031942
SORL1	A528T mutation	1	https://www.jax.org/strain/031940
TREM2	Loss of function mutation (R47H)	30	[289, 290, 305-310]

Genetic models of AD face criticism of their poor predictive validity, construct validity, and induction validity. These concerns have a valid basis. Thousands of compounds have been tested in many of the models described here with great effect, but have failed to pass clinical trials, indicating a failure of predictive validity. Given the low number of AD cases caused by genetic mutation [1], the use of genetic mutation to construct and induce these models is a clear concern. Despite these concerns, there are currently very few alternatives.

One alternative to genetic modeling is the use of Aβ injection into the brain. Researchers have successfully created models via intracerebroventricular injection [311, 312] or bilateral dorsal hippocampus injections [313, 314] of Aβ oligomers. While these models avoid the developmental and genetic validity problems associated with genetic models, they do not solve the induction criteria. Further, the stress of daily brain injections, as is done in these models, creates an additional factor that must be accounted for in model development. Additionally, brain injections risk brain damage that could obscure or bias results.

Intravenous injection of Aβ oligomers avoids the problems of direct brain injections and showed efficacy in a 2018 study [315]. However, daily injections still create stress and still do not accurately model the induction or construct validity.

Because the effects of CypD in reducing Aβ-induced AD pathology are well characterized, we chose to study tau models. Tau pathology poses an interesting target in AD study due to the high correlation between HFT deposits and cognitive decline. For these studies, tau models without amyloid gene mutation were chosen in order isolate effects of tau separate from any effects of Aβ. Aβ and tau have interactions that can confound the determination of pathways [316]. 19 models that fit these criteria were identified and are compared in *Table 2* based on the age at which AD-like symptoms appear. A dash "-" marks criteria that have not been experimentally tested, while negative data appears is labeled "nd". Negative data, in this context, indicates pathology that

was tested and found to be absent; for example, models in which synaptic loss was tested but not identified. While not all models generate neurofibrillary tangles, also known as tau tangles, all models show hyperphosphorylated tau and other abnormal tau pathologies. mitochondrial dysfunction and cognitive impairments

Table 3: Available Tau Models for Alzheimer's Disease

Model	Tau tangles	Neuronal loss	Gliosis	Synaptic loss	Changes in LTP	Cognitive impairment	Reference
hTau-A152T	-	20 mo	-	nd	-	10 mo	[266]
hTau-AT	3 mo	12 mo	10 mo	10-16 mo	-	16 mo	[267]
hTau.P301S	4 mo	3 mo	nd	5-6 mo	nd	2.5 mo	[268]
JNPL3(P301L)	4.5 mo	10 mo	10 mo	nd	nd	nd	[269]
mThy-1 3R Tau	8 mo	8 mo	8 mo	nd	nd	6-10 mo	[270]
rTgTauEC	18 mo	24 mo	24 mo	24 mo	16 mo	16 mo	[272]
rTg(tauP301L)4510	2.5 mo	5.5 mo	nd	8 mo	4.5 mo	2.5 mo	[317]
Tau35	14 mo	nd	-	14 mo	nd	8 mo	[275]
Tau4RTg2652	-	-	nd	nd	nd	3 mo	[276]
Tau609	15 mo	15 mo	12 mo	6 mo	6 mo	6 mo	[274]
TauC3	-	-	-	1.3 mo	nd	1.3 mo	[277]
TauΔK280	24 mo	-	nd	13 mo	nd	nd	[279]
Tau P301L	8 mo	nd	7 mo	1-2 mo	6 mo	5 mo	[280]
Tau P301S*	6 mo	12 mo	3 mo	3 mo	6 mo	6 mo	[281]
Tau R406W	18 mo	nd	nd	nd	nd	16 mo	[283]
TauRDΔK280	2 mo	5 mo	21 mo	9.5 mo	10 mo	10 mo	[284]
Tau V337M	11 mo	10 mo	nd	nd	-	11 mo	[318]
THY-Tau22	3-6 mo	12 mo	-	nd	10 mo	9 mo	[287]
TMHT	4 mo	nd	nd	nd	nd	5 mo	[288]

For this study, the Tau P301S line, also referred to as PS19 mice, was chosen due to the high level of characterization of the model, the timely development of tangles and neuronal loss, and the established memory deficits [281]. Models that developed severe tangle pathology within 2-3 months, like the TauRDΔK280 mice, were avoided due to their particularly poor induction validity [284]; with AD as an aging disease, it was important that the model chosen for these studies be tested in an aging condition. Mice that developed only partial pathology, like the TauC3 mice, were avoided in order to focus on a model that recapitulated the AD-like pathology that these studies would address [277]. Finally, models that developed symptomology after only very late time points, like the rTgTauEC model, were avoided in order to streamline research objectives [272].

One concern with the P301S model is that the tau overexpression is done with human tau.

Statement of Purpose

This dissertation will explore the mechanistic links by which aging and tau pathology contribute to mitochondrial dysfunction and cognitive impairments, as well as the therapeutic possibilities of targeting CypD in Alzheimer's disease. These studies will explore hitherto unknown roles for CypD in aging animals and propose possible therapeutic options for age-induced cognitive failure. Further, this study will build on previous work linking CypD and mPTP opening to Aβ by demonstrating a causal link between HPT and CypD triggering mitochondrial failure. A hypothesis is proposed in Schematic 1.

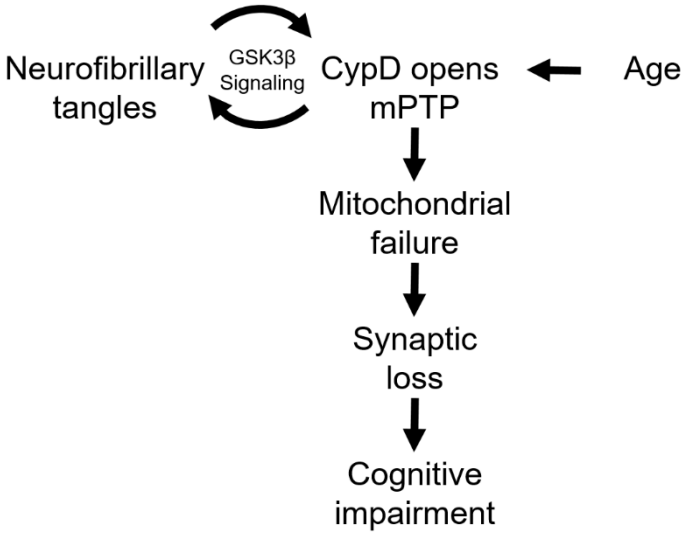

Schematic 1: Dissertation hypothesis of the role of CypD in aging and AD
Aging initiates an opening of the mPTP via CypD triggering mitochondrial failure, which leads to synaptic loss and cognitive impairment. Hyperphosphorylated tau filaments provoke the CypD-mediated opening of the mPTP via GSK3β signaling which leads to mitochondrial failure, synaptic loss, and cognitive impairment.

Methods

Animal Behavior

Open field

Open field was conducted using a force plate actometer developed as described [319, 320]. Briefly, the apparatus consists of a 30 cm by 30 cm box with acrylic walls and lid. Four force transducers operating at 200 samples per second collect force data that is then processed. Mice were acclimated to the procedure room for 30 minutes prior to the experiment beginning. Mice were placed in the apparatus and left alone for the 30-minute test. Locomotion was based on total movement throughout the apparatus. Anxiety was measured by determining time spent in the center of the arena [321, 322]. The center was defined by dividing the arena into two zones, center and outer, of equal area.

Body weight

Body weight measurements were made using the force plate actometer. Mass was calculated from the average force over the 30 minute test period.

$$\frac{F_1}{m_1} = \frac{F_2}{m_2}$$

Analysis of force actometer data

Force data is processed in Matlab following Fowler et al. (2001) in that the force data is analyzed for "center of force" following *equation 1*:

$$X_c = \frac{(x_1 f_1 + x_2 f_2 + x_3 f_3 + x_4 f_4)}{(f_1 + f_2 + f_3 + f_4)}$$

Where X_c is the location in the x coordinate of the mouse at the given time. The same is performed for the y Cartesian coordinate. This provides location data at a rate of 200 samples per second. However, this high volume of data includes a significant portion of noise from locomotive

movements of the mouse that do not affect the mouse's location. To resolve this, a two-stage process was used to eliminate noise in the data and to provide a more accurate estimate of location and distance travelled. First, location data is analyzed for erroneous data, defined as location data that locates the mouse outside of the box. These points are eliminated by replacing the value with the value of the previous data point. Data is replaced with the value of the previous data point to maintain the time location of each data point following the erroneous value. Once the data is processed for erroneous values, it is smoothed by a moving average that is 100 samples long, eliminating much of the vibrational noise of the system. This averaging method has no ill effects on mouse location, but it does reduce the overall length of the analyzed data stream by a total of 100 samples (0.5 seconds) because the first average cannot be performed until there are 50 samples and the last average can only be performed until there are 50 samples remaining. A 100-sample moving average was chosen to reduce the effects of individual values while still maintaining a high enough sampling rate to accurately locate the mouse center of force.

Total distance is calculated between smoothed location points by summing the distance between points as follows:

$$D_i = \sqrt{(x_i - x_{i+1})^2 + (y_i - y_{i+1})^2}$$

Where D_i is the distance between point i and i+1, x_i/y_i is the initial location, and x_i+1/y_i+1 is the next location.

Time in center is calculated by summing the total number of points within the inside box (5 cm away from the edge) and comparing it with the number of points in the outside box (within 5 cm from the edge).

Nesting experiment

Nesting was performed according to the protocol found in [323]. Briefly, mice were given 3 g of compressed cotton nestlet. In group housing, mice were given a new nestlet 2 hours before the dark cycle for 4 subsequent days. On the fifth day, mice were individually housed with a new nestlet and allowed to build a nest. Nests were scored 16 hours later on a scale of 1 to 5 based on published protocols and described in Table 4 [324]. Untorn nestlets were additionally weighed for further analysis.

Table 4: Nest Scoring Protocol

Score	Explanation
1	Less than 10% of nestlet torn
2	10-90% of nestlet torn No nest assembly
3	More than 90% of nestlet torn No nest assembly
4	More than 90% of nestlet torn Nest assembled into less than 25% of cage area No vertical assembly of nest
5	More than 90% of nestlet torn Nest assembled into less than 25% of cage area Vertical assembly of nest, would cover mouse

Mice maintenance

All animals were housed under pathogen-free conditions according to AAALAC guidelines. All animal-related experiments were performed in full compliance with institutional guidelines and approved by the Animal Care and Use Committee of the University of Kansas. Two-month-old SCID mice were purchased from Jackson Laboratories and continuously bred on the Yan breeding protocol to acquire SCID mouse generations for experimental use.

Molecular Experiments

H2O2 Assay

Amplex Red Hydrogen Peroxide/Peroxidase Assay Kit (Cat#A22188; Invitrogen) was used according to the manufacturer's instructions with 10 µG of protein. In short, Amplex Red is combined with horseradish peroxidase to detect H_2O_2 released from cells. Amplex Red reacts 1:1 with H_2O_2 to produce resorufin. Resorufin as an excitation/emission ratio of 571nm/585nm, which allows the amount of H_2O_2 to be measured via spectrophotometer.

Mitochondrial Electron Transport Chain Complex Activity

Complex I and IV were measured via spectrophotometer. A working solution of 25 mM K buffer and an Ultrospec 3100 pro spectrophotometer were used for both assays. Complex assays were expressed as nanomoles of substrate oxidized per $mg^{-}1$ protein $min^{-}1$ $ml^{-}1$ (nmol/mg protein/min/ml) converted to fold increase.

Complex I

Cortical tissue lysates (30-50 µG of protein/ml) and 0.5 ml of Complex I reaction buffer were added to a 2 mL cuvette. 2 µL of 65 µM Coenzyme Q1 begins the reaction and 2 uL of 2 µG/mL rotenone is added at 180 seconds. Oxidation of NADH causes a decrease in absorbance at 340 nm which can be measured in 20 second intervals over 18 readings.

Complex IV

Cortical tissue lysates (30-50 µG of protein/mL) and 0.475 mL of assay buffer were added to a cuvette. A dilution buffer was used to bring the total volume to 0.525 mL 25 µL of 0.22 mM ferrocytochrome c solution is added for incubation. Oxidation of cytochrome c causes a change in absorbance at 550 nm which can be measured every 10 seconds over 6 readings.

Western Blot

Continuous polyacrylamide-gel electrophoresis (SDS-PAGE) was used to measure protein from brain tissue. Protein extracts at 2-5 μg/μL were boiled with 1 X SDS sample buffer for 5 min at 100°C. Samples were separated on a 12% separating gel topped with 4% stacking gel with a visible protein molecular weight standard. Gels were run at 80 V through the stacking gel and then 100 V until the samples reached the bottom of the gel. A 12% separating gel topped with 4% stacking gel was prepared as follows for a standard size SDS gel:

Table 5: Composition of SDS-PAGE gels

Material	1 separating gel	1 stacking gel
H_2O (RT)	2.1 ml	1.0 ml
30% bis-acrylamide (4°C)	1.8 ml	220 μl
Separating buffer (4°C)	560 μl	----
Stacking buffer 4°C)	----	440 μl
10% SDS (RT)	45 μl	18 μl
15% APS (4°C)	23 μl	9 μl
TEMED (4°C)	3 μl	2 μl

After SDS-PAGE, proteins were transferred to a 0.45 μm nitrocellulose membrane (Thermo Fisher Scientific) by wet transfer at constant voltage at 110 V for 80 minutes on ice in Western blot transfer buffer. The membrane was incubated in 5% milk buffer in tris-buffered saline (TBS) for 30 minutes at room temperature to block non-specific binding. Primary antibodies were incubated overnight at 4°C. The membranes were washed 3 times for 15 minutes using TBS at room temperature. The membranes were incubated with secondary antibodies for 1-4 hours at room temperature. Membranes were washed 3 times for 15 minutes at room temperature.

Specific protein bands were visualized by chemiluminescence using Super Signal West Pico Chemiluminescent Substrate and a FluorChem HD2 image system. Table 6 contains information specific to particular antibodies used in this study.

Table 6: Antibodies used for protein quantification

Protein of Interest	Antibody	Source	Concentration	Secondary	Secondary incubation time
HPT	AT8		1:500		2 hours
CypD			1:2000	Mouse	1 hour
Synaptophysin			1:1000	Mouse	1 hour
Neuronal tubulin			1:2000	Mouse	1 hour
pAKT			1:1000		2 hours
tAKT			1:1000		1 hour
p(ser9)GSK3β			1:500		2 hours
p(tyr216)GSK3β			1:500		2 hours
tGSK3β			1:1000		1 hour

TMRM staining

Brain tissue was incubated with 150 nM Mito Tracker Green and 100 nM TMRM for 30 min followed and then washed twice with HBSS media. Tissue was imaged by confocal microscopy and the intensity of fluorescence was recorded to determine the uncollapsed proton gradient.

ATP Assay

ATP levels were measured using the Bioluminescence Assay Kit HS II. following the manufacturer's instructions as previously described. Tissue was sonicated using 50 µL lysis buffer. Protein content was determined using the BCA assay. 25 µL of sample and 25 µL/well ATP Dilution Buffer were added to a 96 well plate. ATP levels were determined using an LMax II 384 Microplate Reader and SoftMax Pro.

CypD Staining

Brains were sectioned and stained with goat anti-CypD and anti-goat antibody conjugated with rhodamine diluted 1:1000. Sections were incubated in Sudan black at 1:100 to

block autofluorescence. Neurotrace 640 was incubated at 1:150 in order to visualize nuclie. Images were taken using confocal microscopy.

Statistical analysis

All statistics were performed using StatView. Comparisons between more than two groups were performed using a one-way ANOVA with Tukey's post hoc test. Sex comparisons were performed using Student's t-test. Motion patterns and binding assays were analyzed using nonlinear regression with analysis of intercept.

Chapter 2 : The role of CypD in Aging Mice

Wild type C57/BL6 mice were used to assess behavioral and biochemical changes in mice as they aged from three months of age to 24 months of age. Complementarily, CypD overexpression (OE) and KO mice were used to determine the role of CypD in this process.

Two behavioral tests were employed. Open field was used to measure gross motor function, patterns of motion, and body weight to measure metrics of health and determine that mice were fit for further testing. Nesting activity was used to assay daily task performance, a sensitive metric of learning and memory that combines long term memory with working memory.

Biochemically, ROS, mitochondrial function, and proteins of interest were measured. ROS was measured via a H_2O_2 assay. Mitochondrial function was measured using a spectrophotometer-based colorimetric assay. Proteins of interest were measured using western blotting. These techniques are described in detail in the methods section.

Aging mice used in the experiments described in 2.1-2.4 are not the same as the cohorts used in experiments described in 2.6-2.12.

This chapter tests the sub-hypothesis presented in Schematic 2. We hypothesize with increased age, there is increased mPTP opening. This leads to mitochondrial failure, and the subsequent energy loss causes synaptic loss and cognitive impairment.

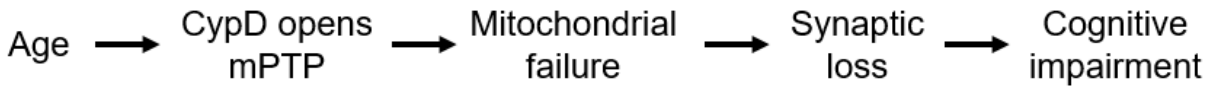

Schematic 2: Chapter 2 sub-hypothesis.

2.1 Gross locomotion, patterns of motion, and body weight

First, novel open field was used to assess total distance traveled in a 30-minute period. Between ages, there were no significant changes in the total distance traveled ($p=0.83$) (Fig. 2-1 A). Males and females were analyzed separately, and no significant differences were observed ($p=0.14$, $p=0.11$) (Fig. 2-1 B-C). Distance traveled in five-minute increments was then assessed to determine whether patterns of exploration and rest were different with age. When analyzed for sex and age, no significant differences were seen ($p=.21$) (Fig. 2-1 D).

Finally, we used force plate measurements to assess changes in body weight with age. This was done as a metric of health in animals as they age, as there are well-established parameters for patterns of healthy weight gain in mice, as identified by Jackson Laboratories. These mice maintained healthy body weights throughout the duration of this experiment (Fig 2-1 E). This data indicates that as mice age from three to twenty four months, they do not experience gross health changes.

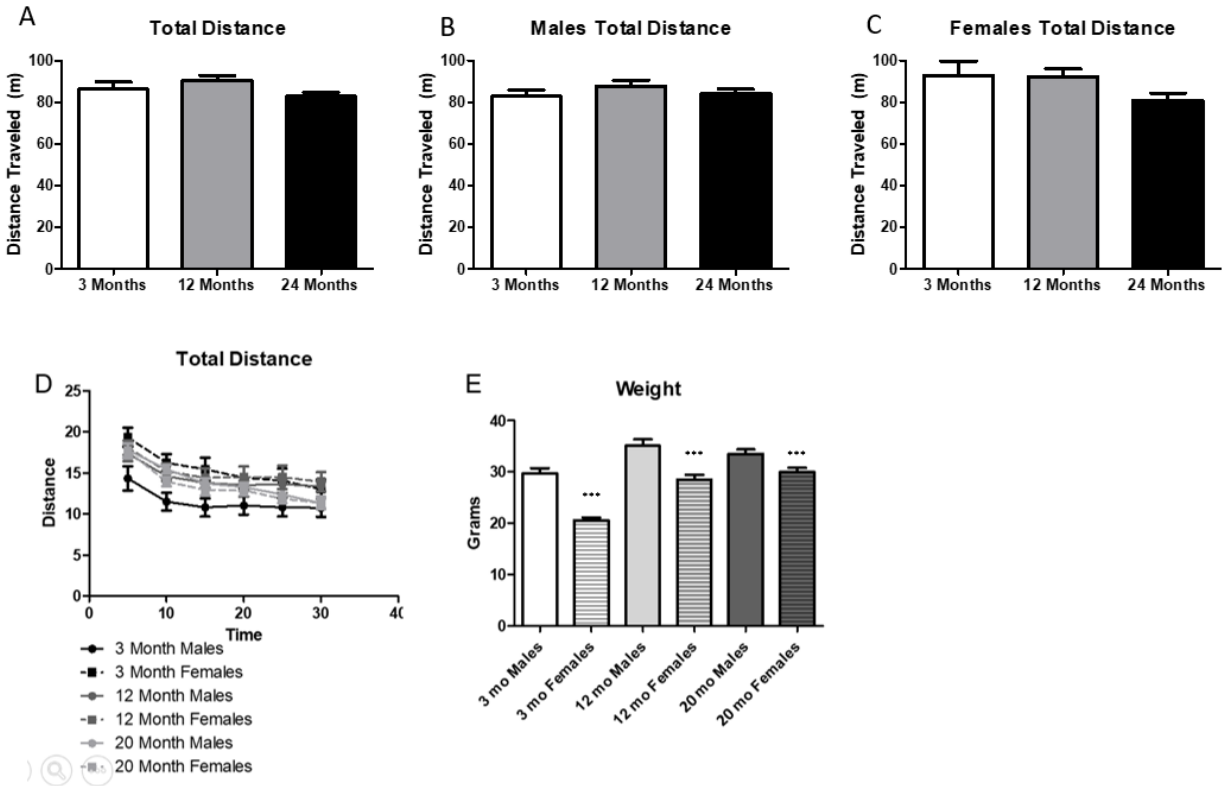

Figure 2-1: Male and female mice maintain similar patterns and levels of general locomotion

Total distance traveled does not change from 3 to 20 months. When analyzed by sex, there is no significant difference in male or females for total distance traveled at any age. When analyzed in five-minute increments, there is no significant change in locomotion patterns based on either sex or age. As animals aged from 3 to 20 months, they maintained healthy body weight conditions.

2.2 Anxiety-like behaviors in aging mice

Anxiety-like behaviors were measured via time spent in the center of a novel open field apparatus. As mice are naturally explorative animals, open field exploration gives a reliable and more physiological assessment of anxiety than other common tests [322]. When assessed with male and female mice combined, there was a significant decrease of time in the center of the arena in both 12- and 24-month-old mice (p=.006) (Fig. 2-2 A/B). Male mice aged 12 and 24 months did not show a significant decrease in time in the center (p=0.83) (Fig. 2-2 C). However, female mice showed significant decreases in time spent in the center at 12 months and 24 months (p=0.001) (Fig. 2-2 D).

To determine whether the different times spent in the center was because of different motion patterns, we assessed time spent in the center in five-minute increments. Linear regression of this data revealed that while the intercepts were significantly different (p=0.005), indicating differences in time, the slopes were not significantly different (p=0.27) (Fig. 2-2 A). This indicates that the overall motion patterns are the same, despite having different total times.

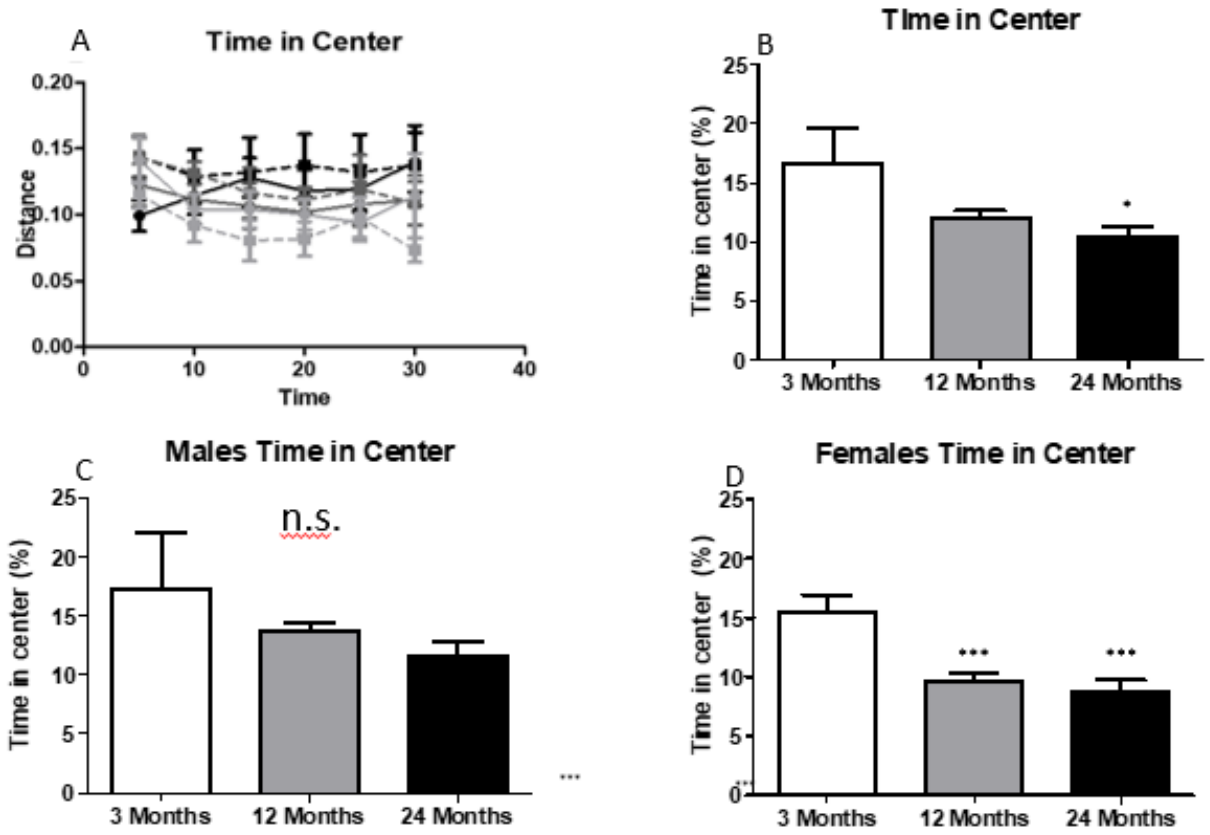

Figure 2-2: Anxiety-like behavior in aging mice

Mice show reduced time spent in the center of the arena. Males, analyzed alone, do not show any decrease in time spent in the center of the arena. Females, analyzed alone, show a significant decrease in time spent in the center of the arena. There is no significant change in exploration patterns in either males or females as they age.

2.3 Daily task performance in aging mice

The nesting paradigm assesses daily task performance based on the quality of a nest built by an individual mouse. Young, 3-month-old mice build nearly perfect nests. By 12 months of age, the nests are less proficiently built ($p=0.001$). From 12 months to 24 months, mice trend towards significantly worse nest building ($p=0.12$) (Fig. 2-2 A). Due to significant sex differences in the open field paradigm, sex differences in nest building were analyzed. There were no significant differences between male and female mice at any age point ($p=0.50$, $p=0.31$, $p=0.20$) (Fig. 2-2 B-D). Untorn nesting material was recorded by weight (Fig. 2-2 D). No 3-month-old mouse failed to completely tear up their nestlet, compared with two 12-month-old mice (6.25%) and seventeen 24-month-old mice (70.83%). The increase in nestlet left untorn was statistically significant ($p < .001$) at 24 months when compared to mice at either 3 or 12 months of age (Fig. 2-2D).

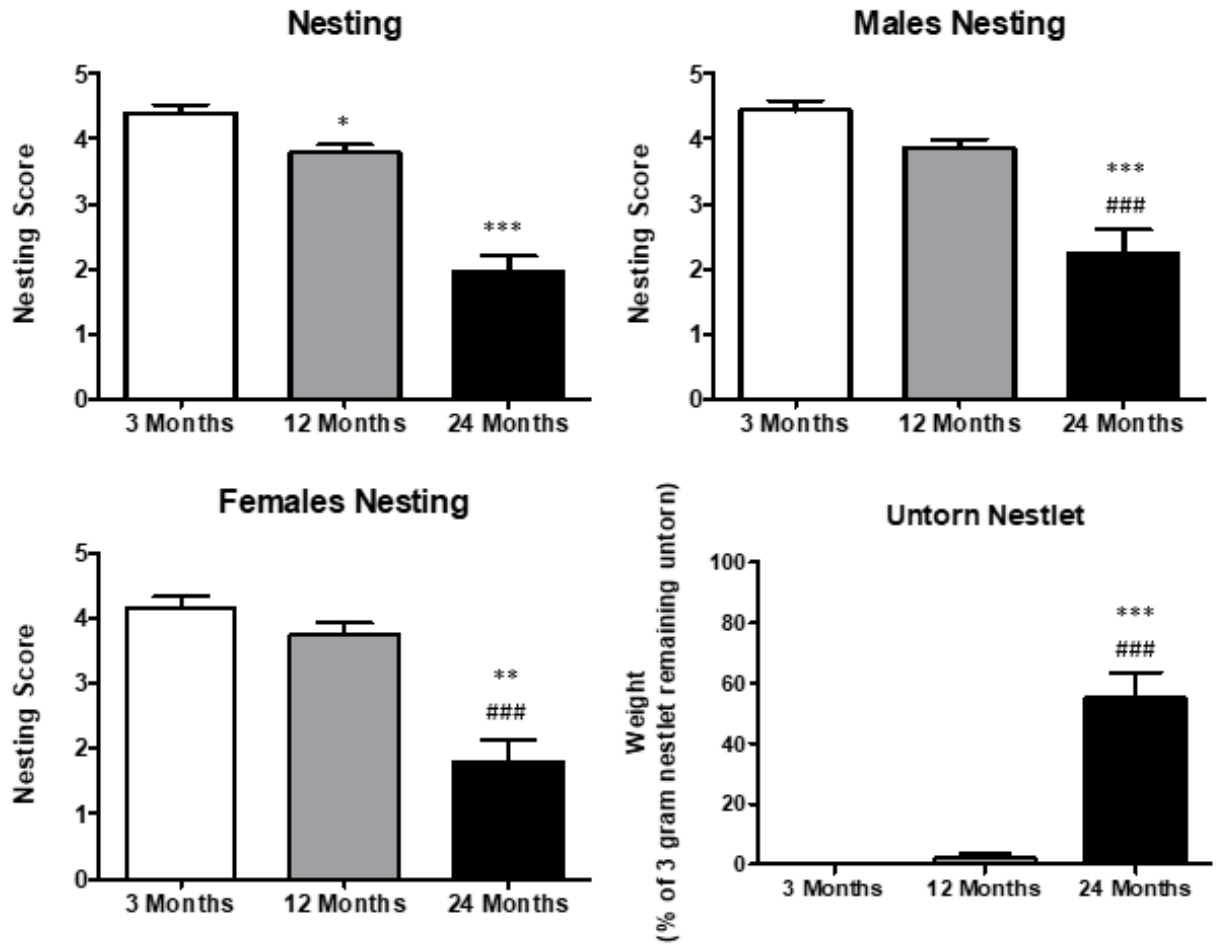

Figure 2-2: Daily task performance in aging mice

Nesting activity decreases with age. Nesting activity is not sex-dependent, and the decrease seen with age is not sex dependent. Untorn nestlet weight increases with age, with a significant increase occurring at 24 months. * $p < 0.05$ vs 3 months, ** $p < 0.01$ vs 3 months, *** $p < 0.001$ vs 3 months ### $p < 0.001$ vs 12 months.

2.5 ROS in Aging Mice

An H_2O_2 assay was utilized to measure ROS in cortical brain tissue from C57/Bl6 mice (Fig. 2-3). When compared to 3-month-old mice, the 12-month and 24-month-old mice have significantly more ROS ($p < 0.05$, $p < 0.01$). From 12 months to 24 months, mice showed a trend towards further increasing of ROS ($p = 0.057$). ROS was not analyzed based on sex differences, but included mixed sex groups with no trend towards differences.

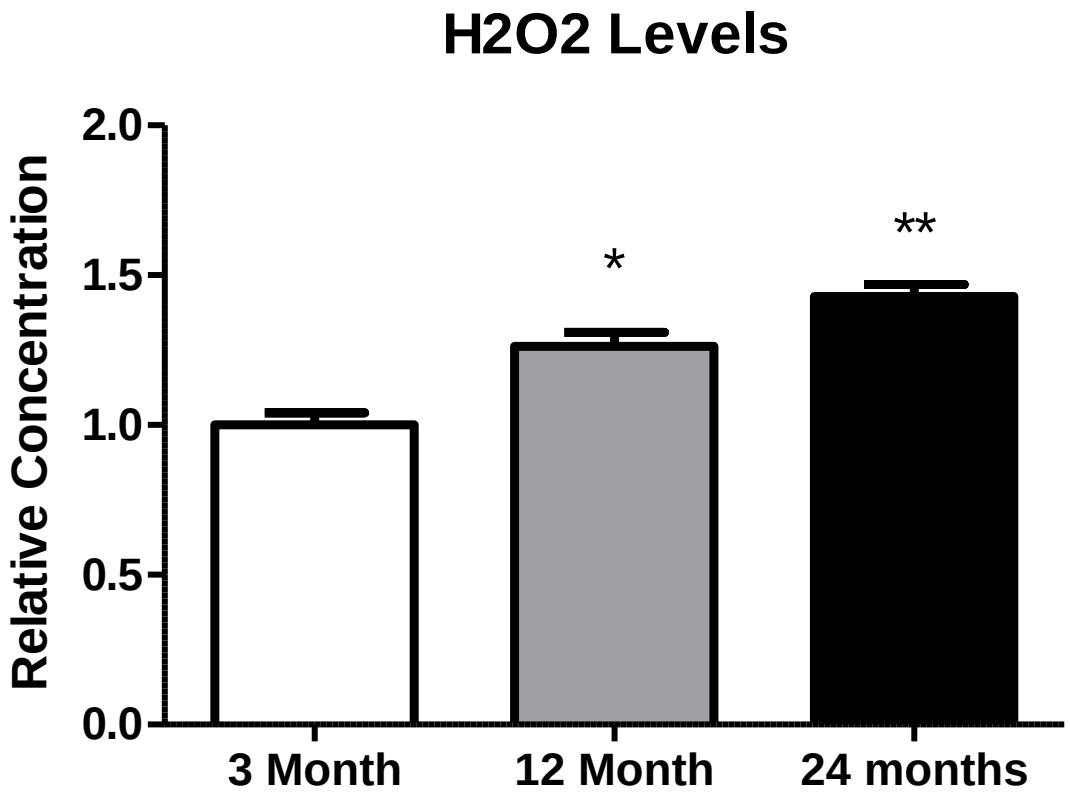

Figure 2-3: Reactive oxygen species in aging mice

Reactive oxygen species increase in aging mice at both 12 and 24 months. * $p < 0.05$ 3 months vs 12 months, ** $p < 0.013$ months vs 24 months.

2.6 Mitochondrial function in Aging mice

The electron transport chain is composed of four complexes, named Complex I-IV, and the ATP synthase complex, sometimes called Complex V. Complex I and IV are measured here due to their importance in this chain. Complex I is the initial step in the ETC and also the largest producer of ROS. Complex IV is the rate limiting step in the ETC.

When compared to 3-month-old mice, 12-month- ($p < 0.001$) and 24-month-old mice ($p < 0.001$) showed significantly lower levels of Complex I activity. 24-month-old mice showed a significant decrease in Complex I activity when compared to 12-month-old mice ($p < 0.01$) (Fig. 2-4 A).

12-month-old mice showed significantly reduced Complex IV activity compared to 3-month-old mice ($p < 0.001$). 24-month-old mice showed significantly reduced Complex IV activity compared to 3-month-old mice ($p < 0.001$) and 12-month-old mice ($p < 0.01$) (Fig. 2-4 B).

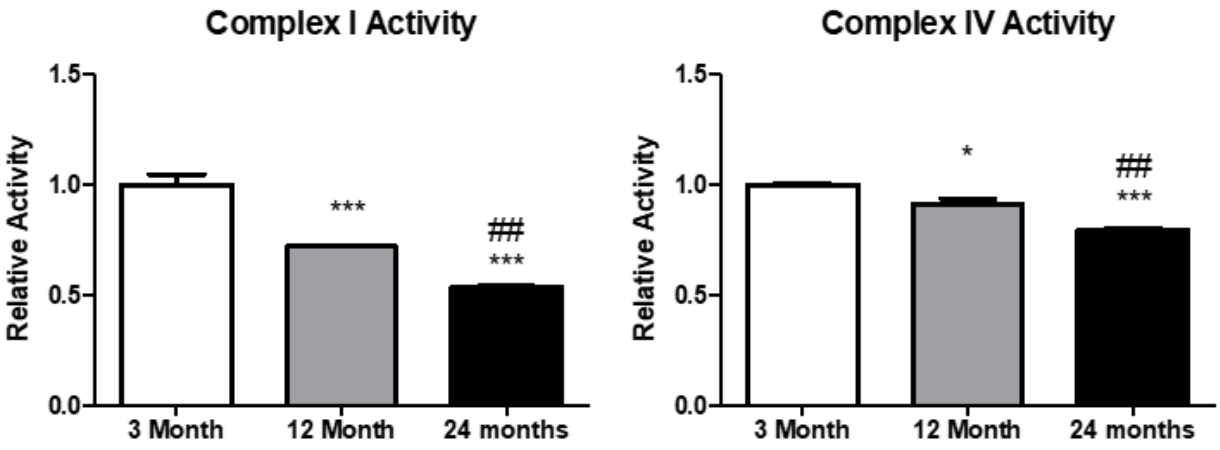

Figure 2-4: Mitochondrial complex activity in aging mice

Mitochondrial function, as measured by electron transport chain activity, decreases steadily with age. By 24 months, complex I activity has decreased by nearly 50%. ** $p < 0.01$ vs 3 months, *** $p < 0.001$ vs 3 months, ## $p < 0.01$ vs 12 months

2.7 CypD expression in aging mice

Our laboratory used antibody-based immunohistochemistry to test expression levels of CypD at 3 and 12 months. While CypD expression was not tested in 24 month, there is a significant increase in CypD levels from 3 to 12 months ($p < 0.01$) (Fig. 2-5).

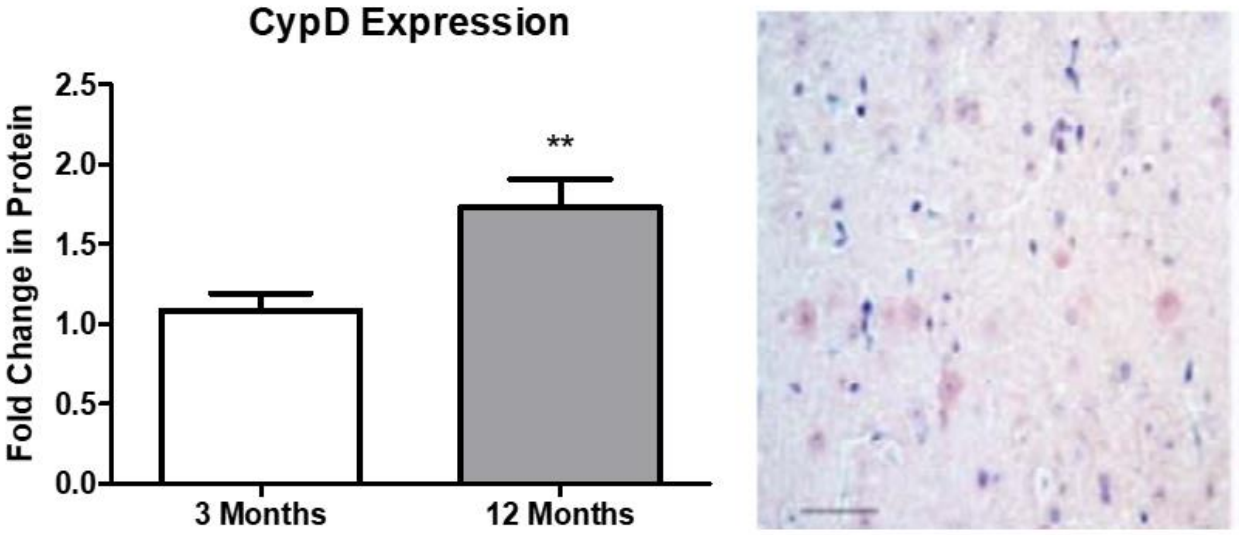

Figure 2-5: CypD Expression in Aging Mice

Data is normalized to 3 Month and represents the results of three separate experiments[23].

2.8 Gross motor function and weight

Due to the increased expression of CypD identified in aging mice, we looked at genetically modified CypD mice: CypD OE and CypD KO. To parallel experiments done in the wild type mice in sections 2.1-2.3, mice were studied at 3-months, 12 months, and 24 months and observed on several behavioral parameters. However, CypD OE mice were only studied at 3 months and 12 months because these mice have an average life expectancy of less than 15 months.

Previous studies have identified that wild type mice do not show changes in gross motor function from 3 months to 24 months [325]. Modification of CypD through overexpression or knock out does not cause changes in gross motor function (Fig. 1 A-C), indicating that these mice are healthy and capable of performing behavioral tests.

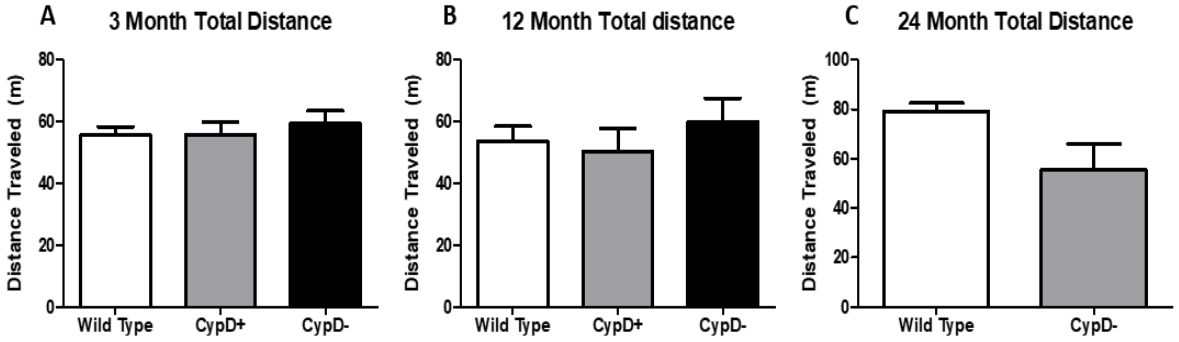

Figure 2-6: Gross locomotion in CypD modified mice

Gross locomotion is not affected by CypD overexpression or knockout at any age. n = 6-15

2.9 Anxiety like behavior

At 3 months, CypD modification does not induce an anxiety-like phenotype (Figure 2-7 A). By 12 months, CypD overexpression mice show significant depression of time spent in the center ($p < 0.01$), indicating a significant anxiety-like phenotype. CypD knock out mice, however, do not show a decrease of time in the center compared to wild type mice (Figure 2.7 B). At 24 months, wild type mice show a significant increase in anxiety-like behavior [325], which is recapitulated here. CypD knock out mice show no such decrease (Figure 2.7 C).

Surprisingly, 24-month CypD knock out mice do not show the age-induced depression in time in center ($p = 0.119$ 3-month wild type vs 24-month CypD knock out). These results indicate that while CypD expression influences anxiety like behavior, with overexpression resulting in anxiety-like behavior earlier and CypD knock out preventing the age-dependent phenotype.

CypD OE and CypD KO mice do not show sex dependent effects at any age point, in contrast to wild type mice which show the same variation presented in earlier figures.

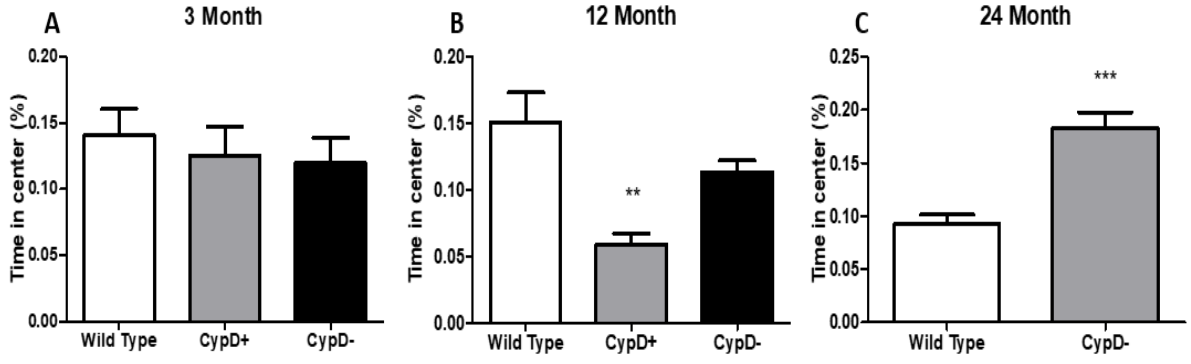

Figure 2-7: Anxiety like behavior in CypD Modified mice

At 3 months, there anxiety-like behavior is not affected by CypD expression status. At 12 months, CypD KO mice show significant reductions of time in the center, while CypD KO mice remain unchanged. At 24 months, CypD KO mice do not show anxiety like behavior while wild type mice do. ** $p < 0.01$ vs wild type, *** $p < 0.001$ vs wild type.

2.10 Daily Task Performance

Daily task performance is an assay of memory that combines both long term memory and working memory [324]. Nest building in mice is a natural behavior done for thermoregulation that the mice learn as pups [326]. Previous studies have identified that mice fail in this assay of daily task performance as they age [325]. At 3 months, mice build nests that score between a 4 and 5 regardless of genotype (Fig. 2.9 A), indicating proficiency at nest building; CypD overexpressing mice built nests that were statistically ($p < 0.05$) better than their wild type counterparts, a nesting score of 4-5 is considered healthy and normal [323, 324]. 12-month old CypD overexpressing mice display significantly diminished nesting activity ($p < 0.01$) compared to wild type mice (Fig. 2.9 B). CypD knockout mice, however, maintain their high level of proficiency in task performance. 24-month wild type mice show impaired nest building activity, in line with previously published work [325]. At this time point, CypD knock out mice do not display the same loss of function ($p < 0.001$) and still build excellent nests (Fig. 2.9 C). These data indicate that CypD overexpression exacerbates age-induced daily task performance failure, while CypD knock out ameliorates them.

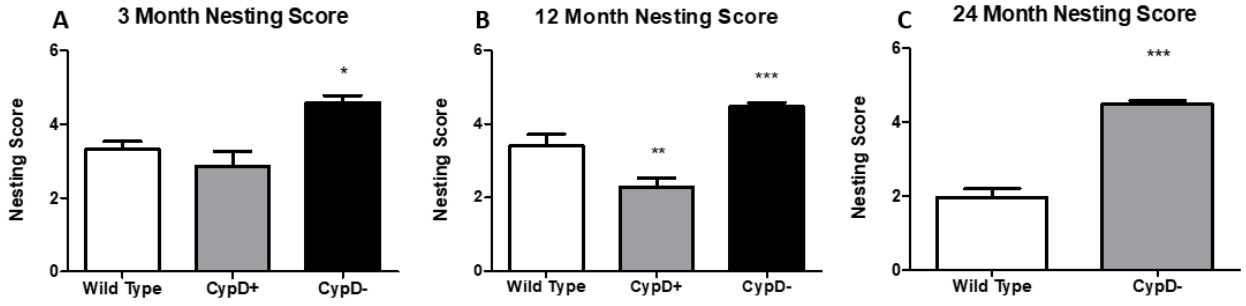

Figure 2-8: Daily task performance in CypD modified mice

CypD KO improves nesting scores at all age points. At 12 months, CypD OE causes significant depression in nesting activity. * $p < 0.05$ wild type vs CypD-, ** $p < 0.01$ wild type vs CypD+, *** $p < 0.001$ wild type vs CypD+

2.11 ROS in CypD KO Aging mice

ROS were measured in 20-month-old CypD KO mice and 20-month-old wild type mice in both the cortex and hippocampus [23]. Brain tissue was stained using MitoSox, which targets the mitochondria and fluoresces upon interaction with superoxide, allowing the measurement of ROS specifically produced by the mitochondria.

CypD KO mice showed significantly reduced MitoSox staining, indicating a significant reduction of ROS (Figure 2.10).

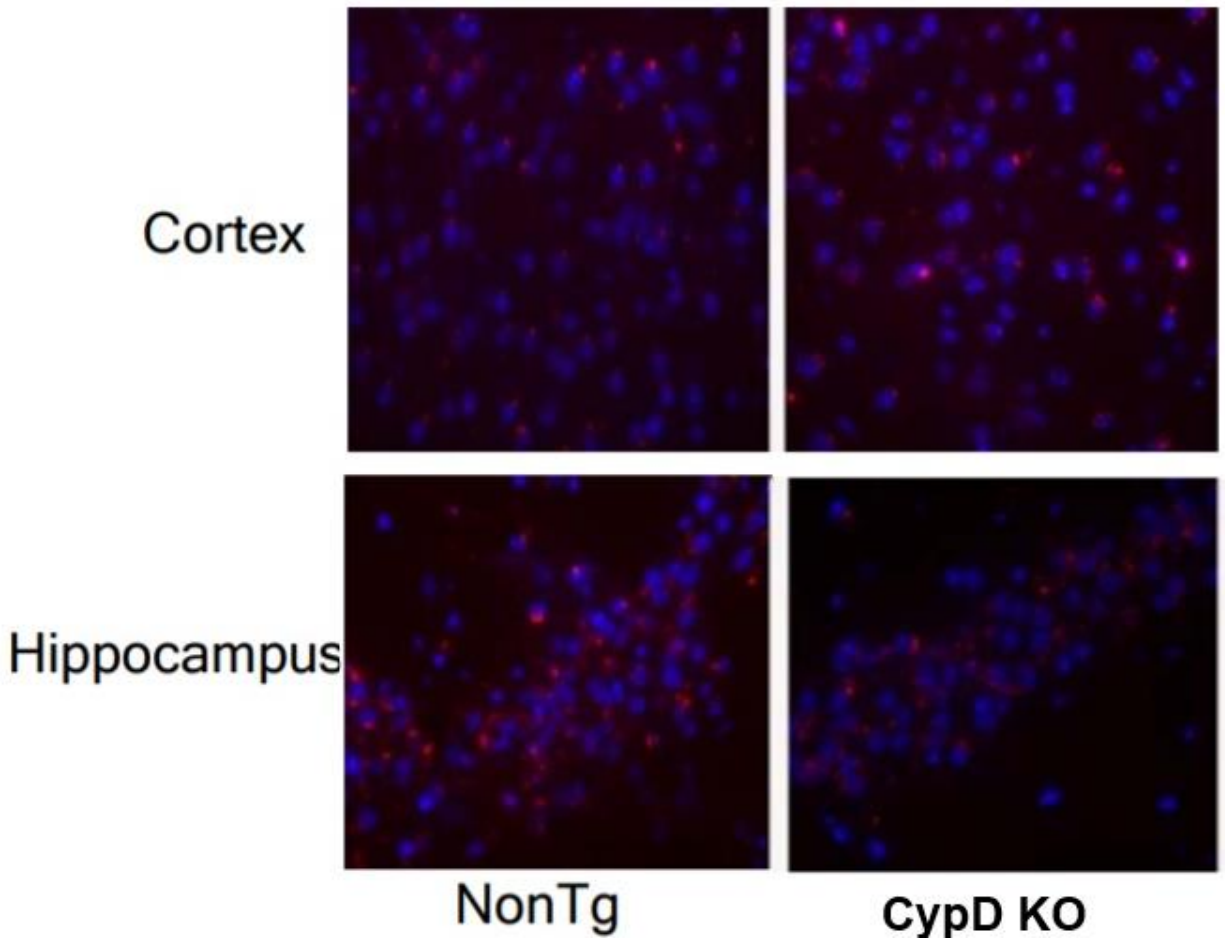

Figure 2-9: CypD KO mice show less ROS in cortex and hippocampus

Mitosox staining revealed reduced mitochondrial-produced ROS in CypD KO mice in 24 month mice.

2.12 Mitochondrial activity in aging CypD KO mice

Mitochondrial membrane polarization was measured via TMRM staining, which is isolated in highly polarized membrane compartments. If the mPTP opens and the mitochondrial membrane polarity gradient is lost, TMRM staining is decreased.

Mitochondrial swelling is measured via optical density. When the mPTP opens, mitochondria swell. This is usually initiated via a calcium bath of cells or tissue, which induce mPTP opening.

Calcium buffering capacity is measured with a calcium sensitive probe. As calcium is added, mitochondria sequester the calcium in the matrix. However, mitochondria do not have limitless buffering capacity, and the mPTP will open at some point in the experiment, resulting in a lack of uptake of the next calcium input.

Wild type and CypD KO mice were used to measured mitochondrial membrane polarization with addition of H_2O_2. H_2O_2 causes damage to mitochondria which can be seen in the decrease in TMRM staining. Brain tissue from wild type mice showed significant decreases in mitochondrial membrane polarization with increasing doses of H_2O_2. CypD KO mice did not show a significant decrease in mitochondrial membrane polarization (Figure 2.11 A). This can be interpreted as CypD KO mice being more resistant to ROS-insult.

Mitochondrial swelling was reliably induced by Ca^{2+} in wild type mice (Figure 2.11 B). However, calcium did not induce mitochondrial swelling in CypD KO mice. CypD KO mice with calcium addition did not significantly differ from CypD KO mice with vehicle addition or wild type mice with vehicle addition.

Calcium buffering capacity was tested in wild type mice and CypD KO mice. CsA was used in wild type mice to serve as positive control for CypD inhibition (Figure 2.11 C). In both

the CsA treated wild type mice and the CypD KO mice, calcium buffering capacity was significantly increased when compared to wild type mice.

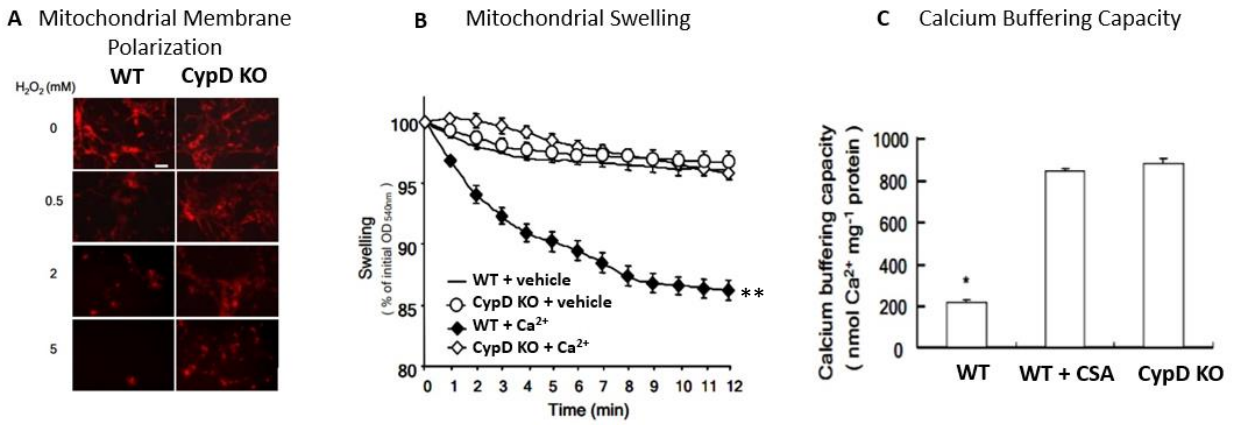

Figure 2-10: Mitochondrial function in CypD modified mice

A. Hydrogen peroxide induced membrane depolarization is increased by CypD KO. B. Mitochondrial swelling induced by calcium is reduced. WT + vehicle vs Wt + Ca^{2+} $p < 0.01$, WT + vehicle vs CypD KO + Ca^{2+} n.s. C. Calcium buffering capacity is increased by CypD KO. * $p < 0.05$ WT vs CypD KO

Chapter 2 Interim conclusion

As mice age from 3 to 24 months, significant cognitive declines were identified. Anxiety-like behaviors were evident in 12- and 24-month female mice that had not been previously identified (Figure 2.2). Additionally, failures in memory and daily task performance were identified in a nesting assay (Figure 2.3), were identified in a nesting assay. We hypothesize that these cognitive failures are the result of mitochondrial failure, both in complex I and IV activity (Figure 2.5) and in increased ROS production (Figure 2.4).

We hypothesized that inhibition of CypD could prevent these cognitive impairments. We used CypD OE and KO mice to assess the role of CypD in aging-induced cognitive impairments.

CypD OE induced cognitive impairments at an earlier age than in wild type mice. CypD OE also showed more pronounced anxiety-like behavior at six months (Figure 2.7) and impaired nesting behavior at 12 months (Figure 2.8). CypD OE mice prematurely died at around 15 months while wild type and CypD KO mice lived beyond 24 months with their general physical health intact (Figure 2.6).

CypD KO mice did not show impaired cognitive function, even at 24 months (Figure 2.7-2.8) when wild type mice were showing anxiety-like behavior and decreased memory and daily task performance, confirming a role for CypD in cognitive impairment.

CypD OE mice were not studied in molecular tests due to the results of the behavioral experiments; because there was a clear degenerative phenotype, we chose to focus on the genetic modifications that represented a potential therapeutic intervention. CypD KO prevented mitochondrial dysfunction as assessed by ROS production (Figure 2.10), membrane potential maintenance (Figure 2.11 A), and calcium buffering capacity (Figure 2.11 B-C).

Taken together, these studies support the hypothesis that elevated CypD expression modulated mitochondrial function which results in cognitive impairments through the course of natural aging.

Chapter 3 : The Role of CypD in Alzheimer's disease Mice

In order to study the role of CypD in a tau model of Alzheimer's disease, several animal lines were developed. First, CypD OE were crossed with the P301S tau mice to create a line of double transgenic CypD OE/Tau+ mice. Cypd OE/Tau+ mice were intended to simulate the elevated levels of CypD seen in AD and to assess the role of CypD in tau-induced AD.

To assess the potential therapeutic role of reducing CypD activity, CypD KO mice were crossed with the P301S mice to generate a line of CypD KO/Tau- mice.

Six genotypes of mice were used for these experiments and are summarized in Table 6.

Table 7: Mouse lines used in Chapter 3

Genotype	Mouse Line	Origin
Wild type	C57/Bl6	Bred internally
Tau+	P301S Tau OE	[281]
CypD OE	CP11	Created internally
CypD KO	BE	[327]
CypD OE/Tau+	Crossed CypD OE / P301S Tau OE	Created internally
CypD KO/Tau+	Crossed CypD KO / P301S Tau OE	Created internally

Experiments for this chapter were divided into two sub-sections based on the type of CypD manipulation:

1. Wild Type, Tau+, CypD OE, and CypD OE/Tau+
2. Wild Type, Tau+, CypD KO, and CypD KO/Tau+

Unique wild type and Tau+ mice were used for the two sub-sections of experiments.

CypD and HPT levels were assessed via western blot. In line with the hypothesis laid out in Schematic 1, mitochondrial failure was assessed with by assaying ETC complex activity. Synaptic and neuronal loss were measured by western blots of synaptophysin and neuronal tubulin. Cognitive levels were measured with two behavioral tests. The open field test was employed to

measure anxiety-like behavior and nesting was used to measure learning and memory in a daily task performance test.

The experiments in this chapter test the two sub-hypothesis presented in Schematic 3. Namely, that overexpression of tau, resulting in higher levels of phosphorylated tau will lead to CypD opening the mPTP. The open mPTP will induce mitochondrial failure and the resulting energy losses will cause synaptic loss. Finally, the summation of these molecular events will be cognitive impairment. Conversely, knock out of CypD will prevent mitochondrial dysfunction and the synaptic loss and cognitive impairment that hypometabolism causes.

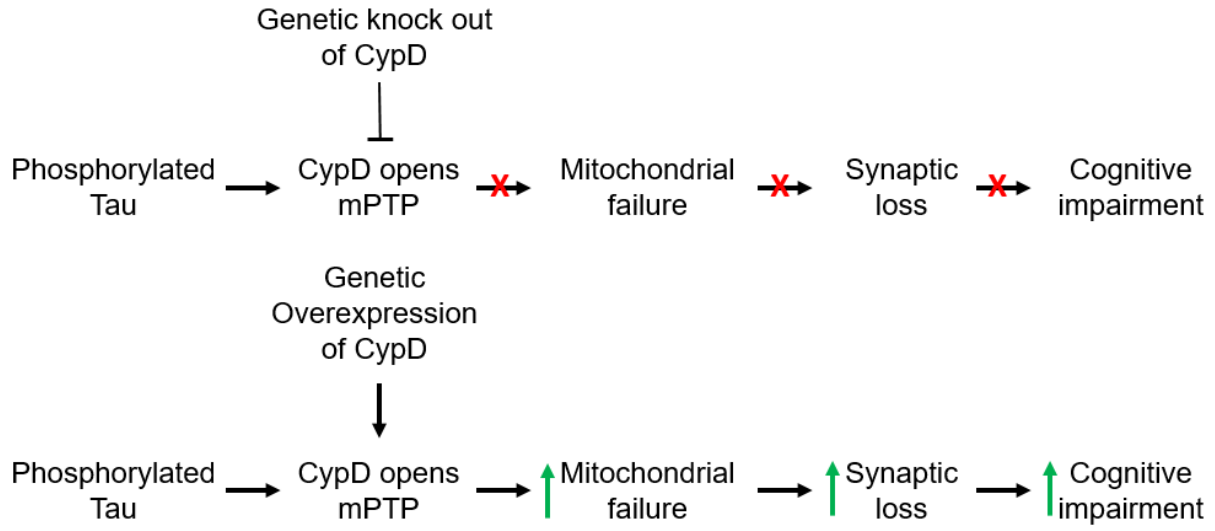

Schematic 3: Sub-hypothesis for chapter 3

3.1 CypD expression in tau-models of Alzheimer's disease with CypD overexpression

CypD OE mice have shortened lifespans (~15 months), as noted in Chapter 2, and this was heightened in CypD OE/Tau+ mice, which survived regularly to 10-12 months. At the 12-month time point, survivor bias made them unsuitable for inclusion in these experiments.

Western blots at 3 months were performed with 15 µG of protein. At 3 months, there is already significantly heightened expression of CypD in the CypD OE/Tau+ mice compared to the CypD OE mice alone ($p < 0.001$). While there was CypD detectible in wild type mice and Tau+ mice, it was far eclipsed by the genetically modified CypD OE models at 3 months (Fig. 3.1A).

Western blots at 6 months were performed with 5 µG of proteins. The amount of protein used for these experiments was determined experimentally for each age group; less protein was used in older mice due to the accumulation of tau that made discerning differences in expression impossible. At 6 months, there was a ceiling effect in which CypD OE and CypD OE/Tau+ mice showed similar levels of CypD expression, although both were significantly elevated when compared to wild type mice ($p < 0.01$). At 6 months, Tau+ mice showed significant increases in expression of CypD when compared to wild type mice ($p < 0.05$). (Fig. 3.1B).

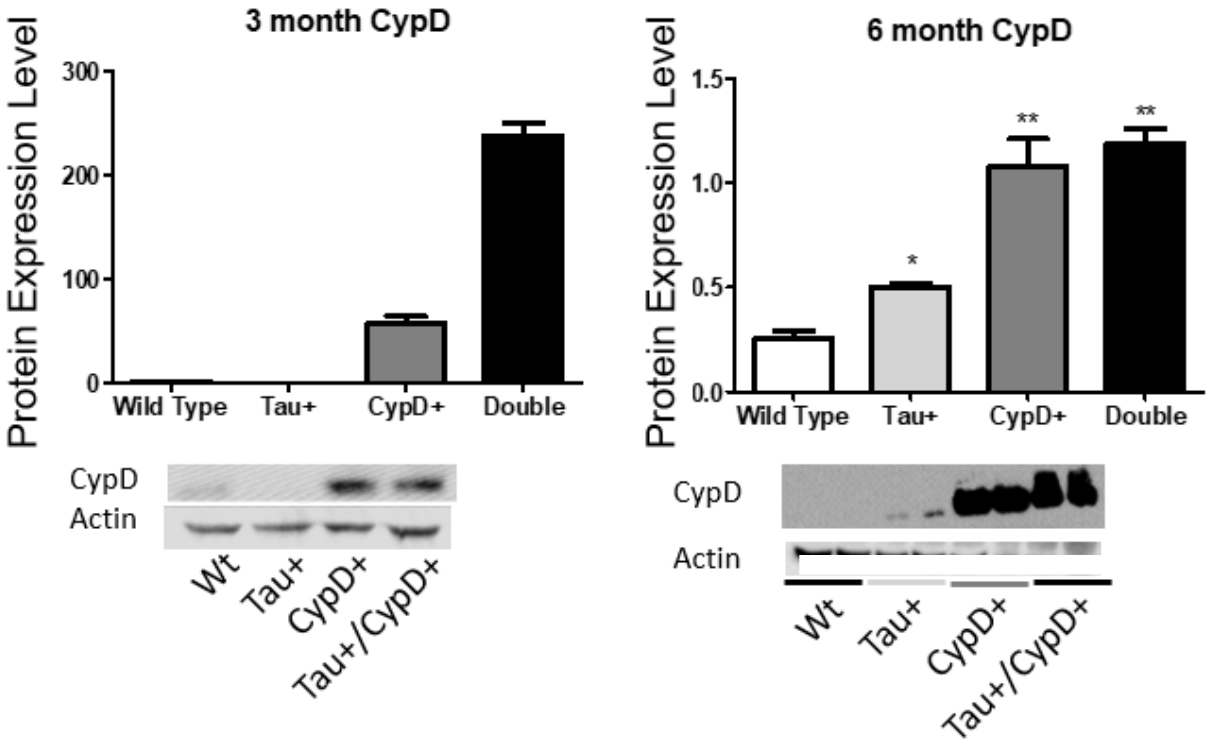

Figure 3-1: Validating CypD Expression in CypD OE/Tau+ mice

*Data is presented as CypD expression normalized to actin expression in relative units. CypD OE mice have higher levels of CypD expression than Wild type or Tau+ mice at 3 and 6 months. *** P < 0.001 vs wild type, ## p < 0.001 CypD+ vs CypD+/Tau+.*

3.2 Hyperphosphorylated tau models of Alzheimer's disease with CypD overexpression

HPT was measured to assess changes in HPT accumulation based on CypD expression. At three months, 15 µG of protein was used, while at six months only 5 µG of protein was used; this change was done based on experiments optimizing the best protein amount for respective ages. With too much protein, particularly in these HPT westerns, there was a higher risk for overexposure from non-specific protein bands that appeared to overlap with tau.

At three months, Tau+ mice showed elevated levels of HPT compared to wild type mice ($p < 0.01$). CypD OE/Tau+ mice showed elevated HPT levels when compared to wild type mice ($p < 0.001$) and when compared to Tau+ mice ($p < 0.01$) Fig. 3.2A

.

At six months of age, Tau+ mice maintained their high levels of HPT compared to wild type mice ($p < 0.01$). CypD OE/Tau+ mice showed an even greater increase in HPT that was significantly different from wild type mice ($p < 0.001$) and from Tau+ mice ($p < 0.05$). Fig. 3.2B

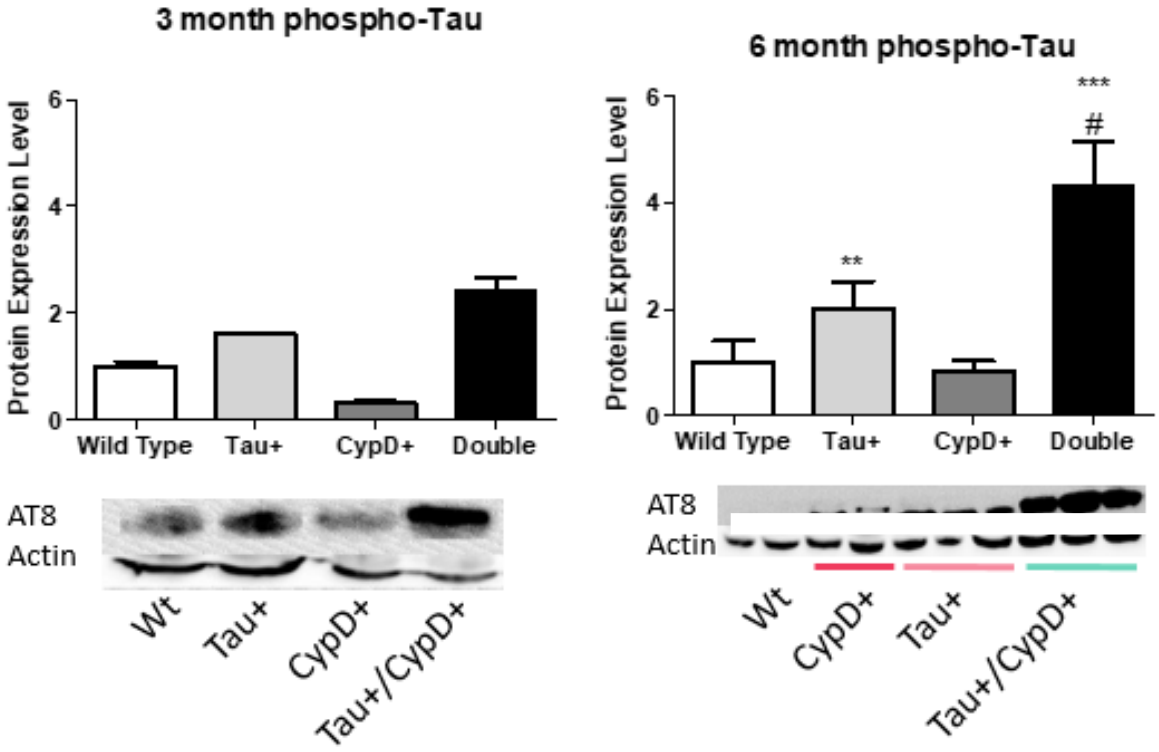

Figure 3-2: Validation of Phosphorylated tau in CypD OE/Tau+ mice

Data is presented as phosphorylated tau normalized to actin and then normalized to wild type levels. Phosphorylated tau is increased in Tau+ and CypD OE/Tau+ mice at 3 and 6 months. n = 4-7 * $p < 0.05$ Wild type vs Tau+, ** $p < 0.01$ wild type vs. Tau+, *** $p < 0.001$ wild type vs CypD+/Tau+, ## $p < 0.01$ Tau+ vs CypD+/Tau+, # $p < 0.05$ Tau+ vs CypD+/Tau+

3.3 Synaptic loss in a tau-induced model of Alzheimer's disease with CypD overexpression

Synaptophysin was analyzed to assess synaptic loss. As with the previous experiments, two conditions were used for the respective age points. 15 µG of protein was used for three month mice and 5 µG of protein was used for six month mice.

At three months, there are no significant changes in synaptic loss despite the significant HPT accumulations identified in Figure 3.2. This may indicate that the three month time point represents an intermediate stage between pathologically accumulated protein and irreversible neuronal damage. Fig. 3.3A

At six months, there is a significant decrease in synaptophysin staining for Tau+ mice ($p < 0.05$) and a decrease in the CypD OE/Tau+ mice. There was a non-significant trend towards CypD OE/Tau+ mice having less synaptophysin expression when compared to Tau+ mice. While a later time point may have helped to clarify this, the early mortality of the CypD OE/Tau+ mice made further study infeasible. Fig. 3.3B

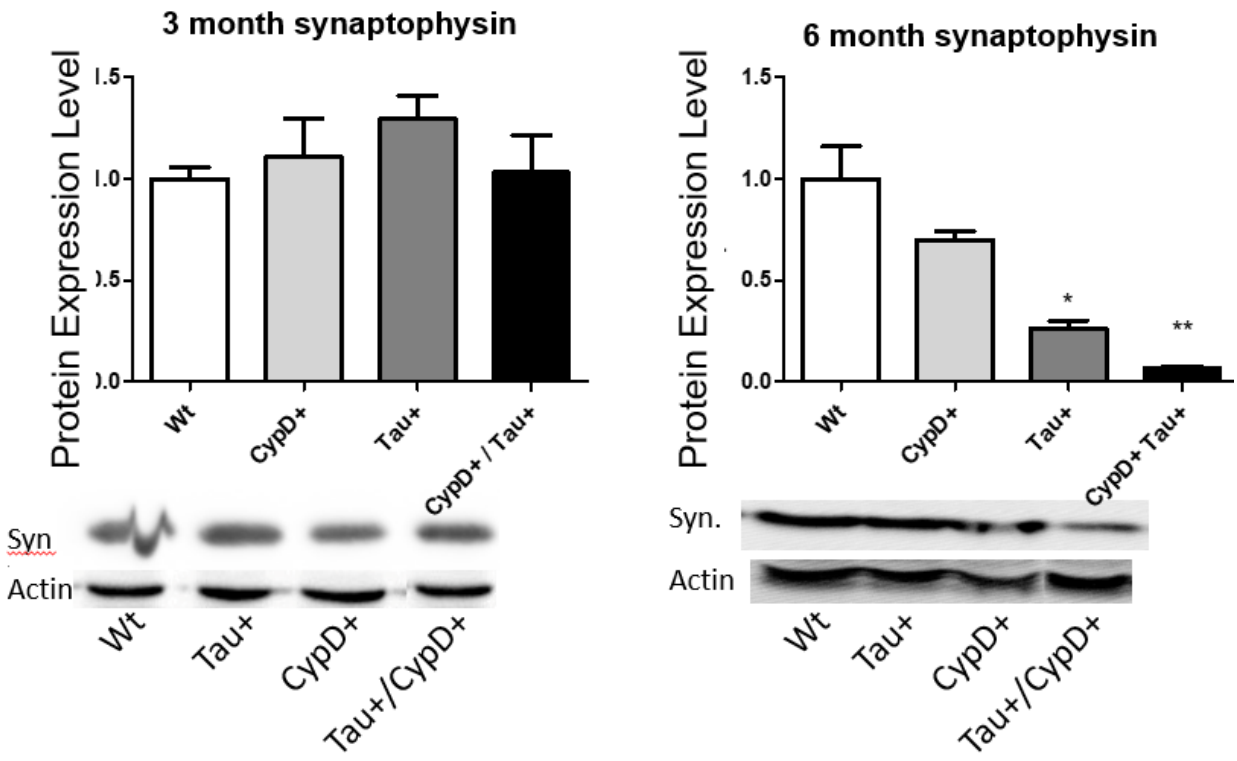

Figure 3-3: Synaptophysin in CypD modified AD mice

At 6 months, synaptophysin is reduced in Tau+ and CypD+/Tau+ mice compared to wild type mice. n = 4 * $p < 0.05$ wild type vs Tau+, ** $p < 0.01$ wild type vs CypD+/Tau+

3.4 Neuronal loss in tau-induced models of Alzheimer's disease with CypD overexpression

Neuronal loss was assessed with western blots for neuronal β-tubulin. As with previous studies, 15 µG of protein was used for the three month time point while 5 µG of protein were used for the six month time point.

Similar to the synaptophysin experiments, at three months there was no significant loss of tubulin expression in the Tau+ or CypD OE/Tau+. Surprisingly, there was a significant increase in tubulin expression in the Tau+ mice ($p < 0.05$). Fig. 3.4A

At 6 months, paralleling synaptic loss, Tau+ mice showed significant decreases in expression of neuronal tubulin ($p < 0.05$) which was also seen in CypD OE/Tau+ mice. Due to floor effects, there was no significant difference in neuronal loss between Tau+ and CypD OE/Tau+ mice. Fig. 3.4B

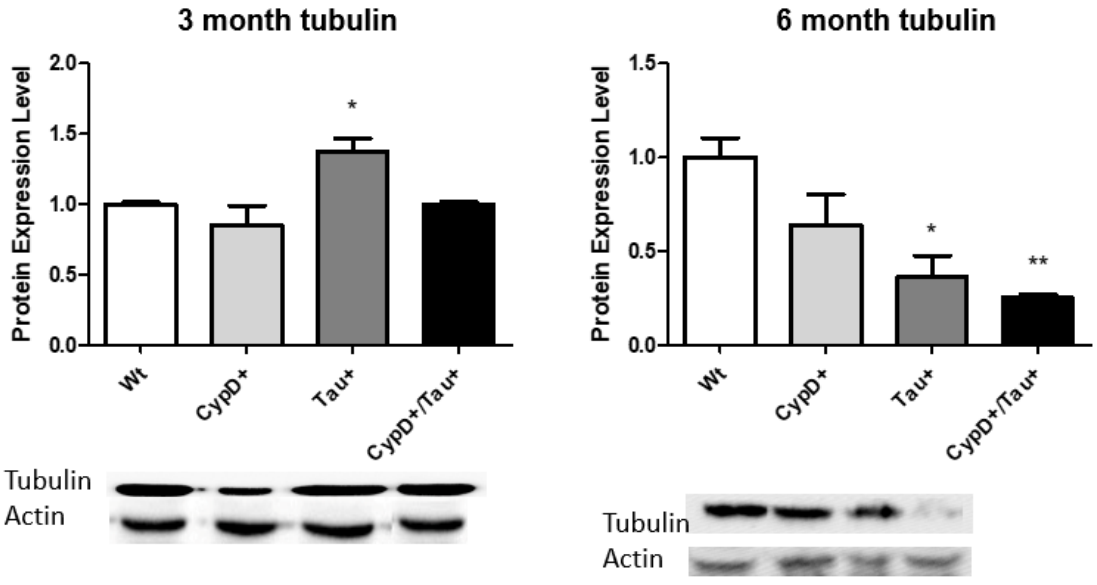

Figure 3-4: Tublin in CypD Modified AD Mice

Tubulin expression is decreased in Tau+ mice and CypD OE/Tau+ mice at six months.

3.5 Mitochondrial electron transport chain activity in tau-induced models of Alzheimer's disease with CypD overexpression

Mitochondrial activity was assessed by assays of complex IV activity. Complex IV was selected because it is the rate limiting step of the ETC. Mice were studied at the 12-month end point for this experiment, and data is presented with the caveat that survivor bias is affecting the outcomes; interpretation of the data should be done with that in mind. While differences in protein accumulation made it necessary to use different amounts of protein for western blotting, no such concern was found in mitochondria studies.

Wild type mice, showed decreases in Complex IV function by 12 months. This same pattern of decrease at both 6 and 12 months was paralleled in Tau+ mice and CypD OE/Tau+ mice. Unexpectedly, CypD OE mice showed preserved mitochondrial function at six months before a sharp decline at 12 months.

That all mice experienced age-related decline in mitochondrial function made comparisons between genotypes somewhat more difficult from a statistical point of view. Fig. 3.5A/B.

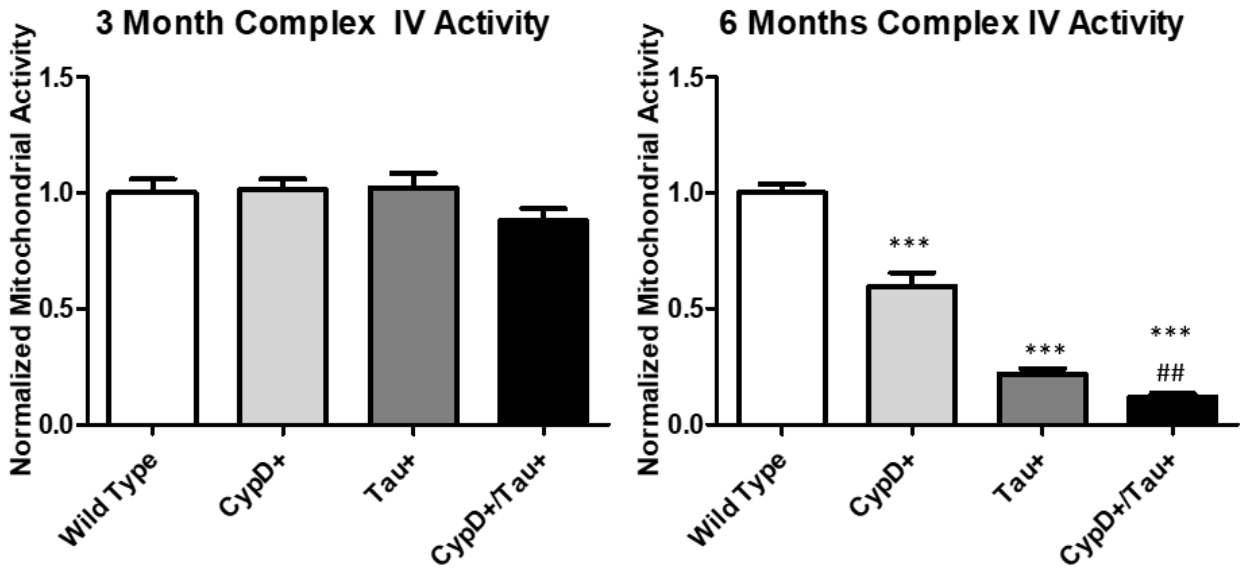

Figure 3-5: Mitochondrial Complex Activity by Genotype in CypD Modified mice

At three months, complex IV activity was unaffected by CypD or Tau expression status. At six months, CypD+, Tau+, and CypD+/Tau+ mice show significantly reduced complex IV activity.

3.7 Gross locomotion in a tau-induced model of Alzheimer's disease with CypD overexpression

Gross locomotion was used to determine the general health and mobility of the animals. Animals were assessed at 12 months and that data is presented here with the caveat that it is biased by survivorship. CypD OE/Tau+ mice that survived to 12 months were relatively healthy, but were the minority of their cohorts, with a majority of mice dying or being humanely euthanized due to complications with tau-induced paralysis prior to the 12 month time point.

There was no significant change in general locomotion in any genotype. The lack of change indicates that further behavioral testing is acceptable and allows for interpretation of this data without concern for mobility.

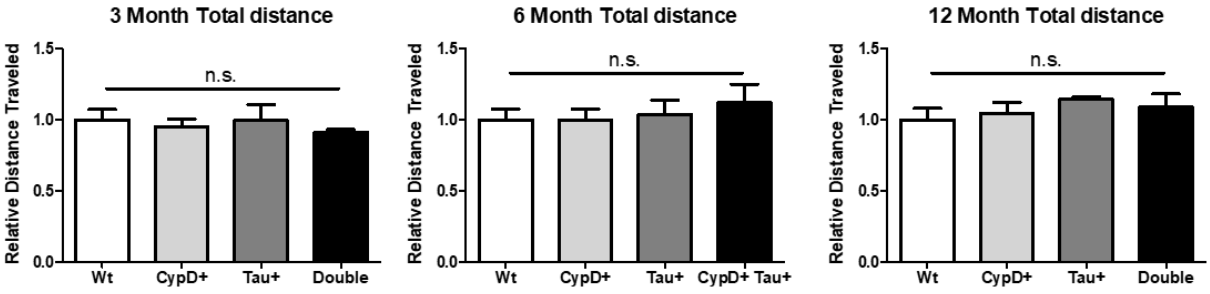

Figure 3-6: General locomotion in CypD Modified AD Mice

General locomotion was not affected by any genotype at any age point.

3.8 Anxiety-like behavior in a tau-induced model of Alzheimer's disease with CypD overexpression

Anxiety-like behavior was assessed in these mice to measure cognitive impairments. At three months, Tau+ mice already display significant anxiety-like behaviors when compared to wild type mice ($p < 0.05$), with CypD OE/Tau+ mice also showing anxiety-like behaviors ($p < 0.01$). Fig. 3.7A

At six months, CypD OE mice ($p < 0.05$) and Tau+ mice ($p < 0.01$) show anxiety-like behavior which is exacerbated in the CypD OE/Tau+ mice ($p < 0.001$). CypD OE/Tau+ mice showed significantly more anxiety-like effects than the Tau+ mice ($p <0.05$). Fig. 3.7B

At 12 months, the data showed significant floor effects with Tau+ mice exhibiting extreme anxiety-like behaviors ($p < 0.001$). CypD OE/Tau+ mice spent nearly no time in the center of the arena. Due to the severely depressed time spent in the center, there was no significant difference between Tau+ and CypD OE/Tau+ mice, although there was a non-significant trend. The non-significant trend, paired with the knowledge that the 12-month mice used here represent the healthiest and least impaired mice of the cohort, shows that CypD OE/Tau+ are likely more impaired than the Tau+ mice. Fig. 3.7C

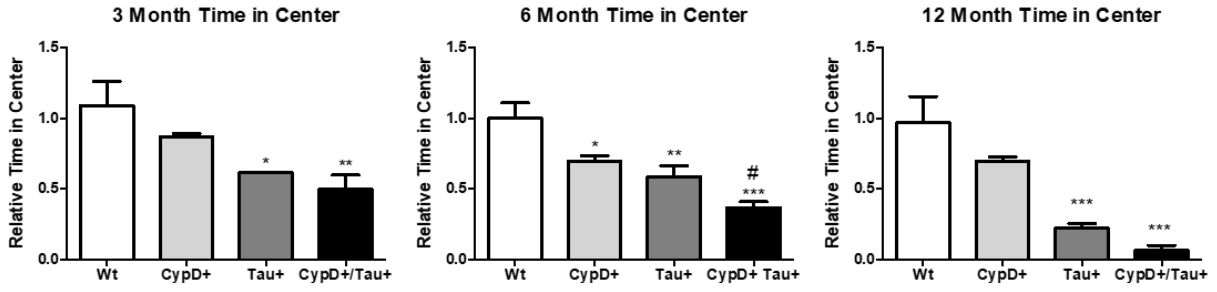

Figure 3-7: Anxiety-like Behavior in CypD Modified AD Mice

At three months, Tau+ and CypD+/Tau+ mice showed significantly decreased time in the center of the arena. At six months, CypD+, Tau+, and CypD+ all show decreased time in the center, with CypD+/Tau+ mice being significantly less than the Tau+ mice. By twelve months, there is significant reduction in time in the center in the Tau+ and CypD+/Tau+ mice. n = 8-10 * $p < 0.05$ vs wild type, ** $p < 0.01$ vs wild type, *** $p < 0.005$ vs wild type, # $p < 0.05$ Tau+ vs CypD+/Tau+

3.9 Daily task performance in a tau-induced model of Alzheimer's disease with CypD overexpression

A nesting assay was used to measure daily task performance and memory. Nesting was done after open field to determine that the mice had normal mobility. Additionally, evidence has shown that changing housing and nesting materials can affect anxiety-like behaviors [328, 329], although not all behaviors are affected. Performing the nesting experiments after open field removed any possibility that the measurement of anxiety-like behaviors may be compromised.

At three months, Tau+ and CypD OE/Tau+ mice show significant impairment in ability to build a nest ($p < 0.05$). These significant differences were preserved into the 6-month time point ($p < 0.05$). CypD OE mice did not show any significant cognitive impairment in this assay. Fig. 3.8A-C

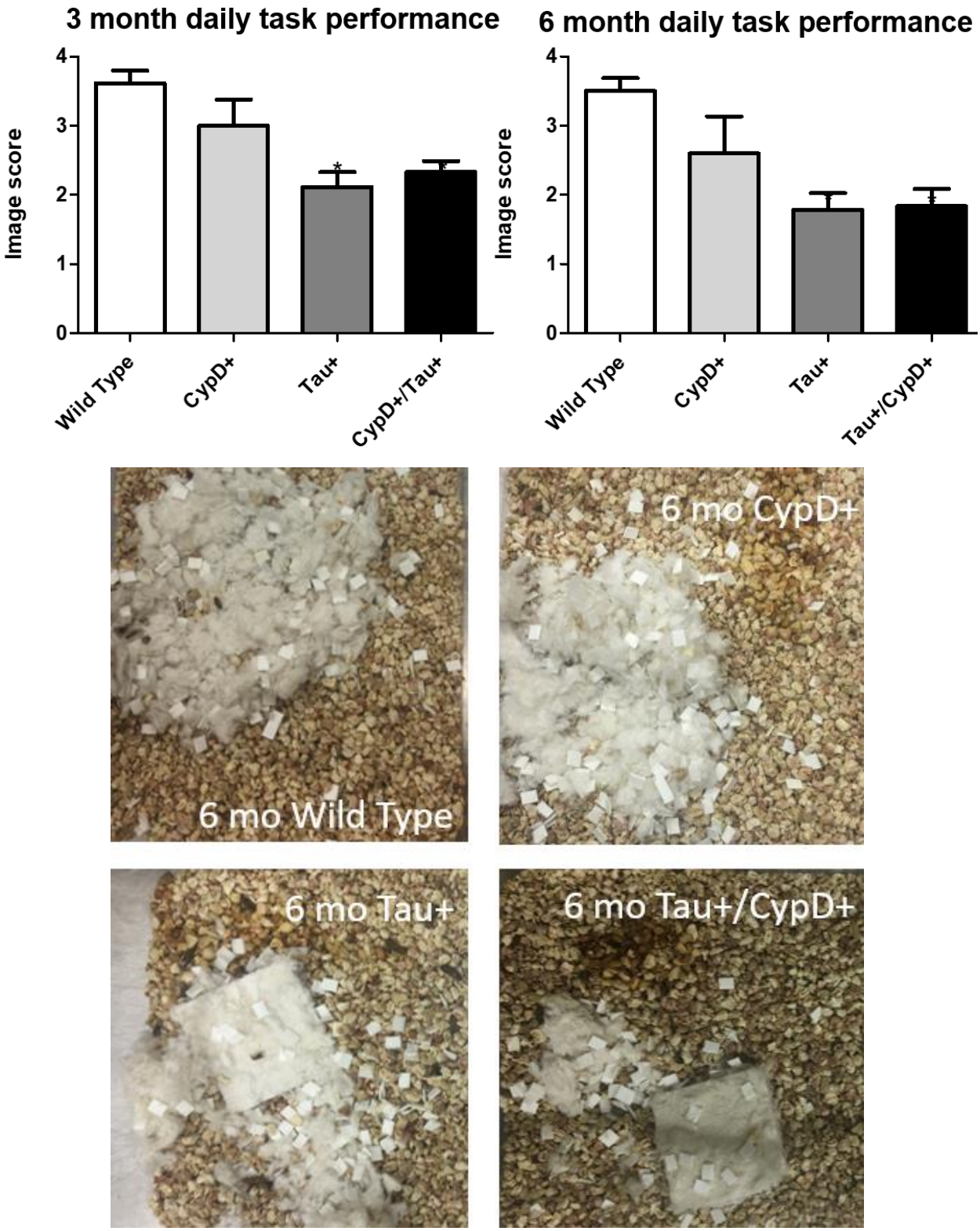

Figure 3-8: Daily task performance of CypD-modified AD mice

At 3 and 6 months, Tau+ mice and CypD+/Tau+ mice show significantly reduced nesting activity. Representative images show the nestlets built by 6- month-old mice.

3.10 CypD and hyperphosphorylated tau expression in a tau-induced model of Alzheimer's disease with CypD knock out

CypD expression was measured to assess the quality of the knock out at six months. CypD KO and CypD KO/Tau+ mice showed a complete knock out. Fig. 3.9A

HPT levels were measured at six months to determine the effect of CypD KO on HPT accumulation. While Tau+ mice showed highly elevated HPT levels compared to wild type mice ($p < 0.001$), CypD KO/Tau+ mice showed no such increase. CypD KO/Tau+ mice had significantly less HPT than Tau+ mice alone ($p < 0.001$). Fig. 3.9B

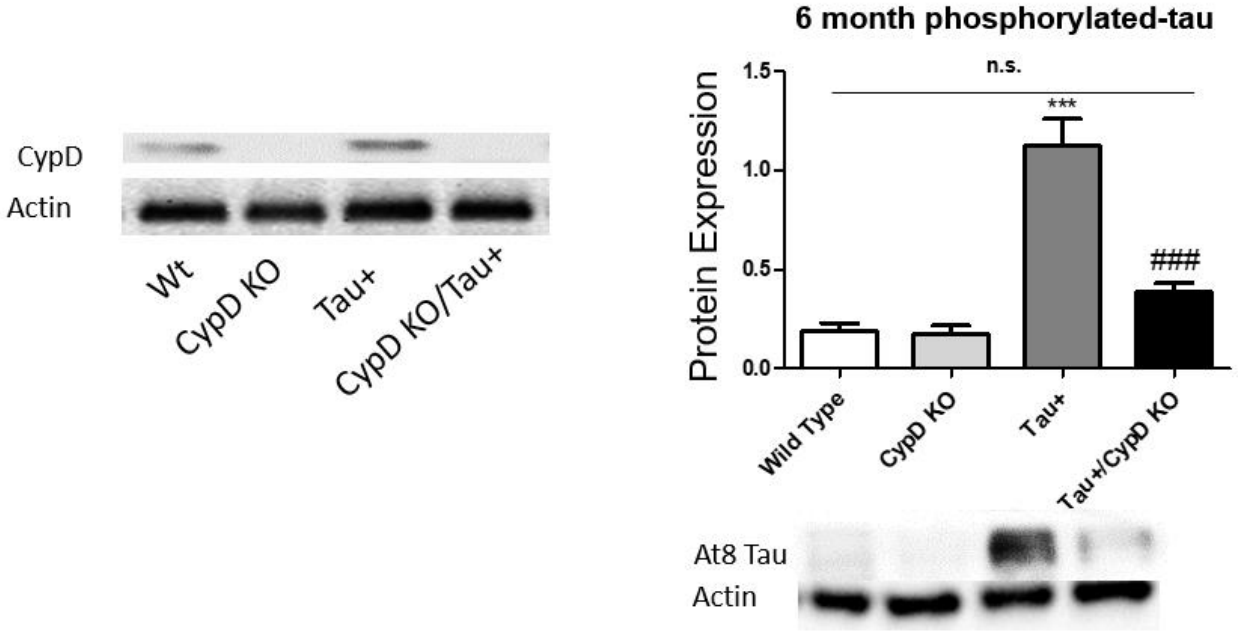

Figure 3-9: CypD and Hyperphosphorylated Tau Expression in CypD Modified AD Mice

Data is presented as phosphorylated tau normalized to actin, normalized to Tau+ levels. Western blots reveal that CypD is successfully knocked out in CypD KO and CypD KO/Tau+ mice. Phosphorylated tau expression is elevated in Tau+ mice, but normalized in Tau+/CypD KO mice. n = 4 *** $p < 0.001$ vs wild type, ### $p < 0.001$ vs Tau+

3.11 Synaptic loss in a tau-induced model of Alzheimer's disease with CypD knock out

Synaptophysin was measured at six months to assess synaptic loss. While Tau+ mice showed significant decreased in synaptophysin expression ($p < 0.001$), CypD KO/Tau+ mice did not. CypD KO/Tau+ mice showed significantly elevated levels of synaptophysin when compared to Tau+ mice ($p < 0.01$). Fig. 3.10A/B

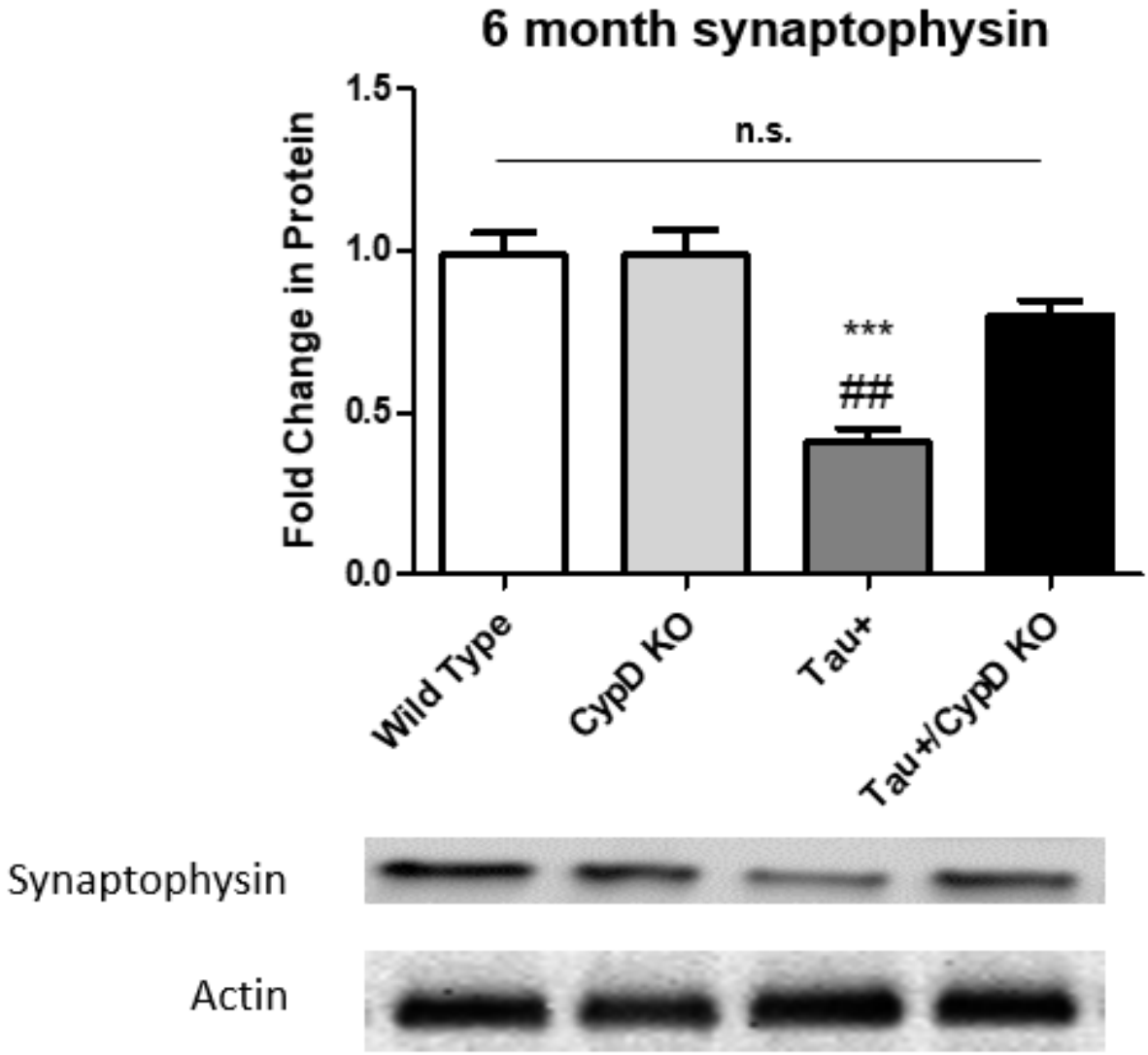

Figure 3-10: Synaptophysin in CypD Modified AD Mice

At six months, Tau+ mice show significantly depressed synaptophysin expression. Tau+/CypD KO mice have normalized synaptophysin expression. N = 3-5 *** $p < 0.001$ vs wild type, ## $p < 0.01$ vs Tau+/CypD KO.

3.12 Mitochondrial electron transport chain activity loss in a tau-induced model of Alzheimer's disease with CypD knock out

Mitochondrial function was assessed with an assay of Complex I. Tau+ mice showed a decrease in Complex I activity ($p < 0.01$), while CypD KO/Tau+ mice did not. CypD KO/Tau+ mice showed significantly increased Complex I function when compared to Tau+ mice ($p < 0.05$). (Fig. 3-11)

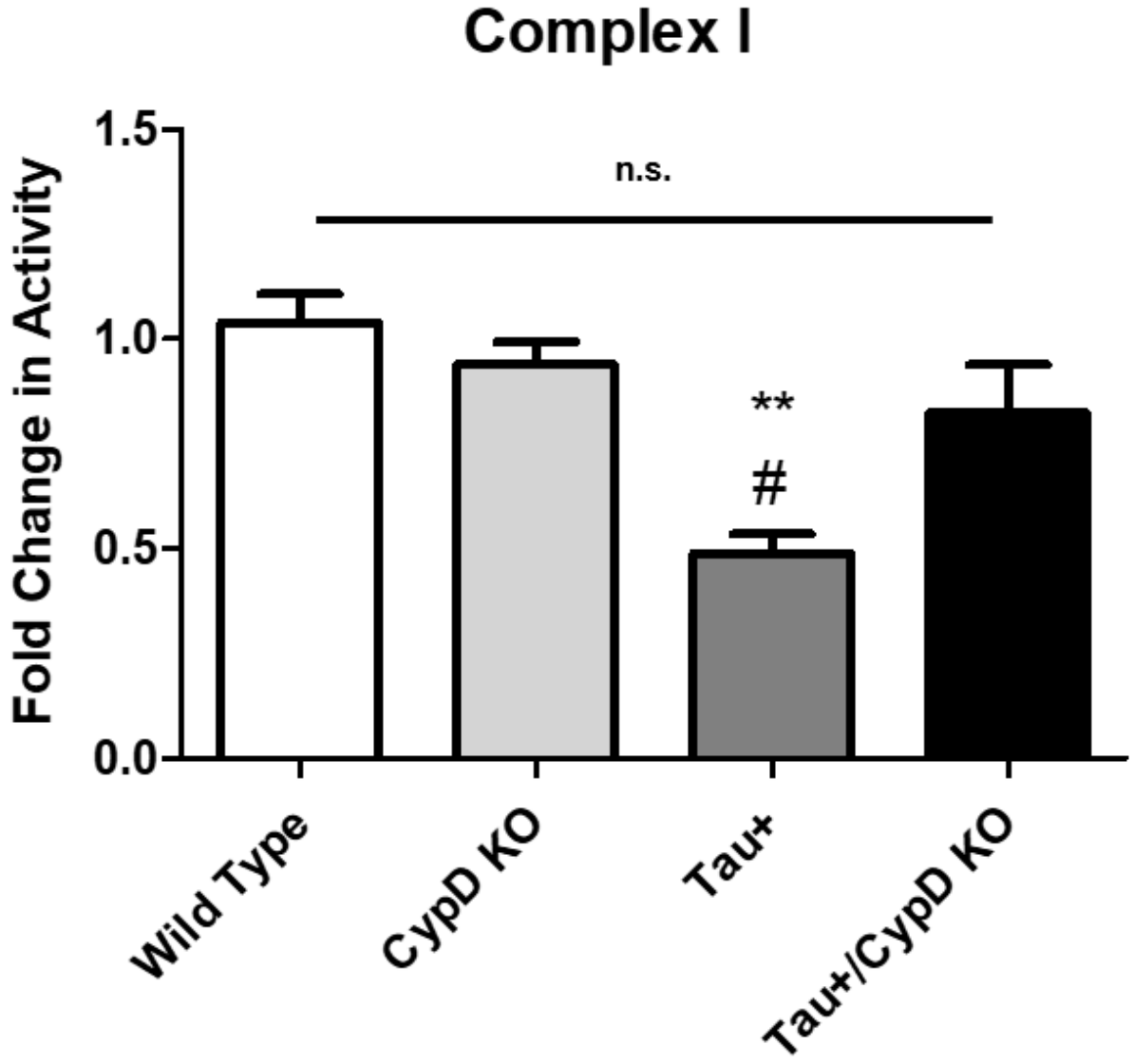

Figure 3-11: Mitochondrial Complex Activity in CypD Modified AD Mice

At six months, complex I shows significantly depressed activity, but Tau+/CypD KO mice show normal complex I activity.

3.13 Gross locomotion in a tau-induced model of Alzheimer's disease with CypD knock out

Gross locomotion was assessed to determine if mice showed relative health problems or differences in motion pattern across genotypes. No changes were detected at 6 or 12 months of age. (Fig. 3-12)

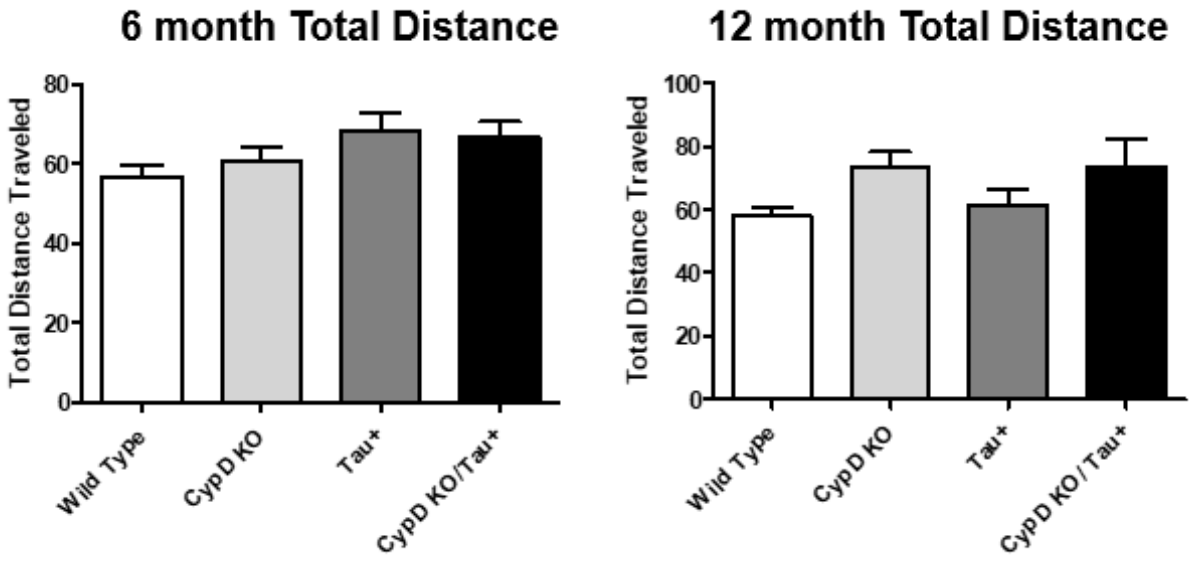

Figure 3-12: General Locomotion in CypD Modified AD Mice

General locomotion is not affected by CypD or Tau expression at six or twelve months.

3.14 Anxiety-like behavior in a tau-induced model of Alzheimer's disease with CypD knock out

Significant anxiety-like behavior, as measured by decreased time spent in the center, was identified in 6-month (Fig. 3-13A) and 12-month (Fig. 3-13B) Tau+ mice ($p < 0.01$). At both time points, CypD KO/Tau+ mice showed less anxiety-like behavior than the Tau+ mice ($p < 0.001$). CypD KO mice showed no significant differences from wild type mice in time spent in the center in either 6 or 12-month mice. This was in line with our previous findings that CypD KO prevented age induced cognitive impairments at 12 months.

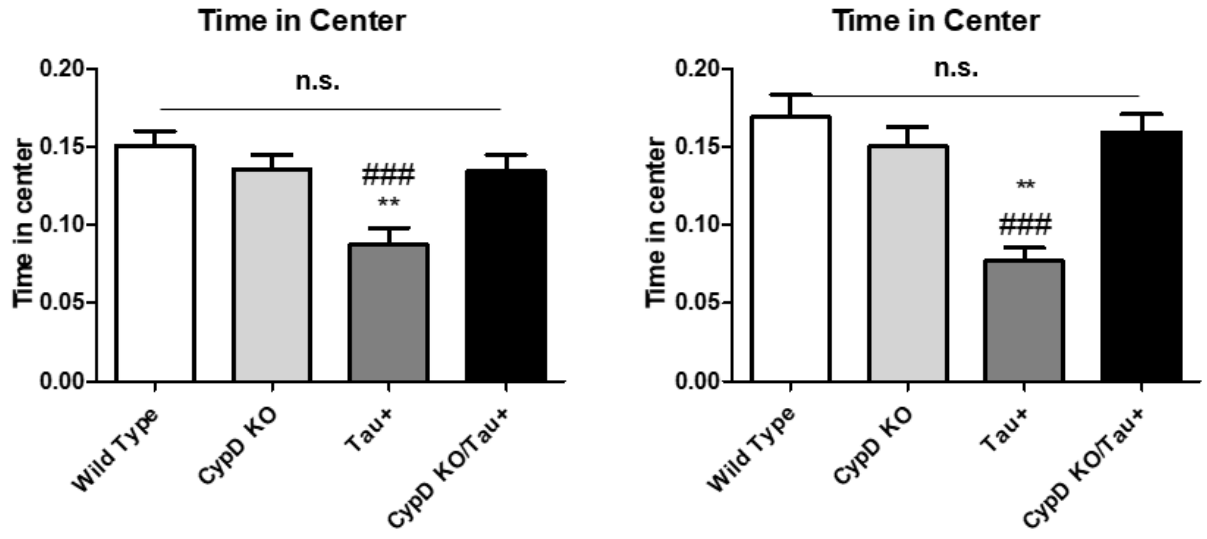

Figure 3-13: Anxiety-like Behavior in CypD Modified AD Mice

At both 6 and 12 months, Tau+ mice show decreased time in the center of the arena. CypD KO/Tau+ mice, however, showed no decrease at six (A) or twelve (B) months. n = 11-19 ## $p < 0.001$ wild type vs Tau+, ** $p < 0.01$ Tau+ vs Tau+/CypD KO

3.15 Daily task performance in a tau-induced model of Alzheimer's disease with CypD knock out

Daily task performance was used to assess the long term and working memory of the mice. At six months (Fig. 3-14A), there Tau+ mice showed significant decreases in nesting activity ($p < 0.001$) which is continued with 12-month-old mice ($p < 0.001$) (Fig. 3-14B). CypD KO mice show significant increased nesting activity when compared to Tau+ mice at both time points ($p < 0.001$). CypD KO mice, in line with our previous findings, do not show any impairment in nesting activity when compared to wild type mice.

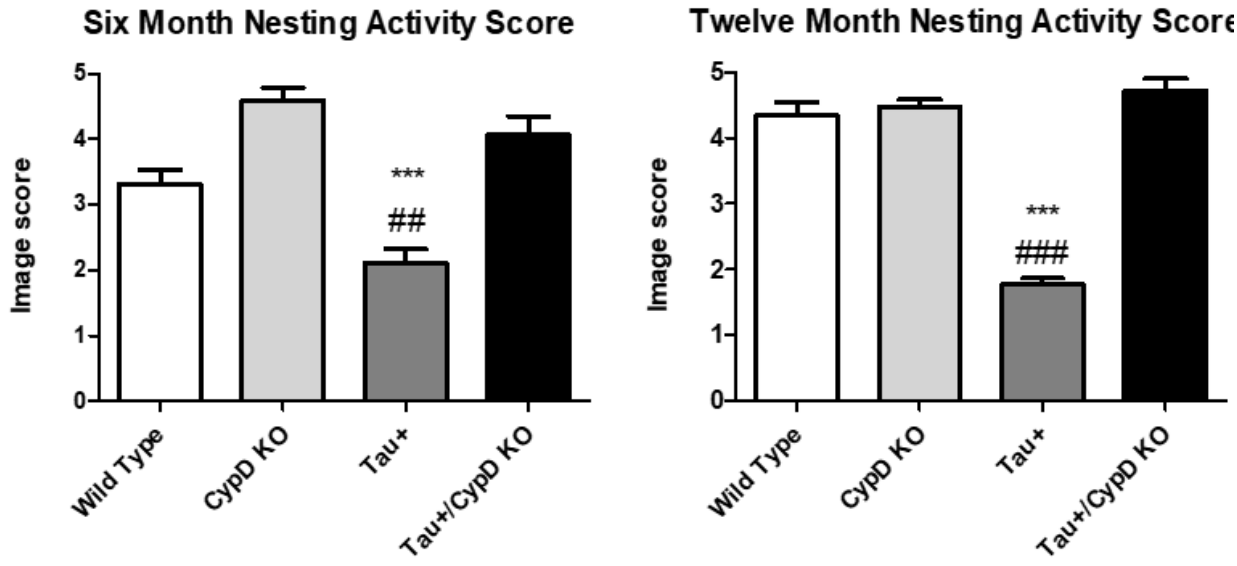

Figure 3-14: General Locomotion in CypD Modified AD Mice

At both six and twelve months, Tau+ mice show significant decreases in nesting activity. CypD KO/Tau+ mice, however, do not have significant impairments in nesting activity. A. n = 6-16 B. n = 13-23, *** $p < 0.001$ vs wild type, ## $p < 0.01$ vs CypD KO/Tau+, ### $p < 0.001$ vs CypD KO/Tau+

3.16 AKT signaling in a tau-induced model of Alzheimer's disease with CypD knock out

To assess mechanisms by which HPT might be interacting with CypD, we measured AKT signaling. AKT becomes activation upon phosphorylation (pAKT). pAKT then phosphorylates and inactivates GSK3β.

At three months (Fig. 3-15A), there were no significant changes in wild type and Tau+ mice for AKT signaling. However, at six months (Fig. 3-15B), there was a significant decrease in pAKT in CypD OE/Tau+ compared to wild type ($p < 0.001$) and Tau+ mice.

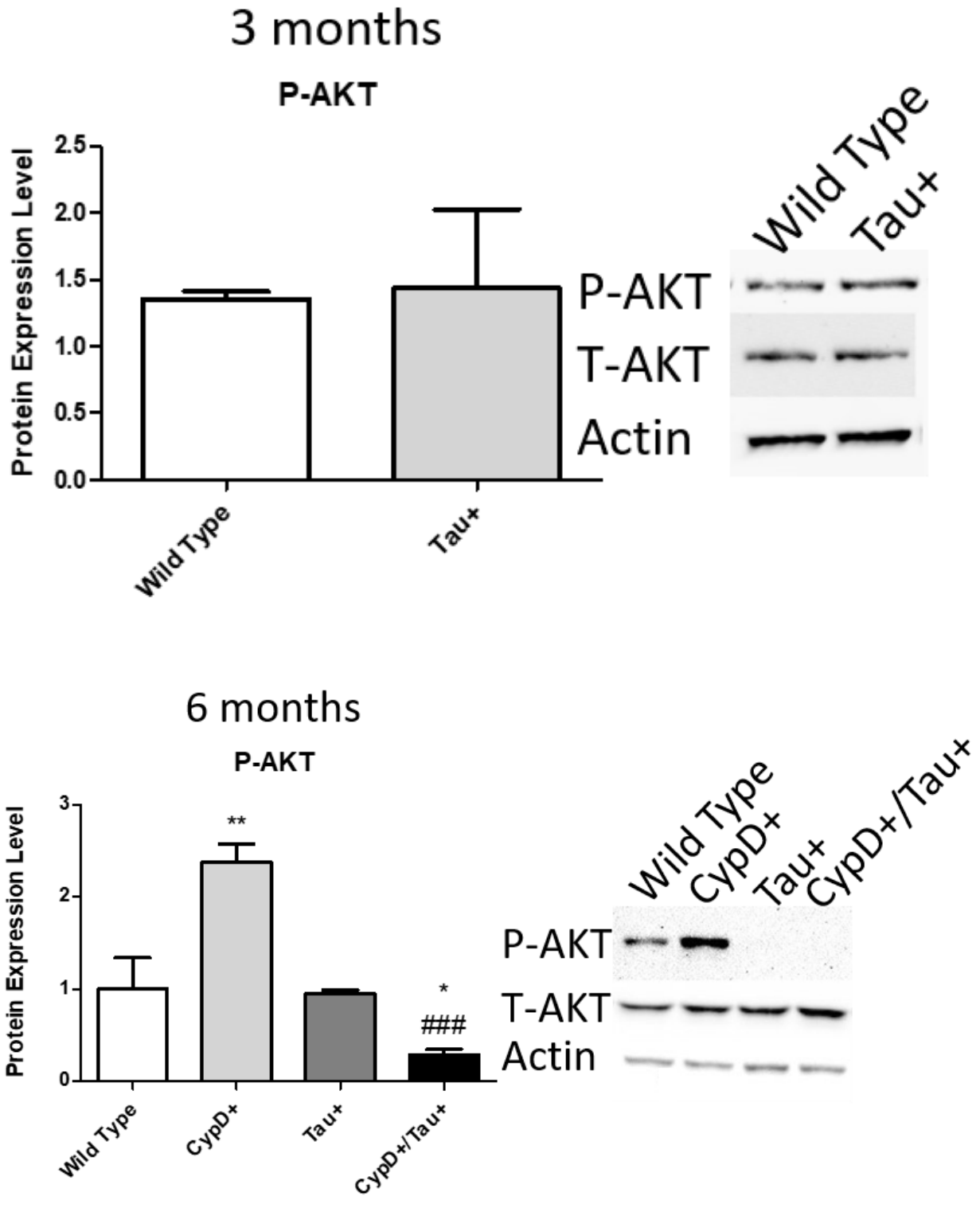

Figure 3-15: AKT Activity in CypD Modified AD Mice

*Data is presented as phosphorylated protein normalized to the total protein and actin; data is normalized to wild type levels. At three months, there is no significant change in Tau+ mice in Akt signaling. At six months, CypD+ mice have high levels of active Akt, while CypD+/Tau+ mice have significantly decreased levels of active Akt. n = 3-6 * $p < 0.05$ vs wild type ** $p < 0.01$ vs wild type, ### $p < 0.001$ vs Tau+.*

3.17 GSK3β signaling in a tau-induced model of Alzheimer's disease with CypD knock out

Based on the lack of change in Akt signaling at three months, we only examined 6-month-old mice for GSK3β activity. GSK3β signaling was measured to assess the downstream effects of changes in Akt signaling. pAkt inhibits GSK3β by phosphorylating the Ser9 inhibitory site. GSK3β activity can be identified by looking at two phosphorylations: p-Ser9 and p-Tyr216. Phosphorylation at serine 9 is inhibitory while phosphorylation at tyrosine 216 is an activation site [330]. Phosphorylation at these sites is not mutually exclusive, so conclusions must be drawn by looking at both sites [331].

At 6 months, p(Try216) GSK3β showed significant increases in the CypD OE/Tau+ mice ($p < 0.05$) (Fig. 3-16A). This change was not seen in the CypD OE or the Tau+ mice. P (Ser9) GSK3β showed significant increases in CypD OE mice ($p < 0.01$), while showing reductions in both Tau+ mice and CypD OE/Tau+ mice ($p < 0.05$) (Fig. 3-16B).

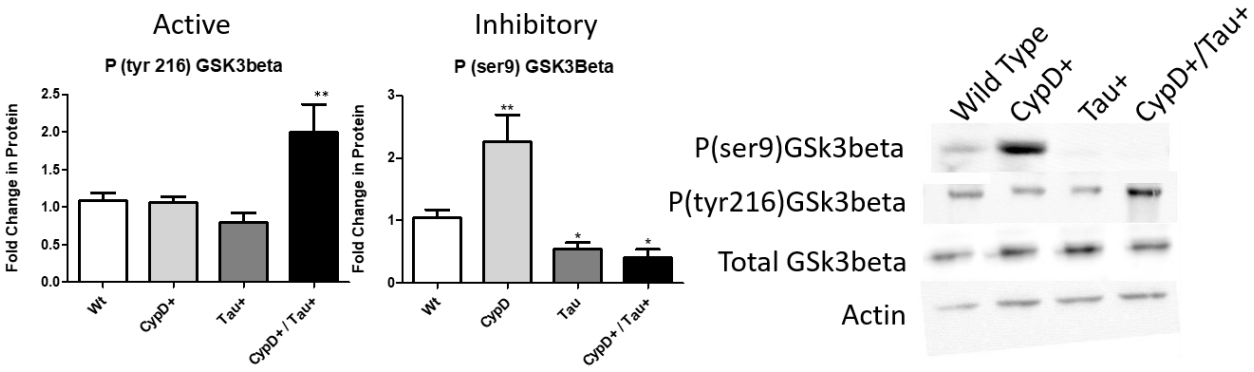

Figure 3-16: GSK3β Activity in AD Mice

At six months, CypD+/Tau+ mice show significant increases in expression of active GSK3β. Tau+ and CypD/Tau+ mice both show decreased expression of inhibitory GSK3β. CypD+ mice showed significant increases in inhibitory GSK3β. n = 5-7 * $p < 0.05$ Wild type vs CypD+/Tau+, Wild type vs Tau+; ** $p < 0.01$ Wild type vs CypD+

Chapter 3 Interim conclusion

These experiments demonstrate that CypD has a significant impact on the AD phenotype in a tau-induced model of AD.

CypD OE increased cognitive dysfunction, while CypD KO preserved cognitive function in AD models. This was supported by molecular experiments that found that CypD OE increased levels of HPT, while CypD KO decreased HPT levels. Further, CypD OE increased synaptic and neuronal loss while CypD KO ameliorated these losses. Finally, CypD OE increased loss of mitochondrial function while CypD KO supported mitochondrial function.

These experiments also suggest a signaling pathway that is affected by the combination of HPT and CypD. Akt, which acts as an inhibitor of GSK3β, was inhibited in the CypD OE/Tau+ mice (Figure 3.16). GSK3β inhibition was severely decreased in the CypD OE/Tau+ mice and its activation was significantly increased. As was described in the introduction, active GSK3β can translocate to the mitochondrial matrix where it directly interacts with CypD to increase opening of the mPTP.

Overall, these results suggest a possible synergistic interaction by which CypD expression worsens the tau-induced AD phenotype, and in turn, the increase HPT modifies signaling pathways to increase mPTP opening.

Chapter 4 Inhibition of CypD as a Therapeutic Target for Alzheimer's disease

Due to the success of CypD KO in ameliorating the Tau+ induced AD phenotype and prior studies identifying CypD KO as a strong ameliorating factor in the Aβ induced AD phenotype [23, 230, 231], we chose to pursue CypD as a target for drug development. The studies in this chapter are split between C-9, a compound we have published on, and a novel compound which is an analog of C-9. For this dissertation, the analog will be called SY1.

Experiments in this chapter used cells and the P301S mice described previously. For the cell experiments SK-N-SH cells were used. In the in vivo pharmacology studies, mice were given a daily intraperitoneal injection of the CypD inhibitor or a vehicle control starting at four months of age. Testing began at six months of age.

These experiments were conducted to test the sub-hypothesis presented in Schematic 4. Namely, that inhibition of CypD can prevent phosphorylated tau induced mitochondrial failure and the resulting synaptic and cognitive loss.

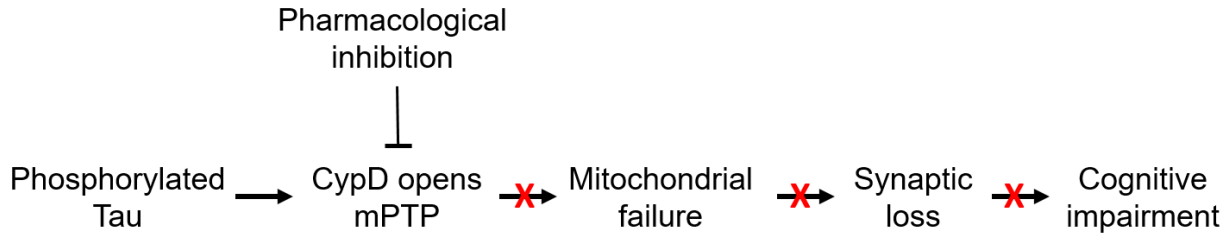

Schematic 4: Sub-hypothesis for Chapter 4

4.1 CypD inhibitor structure

Our lab developed a series of compounds and C-9 was the best compound to come out of this screen [232] (Fig, 4-1). Further screening developed a secondary compound that was used for these experiments, but knowledge of that structure is currently restricted until patent protection is acquired.

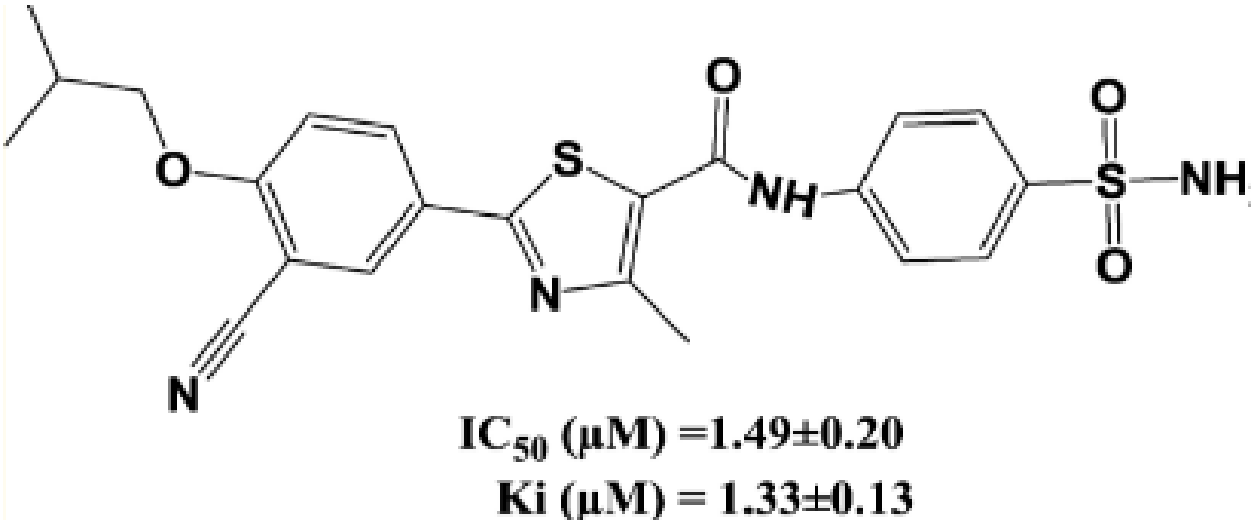

Figure 4-1: Structure of CypD Inhibitor

The structure of C-9 was created based on molecular modeling using the structure of CypD. A newer, modified version of this structure was used in these studies.

4.2 Effectiveness of CypD inhibitor

C-9 was tested for toxicity using SK-N-SH cells in a cell viability assay. Additionally, C-9 was tested in a calcium swelling assay to confirm its effect on the mPTP opening [232].

In the cell viability assay, there were no significant impacts on viability at doses up to 100 μM. No changes in cell morphology were seen with 100 μM C9. (Fig, 4-2)

In the mitochondrial swelling assay, three controls were used: (1) A no Ca^{2+}, no C-9 control provides a baseline for swelling (black triangles), (2) a Ca^{2+} added, no C-9 control provides a maximum swelling (red icons), (3) a Ca^{2+} and CsA control provides a control for CypD inhibition (black squares).

In a dose-dependent manner, C-9 reduced mitochondrial swelling from 10 μM to 100 μM. (Fig, 4-3). C-9 treated cells (green, purple, and yellow icons) showed significantly less swelling when compared to the Ca^{2+} added control (red icons).

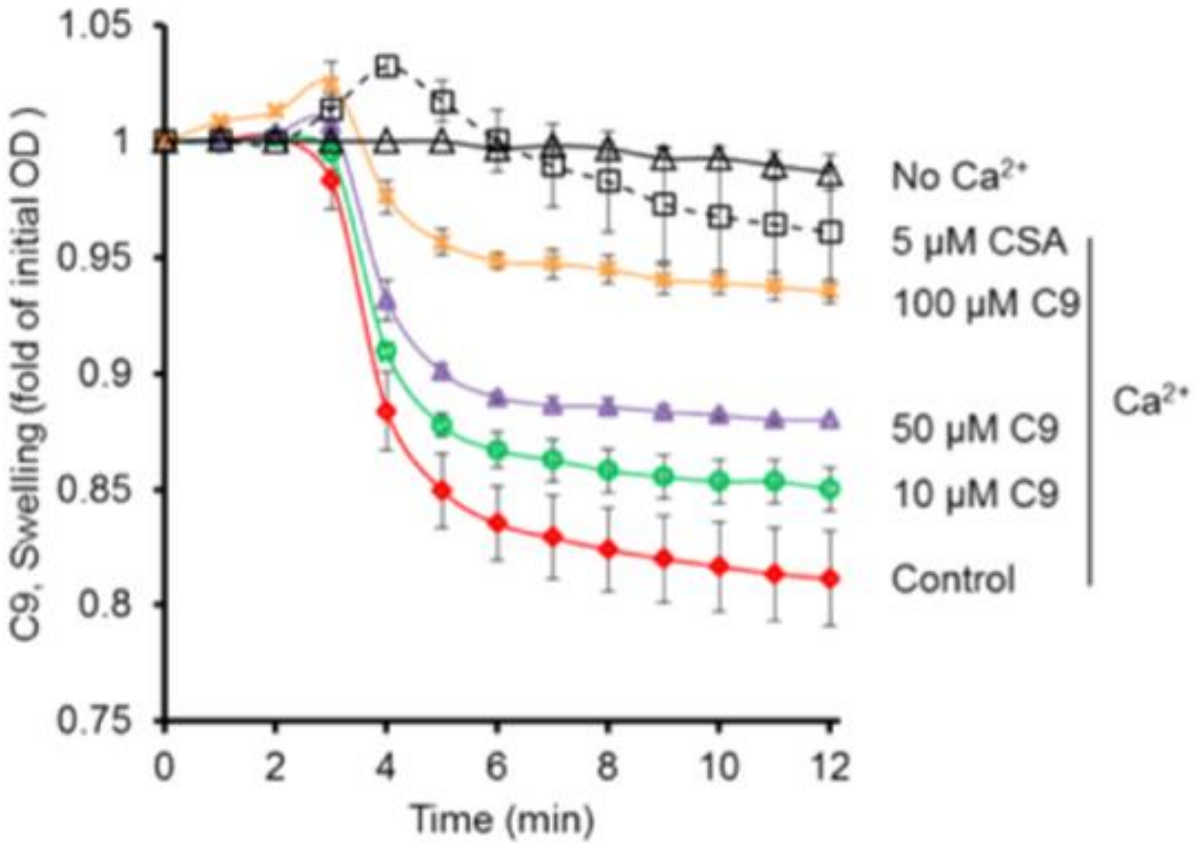

Figure 4-3: A calcium induced swelling assay of C-9 in isolated mitochondria

Isolated mitochondria were exposed to 2 µM of calcium which induced swelling in untreated mitochondria. CsA was used as a control to inhibit CypD and prevent swelling. In a dose dependent manner, C-9 prevented swelling of mitochondria in a dose dependent manner.

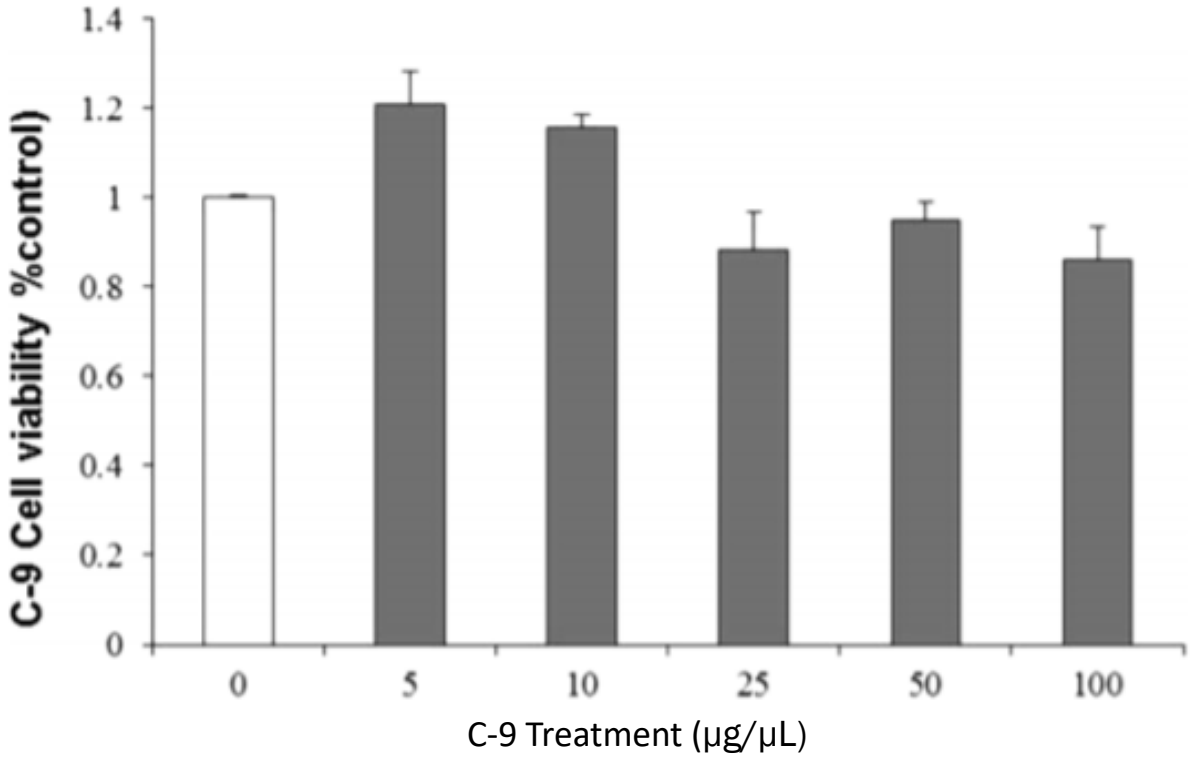

Figure 4-2: Functional Testing of CypD Inhibitor

C-9 was tested in a cell viability assay in SK-N-SH cells. No cell death was detected at any dose tested.

4.3 Inhibition of Cyclophilin D in an Aβ

The effect of C-9 on mitochondrial function was assessed using an ATP assay in conjunction with Aβ oligomers. Aβ caused a significant decrease in ATP ($p < 0.01$) and C-9 dose-dependently increased ATP production in the presence of Aβ ($p < 0.01$). (Fig, 4-4A)

In an Aβ-induced cell death assay, Aβ caused significant cell death ($p < 0.01$) and C-9 dose-dependently prevented cell death induced by Aβ(Fig, 4-4B).

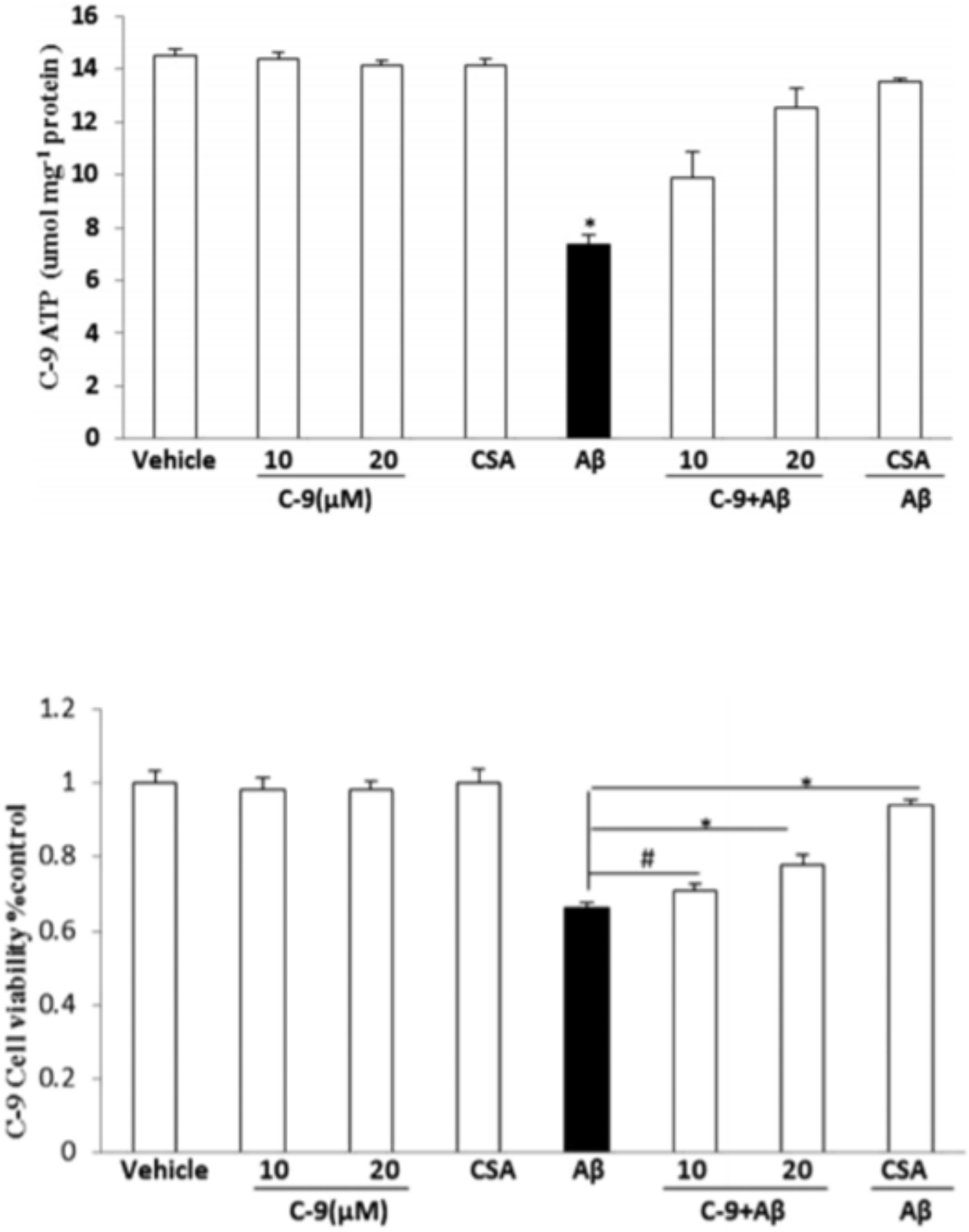

Figure 4-2: Functional Testing of CypD Inhibitor in AD Cell Model

C-9 prevents Aβ induced ATP depletion (A) and Aβ induced cell death in a dose dependent manner in primary neurons?

4.7 Mitochondrial complex activity in tau-induced Alzheimer's disease with CypD inhibitor drug

Mitochondrial complex activity was tested to assess mitochondrial function. Complex I was looked at due to its role in establishing the proton gradient across the inner membrane. Complex IV was chosen due to its role as the rate limiting step in the electron transport chain. Complex I was significantly reduced in Tau+ mice at 6 months when compared to wild type mice. However, Tau+ mice treated with SY1 showed ~60% recovery when compared to wild type. Complex IV activity was also lower in Tau+ vehicle treated mice. In Tau+ mice treated with the SY1, complex IV activity was ~80% recovered.

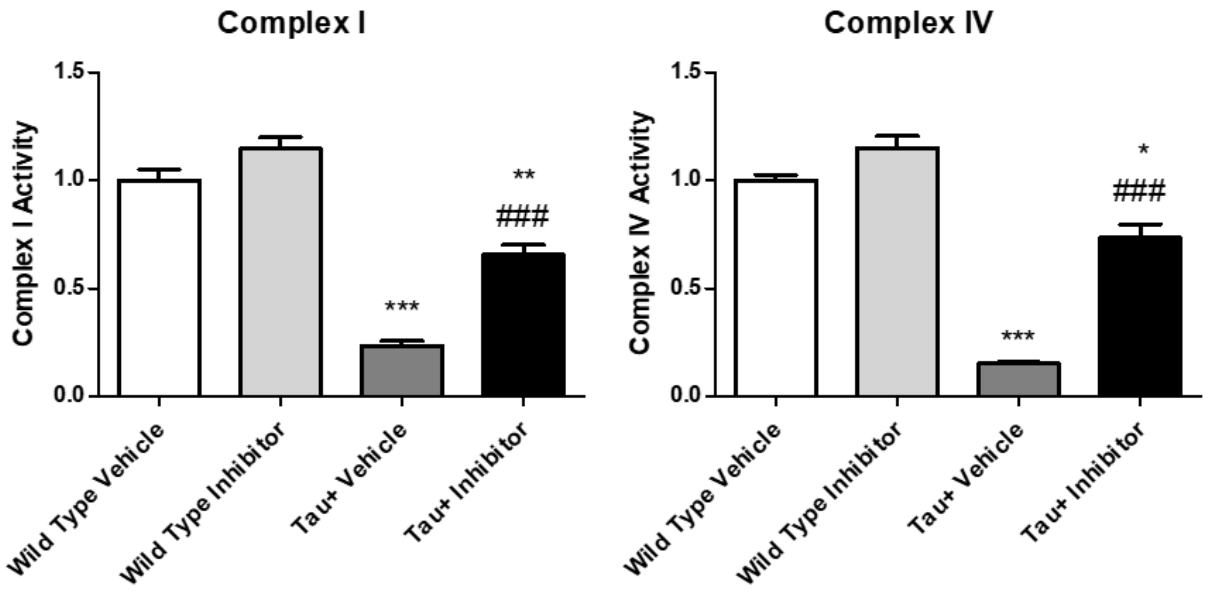

Figure 4-3: Effect on mitochondrial function of CypD inhibitor on Tau+ mice

Six-month-old vehicle-treated mice showed significant reduction of complex I and IV activity from the cortex?, but treatment with the CypD inhibitor ameliorated this effect.

4.8 Gross locomotion in tau-induced Alzheimer's disease with CypD inhibitor drug

Gross locomotion was measured with the SY1 in wild type and Tau+ mice at six months. There were no significant changes in gross locomotion (Fig, 4-4).

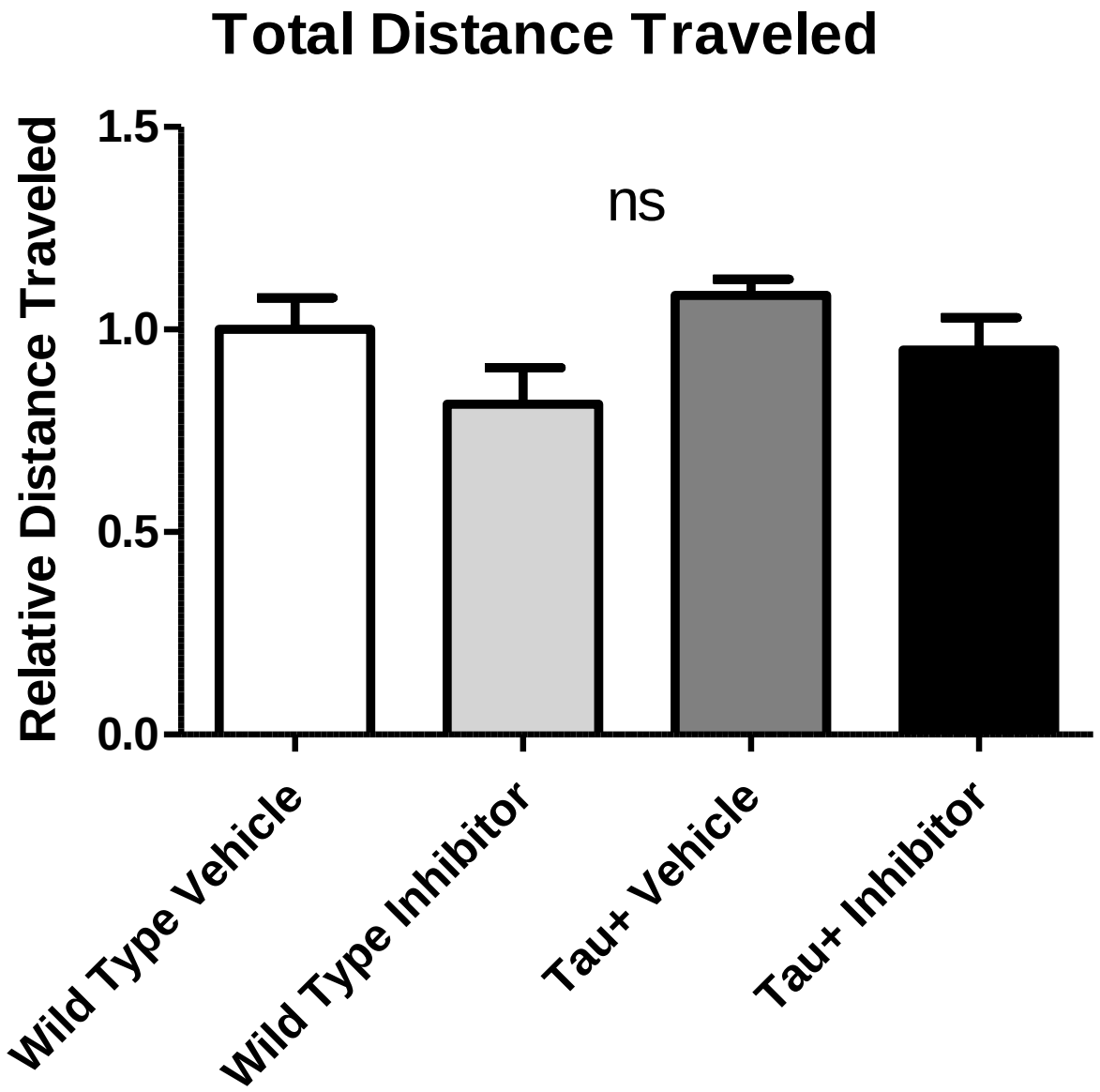

Figure 4-4: General Locomotion with Treatment by a CypD Inhibitor

Neither genotype nor treatment with the CypD inhibitor affected general locomotion.

4.9 Anxiety-like behavior in tau-induced Alzheimer's disease with CypD inhibitor drug

Anxiety-like behavior was measured in open field to assess cognitive impairment in Tau+ mice treated with SY1. Tau+ mice showed significantly decreased time spent in the center of the assay indicating significant anxiety-like behavior ($p < 0.001$). However, treatment with SY1 completely ameliorated these defects ($p < 0.001$) (Fig, 4-5). There was no significant difference between wild type mice treated with vehicle and Tau+ mice treated with the SY1.

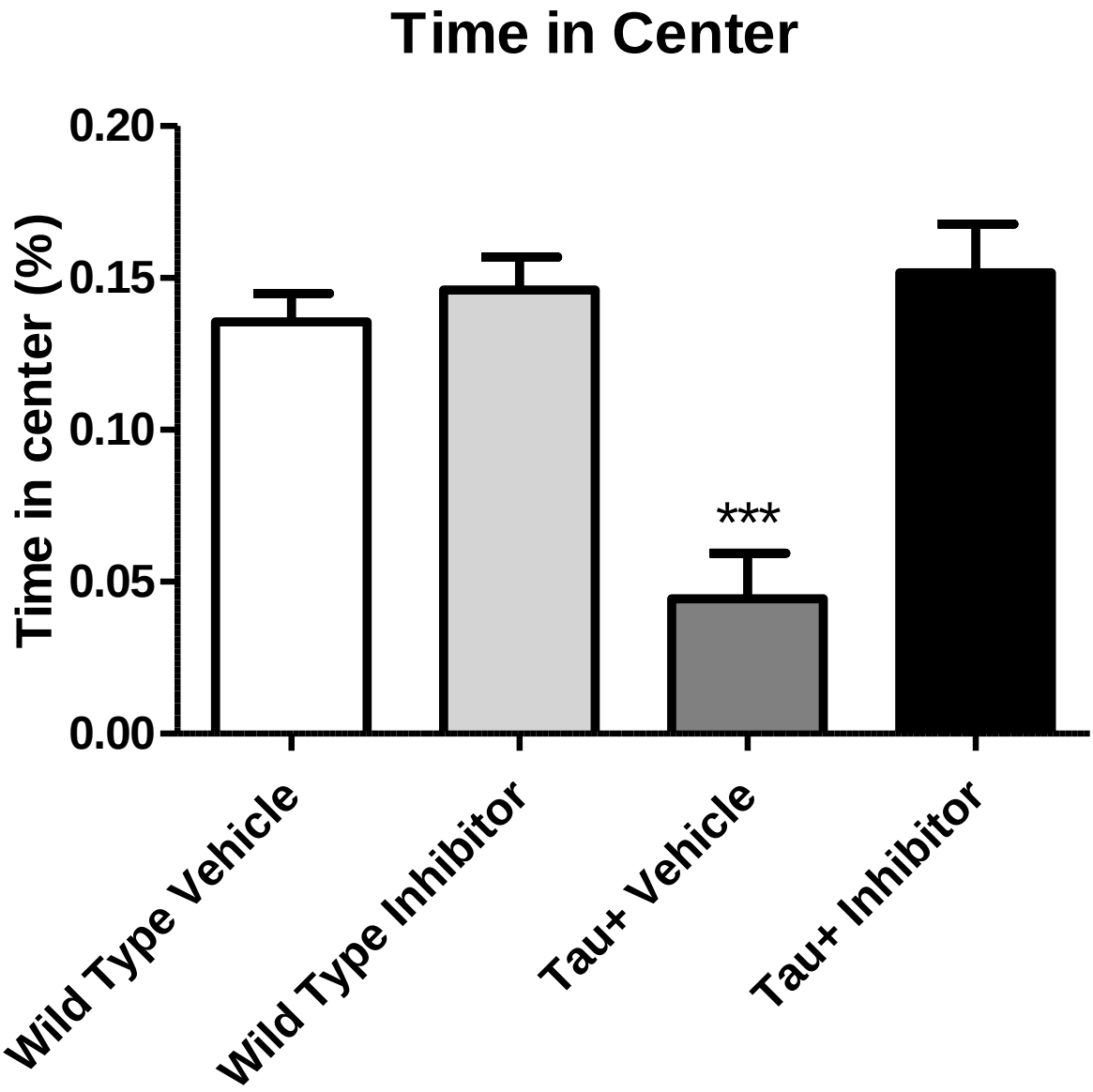

Figure 4-5: Anxiety-like Behavior when Treated with a CypD Inhibitor

Six-month-old vehicle-treated Tau+ mice showed significant reduction in time in the center compared to wild type mice. Tau+ mice treated with the CypD inhibitor showed no change in anxiety-like behavior.

4.10 Daily-task performance in tau-induced Alzheimer's disease with CypD inhibitor drug

A nesting assay was employed to measure memory and task performance in Tau+ mice treated with a CypD inhibitor. Tau+ mice showed significantly impaired ability to build nests ($p < 0.001$) indicating a significant impairment of memory. Tau+ mice treated with a CypD inhibitor did not show impairment of memory. (Fig, 4-8A/B)

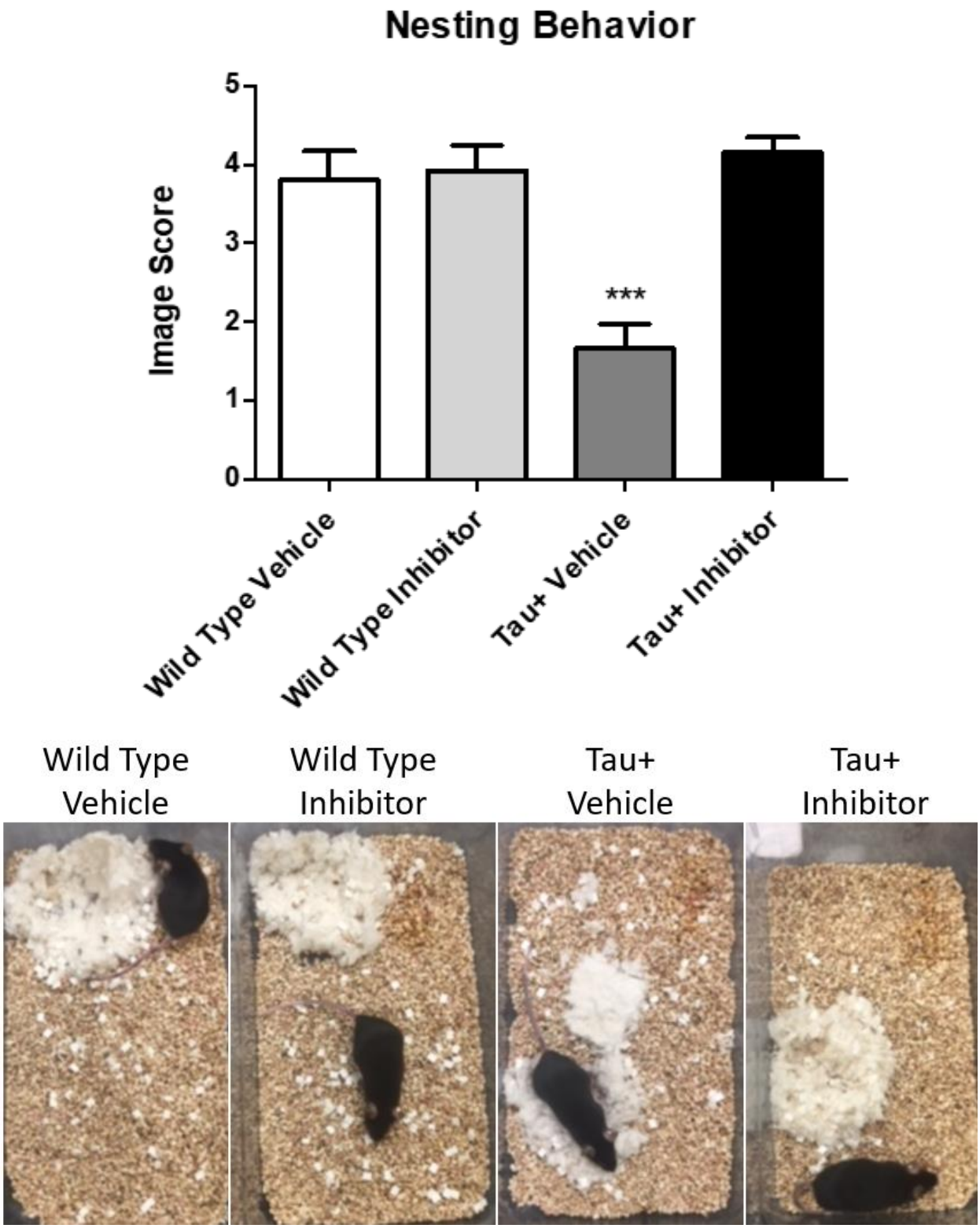

Figure 4-6: Daily Task Performance when Treated with a CypD Inhibitor

Six-month-old Tau+ mice showed significant decreases in nesting activity. Tau+ mice treated with the CypD inhibitor did not show any such deficits.

Chapter 4 Interim conclusions

These studies demonstrate the effects of small molecule CypD inhibitors for the amelioration of AD symptomology. Our inhibitor is effective at preventing mPTP opening and preserving mitochondrial function. The CypD inhibitor is effective at preventing death induced by Aβ and is non-toxic to cells. Further, the CypD inhibitor can prevent cognitive impairments in Tau+ mice.

Chapter 5 Conclusions

Chapter 2: The Role of CypD in Aging Mice

These experiments first demonstrated a cognitive decline in non-transgenic aging mice. We analyzed sex differences on several behavioral tests as mice age. Given new research requirements to include female animals, it is likely that these differences will become more important. Historically, researchers have underestimated the differences between males and females and chosen to only study males.

In the open field paradigm, male and female mice maintained similar general locomotion and motion patterns at all age points. Many behavioral tests, such as elevated plus maze, object exploration, and social recognition tests, rely on the premise that mice are not experiencing difficulty moving or showing different explorative patterns. However, these behavioral tests do not allow for an easy assessment of general locomotion patterns, as demonstrated here. Using a reliable method of identifying gross motor defects will improve the accuracy of other behavioral tests and ensures that behavioral tests as mice age will likely reveal useful, disease-relevant data rather than artifacts of the aging process.

Female mice demonstrate higher levels of anxiety-like behavior with aging. This is of particular importance to research in many aging diseases, such as Alzheimer's disease, which are more common in women. Knowing that male mice do not naturally display increases in anxiety-like behavior is also important, given that aging diseases such as Parkinson's disease and type 2 diabetes are more common in men.

Daily task performance is a useful metric of working and long-term memory. Mice build nests for thermoregulation, meaning that it is not a sex-specific behavior, and is learned as a natural behavior when the mice are pups. This makes nesting activity a particularly good measure of skills that mice naturally have, rather than one that researchers teach to them, like lever pulling or maze

running. This test found declines earlier than other paradigms have found memory impairments due to its specific design. A high-quality nest will use all of the available material shredded, organized into a region less than ¼ the area of the cage, and built up high enough to cover the mouse entirely. Three-month-old mice, whether male or female, rarely fail to build nests fitting this description. However, by 12 months of age, many mice (8/13) fail to utilize the entire nestlet, and none build nests of sufficient height. This is indicative of a failure of memory or performance of a nesting task learned as pups. This trend is continued in 24-month-old mice, where only 6/23 mice built proper nests. Based on data from the open field paradigm showing that 24-month-old mice are capable of similar gross motor, we interpret this to mean that aging mice start to show subtle memory failures.

Having discovered this robust age-dependent cognitive decline, we sought to determine a mechanism by which this may occur in non-transgenic mice. Mitochondrial failure with age and neurodegeneration has been demonstrated in several models [332-334]. Specifically, with age there is a decline in mitochondrial respiratory chain complex activity and an increase in mutations of mitochondrial genes [335-339]. This leads both to a loss of ATP production as well as an increase in ROS [334, 340-342]. Loss of mitochondrial function is even more pronounced at the synaptic level, where losses of energy can lead to synaptic loss [343-346]. We hypothesized that mitochondrial failure was the root cause of this cognitive impairment.

We identified increased ROS production in both males and females with age. This was accompanied by reduced activity in Complex I and Complex IV of the mitochondrial ETC. These correlative results supported the hypothesis that aging mice were experiencing cognitive decline as a result of mitochondrial failure. However, further experimentation would be necessary to definitively prove causation.

We further hypothesized that the mitochondrial failure was directly related to the activity of CypD, given its proposed role in neurodegeneration that was discussed at length in the introduction. We first tested this hypothesis by measuring levels of CypD and determining that aging mice showed increased expression of CypD. Then, CypD OE and CypD KO models were used to manipulate the levels of CypD to test a causative role in cognitive impairment.

We determined that CypD OE mice showed a phenotype that we termed "early aging", in which they showed cognitive impairment at an earlier age than non-transgenic mice. The significant increased expression of CypD induced an anxiety-like phenotype in males and females as early as six months. Additionally, by six months, CypD OE males and females were showing declines in nesting activity. Most interestingly, CypD OE reduced life expectancy of mice to about 15 months, making them unavailable to study at the latest time points used for these aging studies.

CypD KO mice were resilient to cognitive impairments with age. They did not show an anxiety-like phenotype in the open field paradigm, and were still building near perfect nests at 24 months old. While no formal survival curve was done, these mice long out lived their age matched controls.

Studies in the lab demonstrated that CypD KO mice had better mitochondrial function and less reactive oxygen species. These studies also identified increased buffering of calcium and membrane potential more resistant to ROS induced failures.

Taken together, these studies indicate a strong role for CypD in cognitive failure in aging animals. However, these studies were limited by several factors that should be corrected in future study. First, synaptic loss via imaging was not assessed in these mice. While we hypothesize that synaptic loss is the tie between mitochondrial failure and cognitive impairment, this was not proven here. Second, given the ample evidence that synaptic and somatic mitochondria are

separate pools with separate characteristics and different sensitivities to stress [345], these two mitochondria pools should be analyzed separately.

Chapter 3: The Role of CypD in Alzheimer's disease Mice

Given the role of CypD in Aβ models of AD, we hypothesized that tau-induced AD would be equally affected by CypD. Due to the lack of success in drug trials targeting Aβ pathways alone, identifying an effective target in both Aβ pathology and tauopathies would substantially improve the chances of success of a compound in treating AD.

These studies were divided into two sections: those utilizing CypD OE to model a more severe AD pathology and those utilizing CypD KO to model the potential therapeutic effect. CypD OE mice were crossed into the P301S tau mice. The double transgenic mice represent severe AD phenotype when compared to the Tau+ mice; wild type and CypD OE alone mice served as controls. Similarly, CypD KO mice were crossed into P301S tau mice to create a therapeutic model when compared to the Tau+ mice with wild type and CypD KO mice serving as controls.

CypD OE/Tau+ mice showed more significant CypD accumulations than CypD OE alone mice, as well as increased levels of HPT when compared to Tau+ mice. These results indicate more severe AD pathology. Additionally, CypD OE/Tau+ mice show more significant depressions of mitochondrial complex activity. CypD OE/Tau+ mice also showed more significant decreases in synaptophysin and neuronal tubulin, indicating a loss of both synaptic structures and neurons. CypD OE/Tau+ mice also showed more significant cognitive impairments, with increased levels of anxiety-like behavior and decreased daily task performance. Overall, these results suggest that increased expression of CypD causes an earlier onset of AD with worse symptoms.

CypD KO/Tau+ mice showed an amelioration of every tested phenotype of AD. Tau expression, while very high in the Tau+ mice, was significantly reduced with knock out of CypD. CypD KO/Tau+ mice also showed increased mitochondrial ETC activity when compared to Tau+ mice. This was accompanied by an increase in synaptophysin, indicating that CypD KO in Tau+ mice increases the preservation of synaptic structures. As predicted by our hypothesis, CypD KO

prevented tau-induced cognitive deficits, with no increase in anxiety-like behavior and sustained daily task performance behaviors.

These experiments confirm the hypothesis laid out in Schematic 1. CypD OE is sufficient to induce an AD phenotype in some regards: increased mitochondrial failure, increased synaptic loss, increased neuronal loss, and reduced cognitive function. However, CypD OE was not sufficient to induce HPT. When combined with P301S tau, CypD OE did induce a significant increase in HPT, as well as more significantly increasing the other markers of AD measured.

CypD expression was also shown to be necessary for the AD phenotype. When P301S mice had CypD knocked out, there was no significant increase in HPT, no mitochondrial failure, no synaptic loss, and no cognitive failure.

We looked further into mechanisms that may connect the increases in phosphorylated tau to increased mitochondrial damage mediated by CypD. We identified the Akt/GSK3β pathway as potentially important, laid out in Schematic 5. Inhibition of Akt activity results in more active GSK3β, which can then be translocated to the mitochondrial matrix. As discussed previously, active GSK3β can phosphorylate CypD, predisposing mPTP opening. Our results indicate an inhibition of Akt in six-month-old Tau+ mice and CypD+/Tau+ mice. This extended into an increase in active GSK3β in these same genotypes. We interpret this to indicate that the increased tau expression reduced Akt activity, which is in line with previous studies [347].

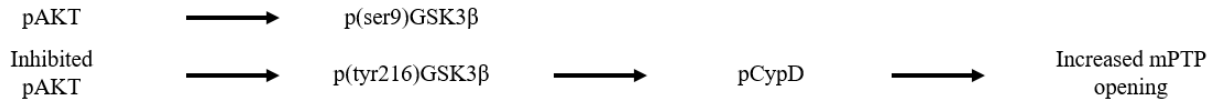

Schematic 5: The AKT/GSK3β pathway.

Surprisingly, the CypD OE genotype alone showed an extreme increase in Akt activity, indicating a pathway by which CypD can alter Akt signaling. Several lines of research indicate

that there is a mechanism of self-regulation in which opening of the mPTP can suppress Akt signaling [348]. In this case, it is possible that this suppression of Akt reduces mPTP opening, resulting in a less dramatic cognitive decline than one may predict.

One may wonder why CypD OE mice and Tau+/CypD OE mice show differential regulation of the Akt/GSK3β signaling. In this case, we can conclude that Tau OE is the dominant, harmful phenotype.

These results demonstrate the effects of a CypD inhibitor developed in our lab. While previous structures of this inhibitor have been published and are referenced in this dissertation, this is the first evidence of a new, effective compound.

The CypD inhibitor used in these studies were developed via a system of intelligent modeling based on improved structures developed in experiments with collaborators in medicinal chemistry.

In molecular binding assays, this small molecule successfully binds to CypD and inhibits its activity. The levels of inhibition are better than that of previous compounds tested by our laboratory and other research groups. Further, the compound is non-toxic to cells even at large doses, and can inhibit Aβ induced cellular death and Aβ induced mitochondrial failure.

This compound was well tolerated in mice, although no explicit toxicology tests were conducted. In mice, the SY1 did not prevent the accumulation of HPT, further supporting that CypD is a target site for ameliorating cognitive deficits induced by tau. Mitochondrial function was also preserved in Tau+ mice treated with the CypD inhibitor. This translated into preserved cognitive function. Tau+ mice treated with the CypD inhibitor did not show an anxiety-like phenotype that is associated with Tau+ mice at six months and retained their daily task performance activity while vehicle-treated mice showed significant reductions.

Final Conclusions

The work presented herein suggests that CypD represents an excellent target for continued investigation in AD and age-related cognitive decline. Genetic ablation of CypD is sufficient to prevent age related cognitive decline as well as the appearance of AD in mice. Pharmacological inhibition of CypD prior to the appearance of neuronal loss similarly prevents cognitive symptoms of decline as well as reduction of molecular markers identified in Tau+ mice.

Chapter 6 Future Directions

Future studies in aging mice

Based on the studies conducted in Chapter 2, the use of the SY1 as used in Chapter 4 for the amelioration of age-induced cognitive dysfunction is warranted. By creating a dosing curve, in which animals begin dosing with the inhibitor at 6, 12, 18, or 20 months and are tested for cognitive dysfunction at 24 months, an essential time point could be determined for the preservation of cognitive function in non-transgenic aging mice. Once said time point is determined, molecular changes with the CypD inhibitor could be determined. ROS and mitochondrial ETC activity are obvious targets of intrigue. However, new technology available, including a 2-photon microscope, could allow for the tracking of synaptic formation and loss over the time course of drug administration [349]. Based on our studies tying mitochondrial failure to synaptic loss, understanding the specific changes of the neural network in aging could explain how mitochondrial failure leads to cognitive impairment. Further, studying these same networks under the effects of CypD inhibition could reveal probative information about how this compound is working to reverse cognitive impairment.

Further mechanistic data could be gathered on the cognitive changes observed in aging mice. Based on changes to GSK3β signaling seen in AD mice, this pathway should be investigated in aging mice. We would expect that aging mice would show decreased Akt activity, as measured by decreased p-Akt on a western blot, and increased GSK3β activity, as measured by increased p(tyr216)GSK3β and decreased p(ser9)GSK3β.

Additionally, measuring calcium induced mitochondrial swelling in an age dependent manner would help to establish mPTP opening in these aging mice beyond just the increase in CypD expression.

Future studies in Alzheimer's disease mice

P301S Tau mice are only one model of tau-induced AD. Testing the effect of CypD in another model would strengthen hypothesis that CypD and HPT are related. One model that might be particularly beneficial for this is the rTGTauEC model, which is a slow developing model that shows HTFs, synaptic and neuronal loss, and impaired cognitive functioning. These studies would confirm that the relationship between CypD-mPTP opening and HPT accumulations.

While this study, combined with previous work in the lab, identifies CypD as a therapeutic target in Tau-induced AD and Aβ-induced AD, CypD has not been tested in a mouse model containing both Aβ and HTFs.

Further establishing the effects of CypD Inhibition

While this compound exerts its effects through inhibition of CypD, we would like to determine whether there is a systematic effect taking place outside of the mitochondria. Specifically, we would like to identify changes in signal transduction that may be occurring in the Tau+ and wild type mice treated with the CypD inhibitor. CypD OE mice showed changes in Akt and GSK3β activity, indicating that there is an effect of CypD expression or activity on signaling pathways. Thus, we hypothesize that there are likely changes in this signaling pathway that have not been identified.

Previous studies have not found an effect of CypD KO on LTP, an important indication that CypD KO does not impair neuronal signaling. For that reason, we hypothesize that there would be no negative impact of CypD inhibition on neuronal signaling. However, our lab has not tested LTP in the Tau+ mice, and doing these experiments could help to bolster the interpretations of the data presented herein, that CypD KO can improve learning and memory.

Toxicity studies for the CypD Inhibitor

While toxicity studies are not the priority with this compound, given our goal of establishing this compound as a candidate for clinical trials, toxicity testing is still a needed component. The earlier proposed time point studies could double as important toxicology studies necessary for this compound to move forward. While no obvious toxicity was registered in any animals in which this compound was used, and the compound was found non-toxic in very high doses in cell culture, formal toxicity studies will be necessary for any effort to move the inhibitor into clinical trials.

There are multiple protocols for assessing toxicity of compounds [350]. While most protocols demand both a rodent and non-rodent species for toxicity studies, the first step would be to complete rodent-based studies in mice. Historically, single dose acute toxicity has been determined by administering a single dose of variable amount to a group of animals and assessing the reaction over 14 days. LD_{50}, the dose toxic to 50% of subject animals, has largely been replaced with metrics that require fewer animals.

The up-and-down (UPD) approach is most commonly used by regulatory agencies. UPD protocols give single animals doses sequentially every 48 hours. Each subsequent dose is double the former dose. If an animal dies, an intermediate dose, one between the non-lethal and lethal dose, is chosen to start upon selection of a new animal.

Repeated dose toxicity tests take longer, a minimum of 28 days. After the 28 days, nearly all of the organs are retained for histological examination. A subgroup must be analyzed at no later than 14 days for immunotoxicity.

Sub chronic toxicity is measured by testing organs after 90 days of administration and chronic toxicity is a measure longer than 90 days. Mice sacrificed after the long-term study of the effect of the compound on cognitive impairment could be used for these chronic (mice dosed from

6, 12, or 18 months) and sub chronic (mice dose from 20 months) conditions. Many protocols recommend assessment of behavioral protocols as well. By using these mice in studies to test our hypotheses and toxicity studies, we would reduce the overall number of mice required in moving this compound from pre-clinical to clinical work.

Beyond toxicity testing, further time point testing is necessary. In these studies, mice were dosed at four months. This time point is after the elevation of HPT and after mild mitochondrial failure, but before any synaptic or neuronal loss. Behavior studies were run at six months, after which, animals were sacrificed and used for molecular studies. We did not confirm if the CypD inhibitor was effective in AD mice over a longer period of time.

The Role of CypD in Other Neurodegenerative Diseases

Given the important role of CypD in cognitive impairment and neurodegeneration established in these experiments, there is likely a role of CypD in other neurodegenerative diseases.

Huntington's disease

Huntington's disease (HD) is an autosomal dominant disease characterized by a pattern of CAG nucleotide repeats [351]. A person having more than 40 repeats will be diagnosed with HD, and the number of repeats is proportional to the age of onset of the disease; the highest reported number of repeats is about 250 [352]. HD leads to the accumulation of huntingtin protein [353]. HD leads to the death of neurons, most characteristically GABAergic neurons [354], which results in a movement disorder with dementia [355].

Huntingtin is a cytosolic protein that has a role in vesicular transport [356]. Mutant huntingtin disrupts axonal transport [357], N-methyl-D-aspartate receptor (NMDAR) signaling [358], and mitochondrial function [359-361]. Mitochondria from HD patients and models undergo increased fission. Additionally, huntingtin can be found in the matrix of mitochondria.

HD is characterized by calcium dyshomeostasis [362]. Mitochondria isolated from patients with HD or from animal models of HD show disrupted calcium uptake capacity in which the mPTP opens at a much lower concentration of calcium compared to healthy controls [363-367]. In HD patients, CypD was upregulated in a progressive, time dependent manner that correlated to the disease progression [361]. Upregulated CypD was also identified in BACHD mice that contain 97 CAG repeats [359]. This irregularity in mPTP opening combined with the increases in CypD expression suggest a role of CypD with potential therapeutic effects to reduce mitochondrial loss and neuronal death.

CypD KO in an R6/2B model of HD increased calcium buffering capacity, indicating a desensitization of the mPTP. However, CypD KO did not reduce weight loss or improve behavioral phenotypes measured for HD. Most importantly, R6/2B CypD KO mice did not survive longer than their R6/2B counterparts [368]. One possible interpretation of this data is that the mPTP is not involved in the HD phenotype. However, mitochondrial function and mitochondrial axonal transport were not assessed in the CypD KO mice. Mutant huntingtin protein impairs mitochondrial trafficking to the synapse, which may mask the effect of reduced mPTP opening. CypD therapeutics may be a necessary part of a drug regimen that also addresses trafficking dysfunction. R6/2B mice have a very rapid onset of HD like symptoms, and have a track record of poor predictive validity [369], which may warrant further testing in a different HD model.

Amyotrophic Lateral Sclerosis

Amyotrophic Lateral Sclerosis (ALS) is a neurodegenerative disease that is fatal within five years of symptom onset [370]. ALS is characterized by muscle weakness and loss of motor control [370], which is caused by degeneration of lower motor neurons in the cerebral cortex and spinal cord [371]. Ten percent of ALS cases are familial with a strong genetic component while 90% occur sporadically with an onset after 55 years of age [372].

ALS patients and models show significant mitochondrial morphology abnormalities [373]. Mitochondria from end plates of ALS patients showed increased mitochondrial volume [374], which has more been associated with mPTP opening. Further, mitochondria isolated from ALS show reduced ETC protein levels and activity [375]. Tissue from ALS patients reveals significant increases in ROS [376]. One of the familial mutations that causes ALS is in the mitochondrial super oxide dismutase (SOD1) gene [377], which further links ALS to mitochondrial dysfunction. The only current FDA treatment for ALS is a glutamate blocker trade name Riluzole; glutamate toxicity is often the result of increased calcium and the inability of mitochondria to buffer it.

Apoptosis in ALS is driven by p53 which, as previously discussed, acts as a regulator of CypD driven mPTP opening [378]. CypD expression levels are increased in models of ALS [376], which could explain the increased mPTP opening that leads to mitochondrial swelling at end plates. Further, CsA improved outcomes for ALS mouse models [379, 380], although, given the immunosuppressive effects of CsA, it is not possible to fully attribute that success to CypD inhibition and reduced mPTP pore opening. CsA is currently in phase II clinical trials for treatment of ALS under the trade name Mitoguard. In G93A high-mSOSD1 mice, a model of ALS, CypD KO delayed the onset of ALS-like symptoms and slowed the progression of the disease after onset [381]. In the same model, CypD KO reduced ROS levels [376]. In a second model of ALS based on SOD1 mutations, CypD KO improved calcium buffering capacity, increased ATP synthesis, and reduced mitochondrial swelling, while also reducing protein aggregation in the cytosol [382].

Based on the excellent results in CypD KO mice, further study with CypD specific inhibitors is indicated in ALS.

Parkinson's disease

Parkinson's disease (PD) is a neurodegenerative disorder characterized by bradykinesia. PD is most commonly associated with tremors [383] . Neuronal loss is most profound in the

dopaminergic neurons of the substantia nigra, but is apparent in other brain regions as well [384]. Less than 10% of PD is familial, with the majority having a sporadic onset after the age of 50 [385]. Molecularly, PD is characterized by the formation of Lewy bodies in the cytoplasm, mostly composed of α-synuclein [386, 387].

α-synuclein aggregation has been proven to directly cause the opening of the mPTP which can be blocked via CsA [388], indicating that α-synuclein likely works through CypD. In a model of PD in which C57BL/6 mice express human A53T-mutant α-synuclein, CypD KO delayed the onset of PD-like symptoms and extended lifespans [389]. In a PD model based on mutation of the motor neuron desecration 2 (MND2) gene, mice are more sensitive to mPTP opening. However, CypD KO did not improve outcomes [390], indicating that the PD model of choice will be important for further characterization of the role of CypD and mPTP opening. Human derived cell lines may help to clarify discrepancies identified here.

Final Conclusions

CypD has roles in many neurodegenerative diseases, likely including some that are not discussed here. Further development of SY1 into a feasible therapeutic option, as well as further study of the role of CypD and mitochondrial dynamics in the brain, will be likely to have a high impact on patient populations.

References

1. McKhann, G., et al., *Clinical diagnosis of Alzheimer's disease: report of the NINCDS-ADRDA Work Group under the auspices of Department of Health and Human Services Task Force on Alzheimer's Disease.* Neurology, 1984. **34**(7): p. 939-44.
2. *United States GDP | 1960-2016.* Trading Economics, World Bank.
3. *Latest Alzheimer's Facts and Figures.* Alzheimer's Association.
4. Menendez, J.A. and J. Joven, *Energy metabolism and metabolic sensors in stem cells: the metabostem crossroads of aging and cancer.* Adv Exp Med Biol, 2014. **824**: p. 117-40.
5. Bernardes de Jesus, B. and M.A. Blasco, *Telomerase at the intersection of cancer and aging.* Trends Genet, 2013. **29**(9): p. 513-20.
6. Falandry, C., et al., *Biology of cancer and aging: a complex association with cellular senescence.* J Clin Oncol, 2014. **32**(24): p. 2604-10.
7. Bao, Q., et al., *Aging and age-related diseases--from endocrine therapy to target therapy.* Mol Cell Endocrinol, 2014. **394**(1-2): p. 115-8.
8. Vuica, A., et al., *Aging and a long-term diabetes mellitus increase expression of 1 alpha-hydroxylase and vitamin D receptors in the rat liver.* Exp Gerontol, 2015. **72**: p. 167-76.
9. Camici, G.G., et al., *Molecular mechanism of endothelial and vascular aging: implications for cardiovascular disease.* Eur Heart J, 2015. **36**(48): p. 3392-403.
10. North, B.J. and D.A. Sinclair, *The intersection between aging and cardiovascular disease.* Circ Res, 2012. **110**(8): p. 1097-108.
11. Kato, Y., et al., *Cardioembolic stroke is the most serious problem in the aging society: Japan standard stroke registry study.* J Stroke Cerebrovasc Dis, 2015. **24**(4): p. 811-4.
12. Arsava, E.M., et al., *The detrimental effect of aging on leptomeningeal collaterals in ischemic stroke.* J Stroke Cerebrovasc Dis, 2014. **23**(3): p. 421-6.
13. Bobela, W., P. Aebischer, and B.L. Schneider, *Alphalpha-Synuclein as a Mediator in the Interplay between Aging and Parkinson's Disease.* Biomolecules, 2015. **5**(4): p. 2675-700.
14. Rodriguez M, R.-S.C., Morales , Sanchez A, Sabate M, *Parkinson's disease as a result of aging.* Aging Cell, 2015. **14**(3): p. 293-308.
15. Giambra, L.M., et al., *Adult life span changes in immediate visual memory and verbal intelligence.* Psychol Aging, 1995. **10**(1): p. 123-39.
16. Freeman, S.H., et al., *Preservation of neuronal number despite age-related cortical brain atrophy in elderly subjects without Alzheimer disease.* J Neuropathol Exp Neurol, 2008. **67**(12): p. 1205-12.
17. Fjell, A.M. and K.B. Walhovd, *Structural brain changes in aging: courses, causes and cognitive consequences.* Rev Neurosci, 2010. **21**(3): p. 187-221.
18. !!! INVALID CITATION !!! [4-12].
19. Serrano-Pozo, A., et al., *Neuropathological alterations in Alzheimer disease.* Cold Spring Harb Perspect Med, 2011. **1**(1): p. a006189.
20. O'Brein, R.J., and Philip C. Wong, *Amyloid Precursor Protein Processing and Alzheimer's Disease.* Annu. Rev. Neurosci 2011. **34**: p. 185-204.
21. Selkoe, D.J., *Alzheimer's Disease Results from the Cerebral Accumulation and Cytotoxicity of Amyloid ß-protein.* Journal of Alzheimer's Disease 2001. **3**: p. 75-80.
22. Du, H. and S.S. Yan, *Mitochondrial permeability transition pore in Alzheimer's disease: cyclophilin D and amyloid beta.* Biochim Biophys Acta, 2010. **1802**(1): p. 198-204.
23. Du, H., et al., *Cyclophilin D deficiency attenuates mitochondrial and neuronal perturbation and ameliorates learning and memory in Alzheimer's disease.* Nat Med, 2008. **14**(10): p. 1097-105.

24. Du, H., et al., *Cyclophilin D deficiency improves mitochondrial function and learning/memory in aging Alzheimer disease mouse model.* Neurobiol Aging, 2011. **32**(3): p. 398-406.
25. Caspersen, C., et al., *Mitochondrial Abeta: a potential focal point for neuronal metabolic dysfunction in Alzheimer's disease.* Faseb j, 2005. **19**(14): p. 2040-1.
26. Barbier, M., D. Wallon, and I. Le Ber, *Monogenic inheritance in early-onset dementia: illustration in Alzheimer's disease and frontotemporal lobar dementia.* Geriatr Psychol Neuropsychiatr Vieil, 2018. **16**(3): p. 289-297.
27. Novotny, R., F. Langer, J. Mahler, A. Skodras, A. Vlachos, B. M. Wegenast-Braun, S. A. Kaeser, J. J. Neher, Y. S. Eisele, M. J. Pietrowski, K. P. R. Nilsson, T. Deller, M. Staufenbiel, B. Heimrich, and M. Jucker, *Conversion of Synthetic A to In Vivo Active Seeds and Amyloid Plaque Formation in a Hippocampal Slice Culture Model.* Journal of Neuroscience, 2016. **36**(18): p. 5084-5093.
28. Satoh, K., Sumiko Abe-Dohmae, Shinji Yokoyama, Peter St George-Hyslop, and Paul E. Fraser, *ATP-binding Cassette Transporter A7 (ABCA7) Loss of Function Alters Alzheimer Amyloid Processing.* Journal of Biological Chemistry J. Biol. Chem, 2015. **290**(40): p. 24152-4165.
29. Song, M., Jingji Jin, Jeong-Eun Lim, Jinghong Kou, Abhinandan Pattanayak, Jamaal A. Rehman, Hong-Duck Kim, Kazuki Tahara, Robert Lalonde, and Ken-Ichiro Fukuchi, *TLR4 Mutation Reduces Microglial Activation, Increases Aβ Deposits and Exacerbates Cognitive Deficits in a Mouse Model of Alzheimer's Disease.* Journal of Neuroinflammation J Neuroinflammation, 2011. **8**(1).
30. Yu, Y., Jue He, Yanbo Zhang, Huanmin Luo, Shenghua Zhu, Yi Yang, Tou Zhao, Jiang Wu, Yuangui Huang, Jiming Kong, Qingrong Tan, and Xin-Min Li, *Increased Hippocampal Neurogenesis in the Progressive Stage of Alzheimer's Disease Phenotype in an APP/PS1 Double Transgenic Mouse Model.* Hippocampus 2009. **19**(12): p. 1247-1253.
31. *Alzforum Networking for a Cure.* Alzforum Networking for a Cure. **Biomedical Research Forum**.
32. Wiley, C.A., *Imaging Brain Amyloid in Alzheimer's Disease With Pittsburgh Compound-B.* Yearbook of Pathology and Laboratory Medicine 2004: p. 190-191.
33. Wiley, C.A., Brian J. Lopresti, Sriram Venneti, Julie Price, William E. Klunk, Steven T. Dekosky, and Chester A. Mathis, *Carbon 11–Labeled Pittsburgh Compound B and Carbon 11–Labeled (R)-PK11195 Positron Emission Tomographic Imaging in Alzheimer Disease.* Arch Neurol Archives of Neurology, 2009. **66**(1).
34. Morris, J.C., Catherine M. Roe, Elizabeth A. Grant, Denise Head, Martha Storandt, Alison M. Goate, Anne M. Fagan, David M. Holtzman, and Mark A. Mintun, *Pittsburgh Compound B Imaging and Prediction of Progression From Cognitive Normality to Symptomatic Alzheimer Disease.* Arch Neurol Archives of Neurology, 2009. **66**(12).
35. Mcnamee, R.L., S.-H. Yee, J. C. Price, W. E. Klunk, B. Rosario, L. Weissfeld, S. Ziolko, M. Berginc, B. Lopresti, S. Dekosky, and C. A. Mathis, *Consideration of Optimal Time Window for Pittsburgh Compound B PET Summed Uptake Measurements.* Journal of Nuclear Medicine 2009. **50**(3): p. 348-355.
36. Grimmer, T., Gjermund Henriksen, Hans-Jürgen Wester, Hans Förstl, William E. Klunk, Chester A. Mathis, Alexander Kurz, and Alexander Drzezga, *Clinical Severity of Alzheimer's Disease Is Associated with PIB Uptake in PET.* Neurobiology of Aging 2009. **30**(12): p. 1902-1909.
37. Rodrigue, K.M., et al., *beta-Amyloid burden in healthy aging: regional distribution and cognitive consequences.* Neurology, 2012. **78**(6): p. 387-95.
38. Wolk, D.A., and William E. Klunk., *Update on Amyloid Imaging: From Healthy Aging to Alzheimer's Disease.* Current Neurology and Neuroscience Reports Curr Neurol Neurosci Rep 2009. **9**(5): p. 345-352.
39. Nelissen, N., K. Van Laere, L. Thurfjell, R. Owenius, M. Vandenbulcke, M. Koole, G. Bormans, D. J. Brooks, and R. Vandenberghe, *Phase 1 Study of the Pittsburgh Compound B Derivative 18F-*

Flutemetamol in Healthy Volunteers and Patients with Probable Alzheimer Disease. Journal of Nuclear Medicine, 2009. **50**(8): p. 1251-1259.
40. Jack, C.R., V. J. Lowe, S. D. Weigand, H. J. Wiste, M. L. Senjem, D. S. Knopman, M. M. Shiung, J. L. Gunter, B. F. Boeve, B. J. Kemp, M. Weiner, and R. C. Petersen, *Serial PIB and MRI in Normal, Mild Cognitive Impairment and Alzheimer's Disease: Implications for Sequence of Pathological Events in Alzheimer's Disease.* Brain, 2009. **32**(5): p. 1355-1365.
41. Rabinovici, G.D., and W. J. Jagust, *Amyloid Imaging in Aging and Dementia: Testing the Amyloid Hypothesis In Vivo.* Behavioural Neurology, 2009. **21**(1-2): p. 117-128.
42. Chételat, G., Renaud La Joie, Nicolas Villain, Audrey Perrotin, Vincent De La Sayette, Francis Eustache, and Rik Vandenberghe, *Amyloid Imaging in Cognitively Normal Individuals, At-risk Populations and Preclinical Alzheimer's Disease.* NeuroImage: Clinical, 2013. **2**: p. 356-65.
43. Herrup, K., *The case for rejecting the amyloid cascade hypothesis.* Nat Neurosci, 2015. **18**(6): p. 794-9.
44. Avila, J., *Role of Tau Protein in Both Physiological and Pathological Conditions.* Physiological Reviews, 2004. **84**(2): p. 361-384.
45. Iqbal, K., Alejandra Del C. Alonso, She Chen, M. Omar Chohan, Ezzat El-Akkad, Cheng-Xin Gong, Sabiha Khatoon, Bin Li, Fei Liu, Abdur Rahman, Hitoshi Tanimukai, and Inge Grundke-Iqbal, *Tau Pathology in Alzheimer Disease and Other Tauopathies.* Biochimica Et Biophysica Acta (BBA) - Molecular Basis of Disease, 2005. **1739**(2-3): p. 198-210.
46. Lee, V.M., M. Goedert, and JQ Trojanowski, *Neurodegenerative Tauopathies.* Annu. Rev. Neurosci 2001. **24**: p. 1121-159.
47. Dixit, R., J. L. Ross, Y. E. Goldman, and E. L. F. Holzbaur, *Differential Regulation of Dynein and Kinesin Motor Proteins by Tau.* Science, 2008. **319**(5866): p. 1086-1089.
48. Drechsel, D.N., Hyman, A. A., Cobb, M. H. and Kirschner, M. W, *Modulation of the dynamic instability of tubulin assembly by the microtubule-associated protein tau.* Mol. Biol. Cell 1992. **3**: p. 1141-1154.
49. Kapitein, L.C., Kah Wai Yau, and Casper C. Hoogenraad, *Microtubule Dynamics in Dendritic Spines.* Microtubules: In Vivo Methods in Cell Biology 2010: p. 111-132.
50. Harada, A., K. Oguchi, S. Okabe, J. Kuno, S. Terada, T. Ohshima, R. Sato-Yoshitake, Y. Takei, T. Noda, and N. Hirokawa, *Altered Microtubule Organization in Small-calibre Axons of Mice Lacking Tau Protein.* Nature, 1994. **369**(6480): p. 488-491.
51. Dawson, H., Ferreira A, Ester MV, Ghoshal N, Binder LL, Viek MP, *Inhibition of neuronal maturation in primary hippocampal neuorons from tau deficient mice.* J. Cell Sci, 2011. **114**(6): p. 1179-1187.
52. Billingsley, M.L., and Randall L. Kincaid, *Regulated Phosphorylation and Dephosphorylation of Tau Protein: Effects on Microtubule Interaction, Intracellular Trafficking and Neurodegeneration.* Biochem. J. Biochemical Journal 1997. **323**(3): p. 577-591.
53. Wang, J.-Z., and Fei Liu, *Microtubule-associated Protein Tau in Development, Degeneration and Protection of Neurons.* Progress in Neurobiology 2008. **85**(2): p. 148-175.
54. Chen, F., Della David, Alessandra Ferrari, and Jurgen Gotz, *Posttranslational Modifications of Tau - Role in Human Tauopathies and Modeling in Transgenic Animals.* Current Drug Targets, 2004. **5**(6): p. 503-515.
55. Petry, F.R., Jérôme Pelletier, Alexis Bretteville, Françoise Morin, Frédéric Calon, Sébastien S. Hébert, Robert A. Whittington, and Emmanuel Planel, *Specificity of Anti-Tau Antibodies When Analyzing Mice Models of Alzheimer's Disease: Problems and Solutions.* PLoS One, 2014. **9**(5).
56. Götz, J., Amadeus Gladbach, Luis Pennanen, Janet Van Eersel, Andreas Schild, Della David, and Lars M. Ittner, *Animal Models Reveal Role for Tau Phosphorylation in Human Disease.* Biochimica et Biophysica Acta (BBA) - Bioenergetics, 2010. **1802**(10): p. 860-871.

57. Adams, S.J., Richard J.p. Crook, Michael Deture, Suzanne J. Randle, Amy E. Innes, Xin Z. Yu, Wen-Lang Lin, Brittany N. Dugger, Melinda Mcbride, Mike Hutton, Dennis W. Dickson, and Eileen Mcgowan., *Overexpression of Wild-Type Murine Tau Results in Progressive Tauopathy and Neurodegeneration.* The American Journal of Pathology 2009. **175**(4): p. 1598-1609.
58. Garcia, M.L., and Don W. Cleveland, *Going New Places Using an Old MAP: Tau, Microtubules and Human Neurodegenerative Disease.* Current Opinion in Cell Biology, 2001. **13**(1): p. 41-48.
59. Lindwall, G., and RD Cole., *Phosphorylation Affects the Ability of Tau Protein to Promote Microtubule Assembly.* Journal of Biological Chemistry, 1984. **259**(8): p. 5301-5305.
60. Alonso, A., T. Zaidi, I. Grundke-Iqbal, and K. Iqbal, *Abnormally Phosphorylated Tau from Alzheimer Disease Brain Depolymerizes Microtubules.* Neurobiology of Aging 1994. **15**: p. 5562-5566.
61. Ihara, Y., N. Nukina, R. Miura, and M. Ogawara, *Phosphorylated Tau Protein Is Integrated into Paired Helical Filaments in Alzheimer's Disease.* Alzheimer Disease and Associated Disorders 1987. **1**(3).
62. Grundke-Iqbal, I., K. Iqbal, Y-C Tung, M. Quinlan, Hm Wisniewski, and Li Binder, *Abnormal Phosphorylation of the Microtubule-associated Protein? (tau) in Alzheimer Cytoskeletal Pathology.* Alzheimer Disease and Associated Disorders 1987. **83**(13): p. 4913-4917.
63. Hasegawa, M., M. Morishima-Kawashima, K. Taiko, M. Suzuki, K. Titani, and Y. Ihara, *Protein Sequence and Mass Spectrometric Analyses of Tau in the Alzheimer's Disease Brain.* J Biol Chem, 1992. **267**(24): p. 17047-17054.
64. Morishima-Kawashima, M., Masato Hasegawa, Koji Takio, Masami Suzuki, Hirotaka Yoshida, Atsushi Watanabe, Koiti Titani, and Yasuo Ihara, *Hyperphosphorylation of Tau in PHF.* Neurobiology of Aging, 1995. **16**(3): p. 365-371.
65. Hanger, D.P., H. L. Byers, S. Wray, K.-Y. Leung, M. J. Saxton, A. Seereeram, C. H. Reynolds, M. A. Ward, and B. H. Anderton, *Novel Phosphorylation Sites in Tau from Alzheimer Brain Support a Role for Casein Kinase 1 in Disease Pathogenesis.* Journal of Biological Chemistry, 2007. **282**(32): p. 23645-23654.
66. Hanger, D.P., Joanna C. Betts, Thérèse L. F. Loviny, Walter P. Blackstock, and Brian H. Anderton, *New Phosphorylation Sites Identified in Hyperphosphorylated Tau (Paired Helical Filament-Tau) from Alzheimer's Disease Brain Using Nanoelectrospray Mass Spectrometry.* Journal of Neurochemistry 2002. **71**(6): p. 2465-2476.
67. Iqbal, K., et al., *Tau in Alzheimer disease and related tauopathies.* Curr Alzheimer Res, 2010. **7**(8): p. 656-64.
68. Chiu, M.J., et al., *Plasma Tau Levels in Cognitively Normal Middle-Aged and Older Adults.* Front Aging Neurosci, 2017. **9**: p. 51.
69. Peters, A., U. Schweiger, L. Pellerin, C. Hubold, KM Oltmanns, M. Conrad, B. Schultes, J. Born, and HL Fehm, *The Selfish Brain: Competition for Energy Resources.* Neuroscience & Biobehavioral Reviews, 2004. **28**(2): p. 143-180.
70. G.I., K., *Non-Invasive Methods for Studying Brain Energy Metabolism: What They Show and What It Means.* Developmental Neuroscience Dev Neuroscience, 2000. **22**(5-6): p. 418-428.
71. Kozloski, J., *Closed-Loop Brain Model of Neocortical Information-Based Exchange.* Front. Neuroanat. Frontiers in Neuroanatomy 2016. **10**.
72. Harris, J.J., Renaud Jolivet, and David Attwell, *Synaptic Energy Use and Supply.* Neuron, 2012. **75**(5): p. 762-777.
73. Ahmed, W.W., and Taher A. Saif, *Active Transport of Vesicles in Neurons Is Modulated by Mechanical Tension.* Sci. Rep. Scientific Reports, 2014. **4**.
74. Hirokawa, N., and Reiko Takemura, *Molecular Motors and Mechanisms of Directional Transport in Neurons.* Nature Reviews Neuroscience Nat Rev Neurosci, 2005. **6**(3): p. 201-214.

75. Frey, E., *Physics in Cell Biology: On the Physics of Biopolymers and Molecular Motors.* ChemPhysChem 2002. **3**(3): p. 270.
76. Wai, T., and Thomas Langer, *Mitochondrial Dynamics and Metabolic Regulation.* Trends in Endocrinology and; Metabolism 2016. **27**(2): p. 105-117.
77. Chen, H., and D. C. Chan, *Mitochondrial Dynamics-fusion, Fission, Movement, and Mitophagy-in Neurodegenerative Diseases.* Human Molecular Genetics 2009. **18**.
78. Santos, R., SC Correia, X. Wang, G. Perry, MA Smith, PI Morera, and X. Zhu, *A Synergistic Dysfunction of Mitochondrial Fission/fusion Dynamics and Mitophagy in Alzheimer's Disease.* Journal of Alzheimer's Disease, 2010. **20**(2): p. 1-12.
79. Van Laar, V.S., and Sarah B. Berman, *The Interplay of Neuronal Mitochondrial Dynamics and Bioenergetics: Implications for Parkinson's Disease.* Neurobiology of Disease, 2013. **51**: p. 43-55.
80. Vives-Bauza, C., and Serge Przedborski, *Mitophagy: The Latest Problem for Parkinson's Disease.* Trends in Molecular Medicine 2011. **17**(3): p. 158-65.
81. Ni, H.-M., Jessica A. Williams, and Wen-Xing Ding, *Mitochondrial Dynamics and Mitochondrial Quality Control.* Redox Biology 2015. **4**: p. 6-13.
82. Chen, H., and David C. Chan, *Critical Dependence of Neurons on Mitochondrial Dynamics.* Current Opinion in Cell Biology 2006. **18**(4): p. 453-459.
83. Campello, S., and Luca Scorrano, *Mitochondrial Shape Changes: Orchestrating Cell Pathophysiology.* EMBO Rep EMBO Reports 2010. **11**(9): p. 678-684.
84. Reddy, P.H., *Abnormal Tau, Mitochondrial Dysfunction, Impaired Axonal Transport of Mitochondria, and Synaptic Deprivation in Alzheimer's Disease.* Brain Research 2011. **14**(15): p. 136-148.
85. Palmer, A.M., *Neuroprotective Therapeutics for Alzheimer's Disease: Progress and Prospects.* Trends in Pharmacological Sciences, 2011. **32**(3): p. 141-147.
86. Sheng, B., Xinglong Wang, Bo Su, Hyoung-Gon Lee, Gemma Casadesus, George Perry, and Xiongwei Zhu, *Impaired Mitochondrial Biogenesis Contributes to Mitochondrial Dysfunction in Alzheimer's Disease.* Journal of Neurochemistry 2012. **120**(3): p. 419-429.
87. Young-Collier, K., M. McArdle, and JP Bennett, *The Dying of the Light: Mitochondrial Failure in Alzheimer's Disease.* Journal of Alzheimer's Disease 2012. **28**(4): p. 771-781.
88. Karbowski, M., and Albert Neutzner, *Neurodegeneration as a Consequence of Failed Mitochondrial Maintenance.* Acta Neuropathologica Acta Neuropathol 2011. **132**(2): p. 157-171.
89. Reddy, P.H., Raghav Tripathi, Quang Troung, Karuna Tirumala, Tejaswini P. Reddy, Vishwanath Anekonda, Ulziibat P. Shirendeb, Marcus J. Calkins, Arubala P. Reddy, Peizhong Mao, and Maria Manczak, *Abnormal Mitochondrial Dynamics and Synaptic Degeneration as Early Events in Alzheimer's Disease: Implications to Mitochondria-targeted Antioxidant Therapeutics.* Biochimica Et Biophysica Acta (BBA) - Molecular Basis of Disease 2012. **1822**(5): p. 639-649.
90. Wang, C., and Richard J. Gorgi, *The Role of Mitochondria in Apoptosis.* Annu. Rev. Genet. Annual Review of Genetics, 2009. **43**(1): p. 95-118.
91. Lustbader, J.W., et al., *ABAD directly links Abeta to mitochondrial toxicity in Alzheimer's disease.* Science, 2004. **304**(5669): p. 448-52.
92. Devi, L., et al., *Accumulation of amyloid precursor protein in the mitochondrial import channels of human Alzheimer's disease brain is associated with mitochondrial dysfunction.* J Neurosci, 2006. **26**(35): p. 9057-68.
93. Hansson Petersen, C.A., et al., *The amyloid beta-peptide is imported into mitochondria via the TOM import machinery and localized to mitochondrial cristae.* Proc Natl Acad Sci U S A, 2008. **105**(35): p. 13145-50.
94. Crouch, P.J., et al., *Copper-dependent inhibition of human cytochrome c oxidase by a dimeric conformer of amyloid-beta1-42.* J Neurosci, 2005. **25**(3): p. 672-9.

95. Chen, J.X. and S.S. Yan, *Role of mitochondrial amyloid-beta in Alzheimer's disease.* J Alzheimers Dis, 2010. **20 Suppl 2**: p. S569-78.
96. Du, H. and S. ShiDu Yan, *Unlocking the Door to Neuronal Woes in Alzheimer's Disease: Abeta and Mitochondrial Permeability Transition Pore.* Pharmaceuticals (Basel), 2010. **3**(6): p. 1936-1948.
97. Patching, S.G., *Roles of facilitative glucose transporter GLUT1 in [18F]FDG positron emission tomography (PET) imaging of human diseases.* Journal of Diagnostic Imaging in Therapy, 2015. **2**(1): p. 30-102.
98. Sun, X., L. Jin, and P. Ling, *Review of drugs for Alzheimer's disease.* Drug Discov Ther, 2012. **6**(6): p. 285-90.
99. Reiman, E.M., et al., *Preclinical evidence of Alzheimer's disease in persons homozygous for the epsilon 4 allele for apolipoprotein E.* N Engl J Med, 1996. **334**(12): p. 752-8.
100. Reiman, E.M., et al., *Declining brain activity in cognitively normal apolipoprotein E epsilon 4 heterozygotes: A foundation for using positron emission tomography to efficiently test treatments to prevent Alzheimer's disease.* Proc Natl Acad Sci U S A, 2001. **98**(6): p. 3334-9.
101. Pimplikar, S.W., *Reassessing the Amyloid Cascade Hypothesis of Alzheimer's Disease." The International Journal of Biochemistry & Cell Biology* The International Journal of Biochemistry & Cell Biology, 2009. **41**(6): p. 1261-1268.
102. Oddo, S., Antonella Caccamo, Jason D. Shepherd, M.paul Murphy, Todd E. Golde, Rakez Kayed, Raju Metherate, Mark P. Mattson, Yama Akbari, and Frank M. Laferla, *Triple-Transgenic Model of Alzheimer's Disease with Plaques and Tangles.* Neuron, 2003. **39**(3): p. 409-421.
103. Oddo, S., et al., *Triple-transgenic model of Alzheimer's disease with plaques and tangles: intracellular Abeta and synaptic dysfunction.* Neuron, 2003. **39**(3): p. 409-21.
104. Elder, G.A., Miguel A. Gama Sosa, and Rita De Gasperi, *Transgenic Mouse Models of Alzheimer's Disease.* Mount Sinai Journal of Medicine: A Journal of Translational and Personalized Medicine Mt Sinai J Med, 2012. **77**(1): p. 69-81.
105. Laferla, F.M., and K. N. Green, *Animal Models of Alzheimer Disease.* Cold Spring Harbor Perspectives in Medicine, 2012. **2**(11).
106. Webster, S.J., Adam D. Bachstetter, Peter T. Nelson, Frederick A. Schmitt, and Linda J. Van Eldik, *Using Mice to Model Alzheimer's Dementia: An Overview of the Clinical Disease and the Preclinical Behavioral Changes in 10 Mouse Models.* Front. Genet. Frontiers in Genetics, 2014. **5**.
107. Laferla, F.M., and Salvatore Oddo, *Alzheimer's Disease: Aβ, Tau and Synaptic Dysfunction.* Trends in Molecular Medicine 2005. **11**(4): p. 170-176.
108. yao, J., R. W. Irwin, L. Zhao, J. Nilsen, R. T. Hamilton, and R. D. Brinton, *Mitochondrial Bioenergetic Deficit Precedes Alzheimer's Pathology in Female Mouse Model of Alzheimer's Disease.* Proceedings of the National Academy of Sciences 2009. **106**(34): p. 14670-14675.
109. Resende, R., Paula Isabel Moreira, Teresa Proença, Atul Deshpande, Jorge Busciglio, Cláudia Pereira, and Catarina Resende Oliveira, *Brain Oxidative Stress in a Triple-transgenic Mouse Model of Alzheimer Disease.* Free Radical Biology and Medicine 2008. **44**(12): p. 2051-2057.
110. Verstreken, P., Cindy V. Ly, Koen J.t. Venken, Tong-Wey Koh, Yi Zhou, and Hugo J. Bellen, *Synaptic Mitochondria Are Critical for Mobilization of Reserve Pool Vesicles at Drosophila Neuromuscular Junctions.* Neuron, 2005. **47**(3): p. 365-378.
111. Du, H., Lan Guo, and Shirley Shidu Yan, *Synaptic Mitochondrial Pathology in Alzheimer's Disease.* Antioxidants and Redox Signaling 2012. **16**(12): p. 1467-1475.
112. Du, H., L. Guo, S. Yan, A. A. Sosunov, G. M. Mckhann, and S. Shidu Yan, *Early Deficits in Synaptic Mitochondria in an Alzheimer's Disease Mouse Model.* Proceedings of the National Academy of Sciences, 2010. **107**(43): p. 18670-8675.
113. Lee, J., Samantha Giordano, and Jianhua Zhang, *Autophagy, Mitochondria and Oxidative Stress: Cross-talk and Redox Signalling.* Biochem. J. Biochemical Journa, 2012. **441**(2): p. 523-540.

114. Lee, S.H., K.-R. Kim, S.-Y. Ryu, S. Son, H. S. Hong, I. Mook-Jung, S.-H. Lee, and W.-K. Ho, *Impaired Short-Term Plasticity in Mossy Fiber Synapses Caused by Mitochondrial Dysfunction of Dentate Granule Cells Is the Earliest Synaptic Deficit in a Mouse Model of Alzheimer's Disease.* Journal of Neuroscience, 2012. **32**(17): p. 5953-5963.
115. Selfridge, J.E., Lezi E, Jianghua Lu, and Russell H. Swerdlow, *Role of Mitochondrial Homeostasis and Dynamics in Alzheimer's Disease.* Neurobiology of Disease, 2013. **51**: p. 3-12.
116. Rintoul G. L., R.I.J., *Mitochondrial trafficking and morphology in neuronal injury.* Biochim. Biophys. Acta, 2010. **1802**: p. 143-150.
117. *Mitochondrial Transport in Neurons: Impact on Synaptic Homeostasis and Neurodegeneration.* Nature Reviews Neuroscience, 2012.
118. Wang, X., and Thomas L. Schwarz, *Imaging Axonal Transport of Mitochondria.* Methods in Enzymology Mitochondrial Function, 2009: p. 319-333.
119. Wang, X., B. Su, S. L. Siedlak, P. I. Moreira, H. Fujioka, Y. Wang, G. Casadesus, and X. Zhu, *Amyloid- Overproduction Causes Abnormal Mitochondrial Dynamics via Differential Modulation of Mitochondrial Fission/fusion Proteins.* Proceedings of the National Academy of Sciences 2008. **105**(49): p. 19318-9323.
120. Baloyannis, S., *Mitochondrial Alterations in Alzheimer's Diseas.* J Alzheimers Dis 2006. **9**(2): p. 119-126.
121. Young B, L.J., Stevens A, Heath JW, *Wheater's Functional Histology: A Text and Atlas*. 6 ed. 2013: Elsevier. 464.
122. Hirai, K., G. Aliev, A. Nunomura, H. Fujioka, RL Russell, CS Atwood, AB Johnson, Y. Kress, HV Vinters, M. Tabaton, S. Shimohama, AD Cash, SL Siedlak, PL Harris, PK Jones, RB Petersen, G. Perry, and MA Smith, *Mitochondrial Abnormalities in Alzheimer's Disease.* Journal of Neuroscience 2001. **21**(9): p. 3017-3023.
123. Melov S, A.P., Morten K, Johnson F, Golden TR, Hinerfeld D, Schilling B, Mavros C, Masters CL, Volitakis I, Li QX, Laughton K, Hubbard A, Cherny RA, Gibson B, Bush AI, *Mitochondrial oxidative stress causes hyperphosphorylation of tau.* Plos One, 2007. **2**(6).
124. Pias, E.K., O. Y. Ekshyyan, C. A. Rhoads, J. Fuseler, L. Harrison, and T. Y. Aw, *Differential Effects of Superoxide Dismutase Isoform Expression on Hydroperoxide-induced Apoptosis in PC-12 Cells.* Journal of Biological Chemistry J. Biol. Chem, 2003. **278**(15): p. 13294-13301.
125. Atlante, A., G. Amadoro, A. Bobba, L. De Bari, V. Corsetti, G. Pappalardo, E. Marra, P. Calissano, and S. Passarella, *A Peptide Containing Residues 26–44 of Tau Protein Impairs Mitochondrial Oxidative Phosphorylation Acting at the Level of the Adenine Nucleotide Translocator.* Biochimica Et Biophysica Acta (BBA) - Bioenergetics 2008. **1777**(10): p. 1289-1300.
126. Amadoro, G., V. Corsetti, A. Stringaro, M. Colone, and P. Calissano, *A NH2 Tau Fragment Targets Neuronal Mitochondria at AD Synapses: Possible Implications for Neurodegeneration.* Journal of Alzheimer's Disease 2010. **21**(2): p. 445-470.
127. Quintanilla, R.A., T. A. Matthews-Roberson, P. J. Dolan, and G. V. W. Johnson, *Caspase-cleaved Tau Expression Induces Mitochondrial Dysfunction in Immortalized Cortical Neurons: Implications for the Pathogenesis of Alzheimer's disease.* Journal of Biological Chemistry 2009. **284**(28): p. 18754-18766.
128. Amadoro, G., V. Corsetti, M.t. Ciotti, F. Florenzano, S. Capsoni, G. Amato, and P. Calissano, *Endogenous Aβ Causes Cell Death via Early Tau Hyperphosphorylation.* Neurobiology of Aging 2011. **32**(6): p. 969-990.
129. Chou, J.L., Deepa V. Shenoy, Nicy Thomas, Pankaj K. Choudhary, Frank M. Laferla, Steven R. Goodman, and Gail A.m. Breen, *Early Dysregulation of the Mitochondrial Proteome in a Mouse Model of Alzheimer's Disease.* Journal of Proteomics 2011. **74**(4): p. 466-479.

130. Terwel, D., R. Lasrado, J. Snauwaert, E. Vandeweert, C. Van Haesendonck, P. Borghgraef, and F. Van Leuven, *Changed Conformation of Mutant Tau-P301L Underlies the Moribund Tauopathy, Absent in Progressive, Nonlethal Axonopathy of Tau-4R/2N Transgenic Mice.* Journal of Biological Chemistry 2005. **280**(5): p. 3963-3973.
131. Rhein, V., X. Song, A. Wiesner, L. M. Ittner, G. Baysang, F. Meier, L. Ozmen, H. Bluethmann, S. Drose, U. Brandt, E. Savaskan, C. Czech, J. Gotz, and A. Eckert, *Amyloid- and Tau Synergistically Impair the Oxidative Phosphorylation System in Triple Transgenic Alzheimer's Disease Mice.* Proceedings of the National Academy of Sciences 2009. **106**(47): p. 20057-20062.
132. Gilley, J., Anjan Seereeram, Kunie Ando, Suzanne Mosely, Simon Andrews, Martin Kerschensteiner, Thomas Misgeld, Jean-Pierre Brion, Brian Anderton, Diane P. Hanger, and Michael P. Coleman, *Age-dependent Axonal Transport and Locomotor Changes and Tau Hypophosphorylation in a "P301L" Tau Knockin Mouse.* Neurobiology of Aging, 2012. **33**(3).
133. Kutty, K.M., *Biological function of cholinesterase.* Clin Biochem, 1980. **13**(6): p. 239-43.
134. *How Is Alzheimer's Disease Treated?* Treatment of Alzheimer's Disease 2014; Available from: https://www.nia.nih.gov/health/how-alzheimers-disease-treated.
135. Lewerenz, J. and P. Maher, *Chronic Glutamate Toxicity in Neurodegenerative Diseases-What is the Evidence?* Front Neurosci, 2015. **9**: p. 469.
136. Collingridge, G.L., et al., *A nomenclature for ligand-gated ion channels.* Neuropharmacology, 2009. **56**(1): p. 2-5.
137. Luscher, C. and R.C. Malenka, *NMDA receptor-dependent long-term potentiation and long-term depression (LTP/LTD).* Cold Spring Harb Perspect Biol, 2012. **4**(6).
138. Olney, J.W., *Inciting excitotoxic cytocide among central neurons.* Adv Exp Med Biol, 1986. **203**: p. 631-45.
139. Choi, D.W., *Glutamate neurotoxicity and diseases of the nervous system.* Neuron, 1988. **1**(8): p. 623-34.
140. Lipton, S.A. and P.A. Rosenberg, *Excitatory amino acids as a final common pathway for neurologic disorders.* N Engl J Med, 1994. **330**(9): p. 613-22.
141. Meldrum, B. and J. Garthwaite, *Excitatory amino acid neurotoxicity and neurodegenerative disease.* Trends Pharmacol Sci, 1990. **11**(9): p. 379-87.
142. Mattson, M.P., et al., *beta-Amyloid peptides destabilize calcium homeostasis and render human cortical neurons vulnerable to excitotoxicity.* J Neurosci, 1992. **12**(2): p. 376-89.
143. Scimemi, A., et al., *Amyloid-beta1-42 slows clearance of synaptically released glutamate by mislocalizing astrocytic GLT-1.* J Neurosci, 2013. **33**(12): p. 5312-8.
144. Choi, D.W., *Ionic dependence of glutamate neurotoxicity.* J Neurosci, 1987. **7**(2): p. 369-79.
145. Choi, D.W., J.Y. Koh, and S. Peters, *Pharmacology of glutamate neurotoxicity in cortical cell culture: attenuation by NMDA antagonists.* J Neurosci, 1988. **8**(1): p. 185-96.
146. Koh, J.Y. and D.W. Choi, *Selective blockade of non-NMDA receptors does not block rapidly triggered glutamate-induced neuronal death.* Brain Res, 1991. **548**(1-2): p. 318-21.
147. Tymianski, M., et al., *Source specificity of early calcium neurotoxicity in cultured embryonic spinal neurons.* J Neurosci, 1993. **13**(5): p. 2085-104.
148. Tripathi, A. and S.K. Chaube, *High cytosolic free calcium level signals apoptosis through mitochondria-caspase mediated pathway in rat eggs cultured in vitro.* Apoptosis, 2012. **17**(5): p. 439-48.
149. Tarasov, A.I., E.J. Griffiths, and G.A. Rutter, *Regulation of ATP production by mitochondrial Ca(2+).* Cell Calcium, 2012. **52**(1): p. 28-35.
150. Ermak, G. and K.J. Davies, *Calcium and oxidative stress: from cell signaling to cell death.* Mol Immunol, 2002. **38**(10): p. 713-21.

151. Lemasters, J.J., Tom P. Theruvath, Zhi Zhong, and Anna-Liisa Nieminen, *Mitochondrial Calcium and the Permeability Transition in Cell Death.* Biochimica Et Biophysica Acta (BBA) - Bioenergetics 2009. **1787**(11): p. 1395-1401.
152. Giorgi, C., Federica Baldassari, Angela Bononi, Massimo Bonora, Elena De Marchi, Saverio Marchi, Sonia Missiroli, Simone Patergnani, Alessandro Rimessi, Jan M. Suski, Mariusz R. Wieckowski, and Paolo Pinton, *Mitochondrial Ca2 and Apoptosis.* Cell Calcium, 2012. **52**(1): p. 36-43.
153. Dubinsky, J.M., and Yael Levi, *Calcium-induced Activation of the Mitochondrial Permeability Transition in Hippocampal Neurons.* J. Neurosci. Res. Journal of Neuroscience Research, 1998. **53**(6): p. 728-741.
154. Kroemer, G., L. Galluzzi, and C. Brenner, *Mitochondrial Membrane Permeabilization in Cell Death.* Physiological Reviews, 2007. **87**(1): p. 99-163.
155. Laferla, F.M., *Calcium Dyshomeostasis and Intracellular Signalling in Alzheimer's Disease.* Nature Reviews Neuroscience 2002. **3**(11): p. 862-872.
156. Fischer, G., H. Bang, and C. Mech, *[Determination of enzymatic catalysis for the cis-trans-isomerization of peptide binding in proline-containing peptides].* Biomed Biochim Acta, 1984. **43**(10): p. 1101-11.
157. Handschumacher, R.E., et al., *Cyclophilin: a specific cytosolic binding protein for cyclosporin A.* Science, 1984. **226**(4674): p. 544-7.
158. Gothel, S.F. and M.A. Marahiel, *Peptidyl-prolyl cis-trans isomerases, a superfamily of ubiquitous folding catalysts.* Cell Mol Life Sci, 1999. **55**(3): p. 423-36.
159. Arevalo-Rodriguez, M., et al., *Prolyl isomerases in yeast.* Front Biosci, 2004. **9**: p. 2420-46.
160. Marks, A.R., *Cellular functions of immunophilins.* Physiol Rev, 1996. **76**(3): p. 631-49.
161. Waldmeier, P.C., et al., *Cyclophilin D as a drug target.* Curr Med Chem, 2003. **10**(16): p. 1485-506.
162. Galat, A., *Peptidylprolyl cis/trans isomerases (immunophilins): biological diversity--targets--functions.* Curr Top Med Chem, 2003. **3**(12): p. 1315-47.
163. Dornan, J., P. Taylor, and M.D. Walkinshaw, *Structures of immunophilins and their ligand complexes.* Curr Top Med Chem, 2003. **3**(12): p. 1392-409.
164. Kallen, J., et al., *Structure of human cyclophilin and its binding site for cyclosporin A determined by X-ray crystallography and NMR spectroscopy.* Nature, 1991. **353**(6341): p. 276-9.
165. Ke, H.M., et al., *Crystal structure of recombinant human T-cell cyclophilin A at 2.5 A resolution.* Proc Natl Acad Sci U S A, 1991. **88**(21): p. 9483-7.
166. Helekar, S.A., et al., *Prolyl isomerase requirement for the expression of functional homo-oligomeric ligand-gated ion channels.* Neuron, 1994. **12**(1): p. 179-89.
167. Ansari, H., G. Greco, and J. Luban, *Cyclophilin A peptidyl-prolyl isomerase activity promotes ZPR1 nuclear export.* Mol Cell Biol, 2002. **22**(20): p. 6993-7003.
168. Brazin, K.N., et al., *Regulation of the tyrosine kinase Itk by the peptidyl-prolyl isomerase cyclophilin A.* Proc Natl Acad Sci U S A, 2002. **99**(4): p. 1899-904.
169. Min, L., D.B. Fulton, and A.H. Andreotti, *A case study of proline isomerization in cell signaling.* Front Biosci, 2005. **10**: p. 385-97.
170. Colgan, J., et al., *Cyclophilin A regulates TCR signal strength in CD4+ T cells via a proline-directed conformational switch in Itk.* Immunity, 2004. **21**(2): p. 189-201.
171. Luban, J., et al., *Human immunodeficiency virus type 1 Gag protein binds to cyclophilins A and B.* Cell, 1993. **73**(6): p. 1067-78.
172. Luban, J., *Absconding with the chaperone: essential cyclophilin-Gag interaction in HIV-1 virions.* Cell, 1996. **87**(7): p. 1157-9.

173. Bosco, D.A., et al., *Catalysis of cis/trans isomerization in native HIV-1 capsid by human cyclophilin A.* Proc Natl Acad Sci U S A, 2002. **99**(8): p. 5247-52.
174. Braaten, D., et al., *Cyclosporine A-resistant human immunodeficiency virus type 1 mutants demonstrate that Gag encodes the functional target of cyclophilin A.* J Virol, 1996. **70**(8): p. 5170-6.
175. Braaten, D., E.K. Franke, and J. Luban, *Cyclophilin A is required for an early step in the life cycle of human immunodeficiency virus type 1 before the initiation of reverse transcription.* J Virol, 1996. **70**(6): p. 3551-60.
176. Braaten, D. and J. Luban, *Cyclophilin A regulates HIV-1 infectivity, as demonstrated by gene targeting in human T cells.* Embo j, 2001. **20**(6): p. 1300-9.
177. Sokolskaja, E., D.M. Sayah, and J. Luban, *Target cell cyclophilin A modulates human immunodeficiency virus type 1 infectivity.* J Virol, 2004. **78**(23): p. 12800-8.
178. Liu, J., et al., *Calcineurin is a common target of cyclophilin-cyclosporin A and FKBP-FK506 complexes.* Cell, 1991. **66**(4): p. 807-15.
179. O'Keefe, S.J., et al., *FK-506- and CsA-sensitive activation of the interleukin-2 promoter by calcineurin.* Nature, 1992. **357**(6380): p. 692-4.
180. Foor, F., et al., *Calcineurin mediates inhibition by FK506 and cyclosporin of recovery from alpha-factor arrest in yeast.* Nature, 1992. **360**(6405): p. 682-4.
181. Liu, J., et al., *Inhibition of T cell signaling by immunophilin-ligand complexes correlates with loss of calcineurin phosphatase activity.* Biochemistry, 1992. **31**(16): p. 3896-901.
182. Breuder, T., et al., *Calcineurin is essential in cyclosporin A- and FK506-sensitive yeast strains.* Proc Natl Acad Sci U S A, 1994. **91**(12): p. 5372-6.
183. Mikol, V., J. Kallen, and M.D. Walkinshaw, *X-ray structure of a cyclophilin B/cyclosporin complex: comparison with cyclophilin A and delineation of its calcineurin-binding domain.* Proc Natl Acad Sci U S A, 1994. **91**(11): p. 5183-6.
184. Rycyzyn, M.A. and C.V. Clevenger, *The intranuclear prolactin/cyclophilin B complex as a transcriptional inducer.* Proc Natl Acad Sci U S A, 2002. **99**(10): p. 6790-5.
185. Obata, Y., et al., *Role of cyclophilin B in activation of interferon regulatory factor-3.* J Biol Chem, 2005. **280**(18): p. 18355-60.
186. Bergsma, D.J., et al., *The cyclophilin multigene family of peptidyl-prolyl isomerases. Characterization of three separate human isoforms.* J Biol Chem, 1991. **266**(34): p. 23204-14.
187. Andreeva, L., R. Heads, and C.J. Green, *Cyclophilins and their possible role in the stress response.* Int J Exp Pathol, 1999. **80**(6): p. 305-15.
188. Hamilton, G.S. and J.P. Steiner, *Immunophilins: beyond immunosuppression.* J Med Chem, 1998. **41**(26): p. 5119-43.
189. Mi, H., et al., *A nuclear RNA-binding cyclophilin in human T cells.* FEBS Lett, 1996. **398**(2-3): p. 201-5.
190. Taylor, P., et al., *Two structures of cyclophilin 40: folding and fidelity in the TPR domains.* Structure, 2001. **9**(5): p. 431-8.
191. Ratajczak, T., et al., *The cyclophilin component of the unactivated estrogen receptor contains a tetratricopeptide repeat domain and shares identity with p59 (FKBP59).* J Biol Chem, 1993. **268**(18): p. 13187-92.
192. Chang, H.C. and S. Lindquist, *Conservation of Hsp90 macromolecular complexes in Saccharomyces cerevisiae.* J Biol Chem, 1994. **269**(40): p. 24983-8.
193. Leverson, J.D. and S.A. Ness, *Point mutations in v-Myb disrupt a cyclophilin-catalyzed negative regulatory mechanism.* Mol Cell, 1998. **1**(2): p. 203-11.
194. Duina, A.A., H.M. Kalton, and R.F. Gaber, *Requirement for Hsp90 and a CyP-40-type cyclophilin in negative regulation of the heat shock response.* J Biol Chem, 1998. **273**(30): p. 18974-8.

195. Anderson, S.K., et al., *A cyclophilin-related protein involved in the function of natural killer cells.* Proc Natl Acad Sci U S A, 1993. **90**(2): p. 542-6.
196. Rinfret, A., et al., *The N-terminal cyclophilin-homologous domain of a 150-kilodalton tumor recognition molecule exhibits both peptidylprolyl cis-trans-isomerase and chaperone activities.* Biochemistry, 1994. **33**(7): p. 1668-73.
197. Montague, J.W., et al., *A calcium-dependent nuclease from apoptotic rat thymocytes is homologous with cyclophilin. Recombinant cyclophilins A, B, and C have nuclease activity.* J Biol Chem, 1994. **269**(29): p. 18877-80.
198. Montague, J.W., F.M. Hughes, Jr., and J.A. Cidlowski, *Native recombinant cyclophilins A, B, and C degrade DNA independently of peptidylprolyl cis-trans-isomerase activity. Potential roles of cyclophilins in apoptosis.* J Biol Chem, 1997. **272**(10): p. 6677-84.
199. Connern, C.P. and A.P. Halestrap, *Purification and N-terminal sequencing of peptidyl-prolyl cis-trans-isomerase from rat liver mitochondrial matrix reveals the existence of a distinct mitochondrial cyclophilin.* Biochem J, 1992. **284 (Pt 2)**: p. 381-5.
200. Fournier, N., G. Ducet, and A. Crevat, *Action of cyclosporine on mitochondrial calcium fluxes.* J Bioenerg Biomembr, 1987. **19**(3): p. 297-303.
201. Valasani, K.R., et al., *High-resolution crystal structures of two crystal forms of human cyclophilin D in complex with PEG 400 molecules.* Acta Crystallogr F Struct Biol Commun, 2014. **70**(Pt 6): p. 717-22.
202. Davis, T.L., et al., *Structural and biochemical characterization of the human cyclophilin family of peptidyl-prolyl isomerases.* PLoS Biol, 2010. **8**(7): p. e1000439.
203. Gutierrez-Aguilar, M. and C.P. Baines, *Structural mechanisms of cyclophilin D-dependent control of the mitochondrial permeability transition pore.* Biochim Biophys Acta, 2015. **1850**(10): p. 2041-7.
204. Crompton, M., S. Virji, and J.M. Ward, *Cyclophilin-D binds strongly to complexes of the voltage-dependent anion channel and the adenine nucleotide translocase to form the permeability transition pore.* Eur J Biochem, 1998. **258**(2): p. 729-35.
205. Kokoszka, J.E., et al., *The ADP/ATP translocator is not essential for the mitochondrial permeability transition pore.* Nature, 2004. **427**(6973): p. 461-5.
206. Baines, C.P., et al., *Voltage-dependent anion channels are dispensable for mitochondrial-dependent cell death.* Nat Cell Biol, 2007. **9**(5): p. 550-5.
207. Kwong, J.Q., et al., *Genetic deletion of the mitochondrial phosphate carrier desensitizes the mitochondrial permeability transition pore and causes cardiomyopathy.* Cell Death Differ, 2014. **21**(8): p. 1209-17.
208. Giorgio, V., et al., *Dimers of mitochondrial ATP synthase form the permeability transition pore.* Proc Natl Acad Sci U S A, 2013. **110**(15): p. 5887-92.
209. Alavian, K.N., et al., *An uncoupling channel within the c-subunit ring of the F1FO ATP synthase is the mitochondrial permeability transition pore.* Proc Natl Acad Sci U S A, 2014. **111**(29): p. 10580-5.
210. Gauba, E., L. Guo, and H. Du, *Cyclophilin D Promotes Brain Mitochondrial F1FO ATP Synthase Dysfunction in Aging Mice.* J Alzheimers Dis, 2017. **55**(4): p. 1351-1362.
211. Beutner, G., R.E. Alanzalon, and G.A. Porter, Jr., *Cyclophilin D regulates the dynamic assembly of mitochondrial ATP synthase into synthasomes.* Sci Rep, 2017. **7**(1): p. 14488.
212. Giorgio, V., et al., *Cyclophilin D modulates mitochondrial F0F1-ATP synthase by interacting with the lateral stalk of the complex.* J Biol Chem, 2009. **284**(49): p. 33982-8.
213. Kajitani, K., et al., *Crystal structure of human cyclophilin D in complex with its inhibitor, cyclosporin A at 0.96-A resolution.* Proteins, 2008. **70**(4): p. 1635-9.

214. Tanveer, A., et al., *Involvement of cyclophilin D in the activation of a mitochondrial pore by Ca2+ and oxidant stress.* Eur J Biochem, 1996. **238**(1): p. 166-72.
215. Clarke, S.J., G.P. McStay, and A.P. Halestrap, *Sanglifehrin A acts as a potent inhibitor of the mitochondrial permeability transition and reperfusion injury of the heart by binding to cyclophilin-D at a different site from cyclosporin A.* J Biol Chem, 2002. **277**(38): p. 34793-9.
216. Linard, D., et al., *Redox characterization of human cyclophilin D: identification of a new mammalian mitochondrial redox sensor?* Arch Biochem Biophys, 2009. **491**(1-2): p. 39-45.
217. Kohr, M.J., et al., *Characterization of potential S-nitrosylation sites in the myocardium.* Am J Physiol Heart Circ Physiol, 2011. **300**(4): p. H1327-35.
218. Gourlay, L.J., et al., *The three-dimensional structure of two redox states of cyclophilin A from Schistosoma mansoni. Evidence for redox regulation of peptidyl-prolyl cis-trans isomerase activity.* J Biol Chem, 2007. **282**(34): p. 24851-7.
219. Lebedev, I., et al., *A Novel In Vitro CypD-Mediated p53 Aggregation Assay Suggests a Model for Mitochondrial Permeability Transition by Chaperone Systems.* J Mol Biol, 2016. **428**(20): p. 4154-4167.
220. Hensley, K., et al., *A model for beta-amyloid aggregation and neurotoxicity based on free radical generation by the peptide: relevance to Alzheimer disease.* Proc Natl Acad Sci U S A, 1994. **91**(8): p. 3270-4.
221. Bores, G.M., et al., *Amyloid beta-peptides inhibit Na+/K+-ATPase: tissue slices versus primary cultures.* Brain Res Bull, 1998. **46**(5): p. 423-7.
222. Mark, R.J., et al., *Amyloid beta-peptide impairs ion-motive ATPase activities: evidence for a role in loss of neuronal Ca2+ homeostasis and cell death.* J Neurosci, 1995. **15**(9): p. 6239-49.
223. Abramov, A.Y., L. Canevari, and M.R. Duchen, *Beta-amyloid peptides induce mitochondrial dysfunction and oxidative stress in astrocytes and death of neurons through activation of NADPH oxidase.* J Neurosci, 2004. **24**(2): p. 565-75.
224. Morais Cardoso, S., R.H. Swerdlow, and C.R. Oliveira, *Induction of cytochrome c-mediated apoptosis by amyloid beta 25-35 requires functional mitochondria.* Brain Res, 2002. **931**(2): p. 117-25.
225. Moreira, P.I., et al., *Effect of amyloid beta-peptide on permeability transition pore: a comparative study.* J Neurosci Res, 2002. **69**(2): p. 257-67.
226. Moreira, P.I., et al., *Amyloid beta-peptide promotes permeability transition pore in brain mitochondria.* Biosci Rep, 2001. **21**(6): p. 789-800.
227. Shevtzova, E.F., E.G. Kireeva, and S.O. Bachurin, *Effect of beta-amyloid peptide fragment 25-35 on nonselective permeability of mitochondria.* Bull Exp Biol Med, 2001. **132**(6): p. 1173-6.
228. Gauba, E., et al., *Cyclophilin D deficiency attenuates mitochondrial F1Fo ATP synthase dysfunction via OSCP in Alzheimer's disease.* Neurobiol Dis, 2019. **121**: p. 138-147.
229. Du, H., Lan Guo, Fang Fang, Doris Chen, Alexander A. Sosunov, Guy M. Mckhann, Yilin Yan, Chunyu Wang, Hong Zhang, Jeffery D. Molkentin, Frank J. Gunn-Moore, Jean Paul Vonsattel, Ottavio Arancio, John Xi Chen, and Shi Du Yan, *Cyclophilin D Deficiency Attenuates Mitochondrial and Neuronal Perturbation and Ameliorates Learning and Memory in Alzheimer's Disease.* Nature Medicine 2008. **14**(10): p. 1097-1105.
230. Guo, L., et al., *Cyclophilin D deficiency rescues axonal mitochondrial transport in Alzheimer's neurons.* PLoS One, 2013. **8**(1): p. e54914.
231. Du, H., et al., *Cyclophilin D deficiency rescues Abeta-impaired PKA/CREB signaling and alleviates synaptic degeneration.* Biochim Biophys Acta, 2014. **1842**(12 Pt A): p. 2517-27.
232. Valasani, K.R., et al., *Structure based design, synthesis, pharmacophore modeling, virtual screening, and molecular docking studies for identification of novel cyclophilin D inhibitors.* J Chem Inf Model, 2014. **54**(3): p. 902-12.

233. Park, I., et al., *Discovery of non-peptidic small molecule inhibitors of cyclophilin D as neuroprotective agents in Abeta-induced mitochondrial dysfunction.* J Comput Aided Mol Des, 2017. **31**(10): p. 929-941.
234. Rao, V.K., E.A. Carlson, and S.S. Yan, *Mitochondrial permeability transition pore is a potential drug target for neurodegeneration.* Biochim Biophys Acta, 2014. **1842**(8): p. 1267-72.
235. Elkamhawy, A., et al., *Pyrazinyl ureas revisited: 1-(3-(Benzyloxy)pyrazin-2-yl)-3-(3,4-dichlorophenyl)urea, a new blocker of Abeta-induced mPTP opening for Alzheimer's disease.* Eur J Med Chem, 2018. **157**: p. 268-278.
236. Jia, Y.L., et al., *SS31, a Small Molecule Antioxidant Peptide, Attenuates beta-Amyloid Elevation, Mitochondrial/Synaptic Deterioration and Cognitive Deficit in SAMP8 Mice.* Curr Alzheimer Res, 2016. **13**(3): p. 297-306.
237. Wischik, C.M., P. C. Edwards, R. Y. Lai, M. Roth, and C. R. Harrington, *Selective Inhibition of Alzheimer Disease-like Tau Aggregation by Phenothiazines.* Proceedings of the National Academy of Sciences, 1996. **93**(20): p. 11213-11218.
238. Wischik, C., D. Horsley, JE Rickard, and CR Harrington, *Materials and Methods Relating to Protein Aggregation in Neurodegenerative Disease.* PCT International Application, 2002.
239. A. Crowe, W.H., C. Ballatore, R.L. Johnson, A.-M.L. Hogan, R. Huang, *The identification of aminothienopyridazine inhibitors of tau assembly by quantitative high-throughput screening.* Biochemistry, 2009. **48**: p. 7732–7745.
240. Wischik, C.M., Charles R. Harrington, and John M.d. Storey, *Tau-aggregation Inhibitor Therapy for Alzheimer's Disease.* Biochemical Pharmacology, 2014. **88**(4).
241. O'brien, J.T., M. J. Firbank, C. Davison, N. Barnett, C. Bamford, C. Donaldson, K. Olsen, K. Herholz, D. Williams, and J. Lloyd, *18F-FDG PET and Perfusion SPECT in the Diagnosis of Alzheimer and Lewy Body Dementias.* Journal of Nuclear Medicine 2014. **55**(12): p. 1959-1965.
242. Wischik, C.M., Peter Bentham, Damon J. Wischik, and Kwang Meng Seng, *O3-04-07: Tau Aggregation Inhibitor (TAI) Therapy with Rember™ Arrests Disease Progression in Mild and Moderate Alzheimer's Disease over 50 Weeks.* Alzheimer's & Dementia, 2008. **4**(4).
243. Yagi, H., et al., *Age-related deterioration of ability of acquisition in memory and learning in senescence accelerated mouse: SAM-P/8 as an animal model of disturbances in recent memory.* Brain Res, 1988. **474**(1): p. 86-93.
244. von Koch, C.S., et al., *Generation of APLP2 KO mice and early postnatal lethality in APLP2/APP double KO mice.* Neurobiol Aging, 1997. **18**(6): p. 661-9.
245. Mann, K.M., et al., *Independent effects of APOE on cholesterol metabolism and brain Abeta levels in an Alzheimer disease mouse model.* Hum Mol Genet, 2004. **13**(17): p. 1959-68.
246. Sullivan, P.M., et al., *Type III hyperlipoproteinemia and spontaneous atherosclerosis in mice resulting from gene replacement of mouse Apoe with human Apoe*2.* J Clin Invest, 1998. **102**(1): p. 130-5.
247. Sullivan, P.M., et al., *Targeted replacement of the mouse apolipoprotein E gene with the common human APOE3 allele enhances diet-induced hypercholesterolemia and atherosclerosis.* J Biol Chem, 1997. **272**(29): p. 17972-80.
248. Knouff, C., et al., *Apo E structure determines VLDL clearance and atherosclerosis risk in mice.* J Clin Invest, 1999. **103**(11): p. 1579-86.
249. Piedrahita, J.A., et al., *Generation of mice carrying a mutant apolipoprotein E gene inactivated by gene targeting in embryonic stem cells.* Proc Natl Acad Sci U S A, 1992. **89**(10): p. 4471-5.
250. Youmans, K.L., et al., *APOE4-specific changes in Abeta accumulation in a new transgenic mouse model of Alzheimer disease.* J Biol Chem, 2012. **287**(50): p. 41774-86.

251. Sun, Y., et al., *Glial fibrillary acidic protein-apolipoprotein E (apoE) transgenic mice: astrocyte-specific expression and differing biological effects of astrocyte-secreted apoE3 and apoE4 lipoproteins.* J Neurosci, 1998. **18**(9): p. 3261-72.
252. Raber, J., et al., *Isoform-specific effects of human apolipoprotein E on brain function revealed in ApoE knockout mice: increased susceptibility of females.* Proc Natl Acad Sci U S A, 1998. **95**(18): p. 10914-9.
253. Oakley, H., et al., *Intraneuronal beta-amyloid aggregates, neurodegeneration, and neuron loss in transgenic mice with five familial Alzheimer's disease mutations: potential factors in amyloid plaque formation.* J Neurosci, 2006. **26**(40): p. 10129-40.
254. Yamada, K., et al., *Abeta immunotherapy: intracerebral sequestration of Abeta by an anti-Abeta monoclonal antibody 266 with high affinity to soluble Abeta.* J Neurosci, 2009. **29**(36): p. 11393-8.
255. Saito, T., et al., *Potent amyloidogenicity and pathogenicity of Abeta43.* Nat Neurosci, 2011. **14**(8): p. 1023-32.
256. Fukuchi, K., et al., *High levels of circulating beta-amyloid peptide do not cause cerebral beta-amyloidosis in transgenic mice.* Am J Pathol, 1996. **149**(1): p. 219-27.
257. Herzig, M.C., et al., *Abeta is targeted to the vasculature in a mouse model of hereditary cerebral hemorrhage with amyloidosis.* Nat Neurosci, 2004. **7**(9): p. 954-60.
258. Tomiyama, T., et al., *A mouse model of amyloid beta oligomers: their contribution to synaptic alteration, abnormal tau phosphorylation, glial activation, and neuronal loss in vivo.* J Neurosci, 2010. **30**(14): p. 4845-56.
259. Zheng, H., et al., *beta-Amyloid precursor protein-deficient mice show reactive gliosis and decreased locomotor activity.* Cell, 1995. **81**(4): p. 525-31.
260. Ou-Yang, M.H., et al., *Axonal organization defects in the hippocampus of adult conditional BACE1 knockout mice.* Sci Transl Med, 2018. **10**(459).
261. Dominguez, D., et al., *Phenotypic and biochemical analyses of BACE1- and BACE2-deficient mice.* J Biol Chem, 2005. **280**(35): p. 30797-806.
262. Coomaraswamy, J., et al., *Modeling familial Danish dementia in mice supports the concept of the amyloid hypothesis of Alzheimer's disease.* Proc Natl Acad Sci U S A, 2010. **107**(17): p. 7969-74.
263. Vidal, R., et al., *Cerebral amyloid angiopathy and parenchymal amyloid deposition in transgenic mice expressing the Danish mutant form of human BRI2.* Brain Pathol, 2009. **19**(1): p. 58-68.
264. Jackson, R.J., et al., *Human tau increases amyloid beta plaque size but not amyloid beta-mediated synapse loss in a novel mouse model of Alzheimer's disease.* Eur J Neurosci, 2016. **44**(12): p. 3056-3066.
265. Andorfer, C., et al., *Hyperphosphorylation and aggregation of tau in mice expressing normal human tau isoforms.* J Neurochem, 2003. **86**(3): p. 582-90.
266. Maeda, S., et al., *Expression of A152T human tau causes age-dependent neuronal dysfunction and loss in transgenic mice.* EMBO Rep, 2016. **17**(4): p. 530-51.
267. Decker, J.M., et al., *The Tau/A152T mutation, a risk factor for frontotemporal-spectrum disorders, leads to NR2B receptor-mediated excitotoxicity.* EMBO Rep, 2016. **17**(4): p. 552-69.
268. Allen, B., et al., *Abundant tau filaments and nonapoptotic neurodegeneration in transgenic mice expressing human P301S tau protein.* J Neurosci, 2002. **22**(21): p. 9340-51.
269. Lewis, J., et al., *Neurofibrillary tangles, amyotrophy and progressive motor disturbance in mice expressing mutant (P301L) tau protein.* Nat Genet, 2000. **25**(4): p. 402-5.
270. Rockenstein, E., et al., *A novel triple repeat mutant tau transgenic model that mimics aspects of pick's disease and fronto-temporal tauopathies.* PLoS One, 2015. **10**(3): p. e0121570.
271. Platt, B., et al., *Abnormal cognition, sleep, EEG and brain metabolism in a novel knock-in Alzheimer mouse, PLB1.* PLoS One, 2011. **6**(11): p. e27068.

272. de Calignon, A., et al., *Propagation of tau pathology in a model of early Alzheimer's disease.* Neuron, 2012. **73**(4): p. 685-97.
273. Santacruz, K., et al., *Tau suppression in a neurodegenerative mouse model improves memory function.* Science, 2005. **309**(5733): p. 476-81.
274. Umeda, T., et al., *Neurodegenerative disorder FTDP-17-related tau intron 10 +16C --> T mutation increases tau exon 10 splicing and causes tauopathy in transgenic mice.* Am J Pathol, 2013. **183**(1): p. 211-25.
275. Bondulich, M.K., et al., *Tauopathy induced by low level expression of a human brain-derived tau fragment in mice is rescued by phenylbutyrate.* Brain, 2016. **139**(Pt 8): p. 2290-306.
276. Wheeler, J.M., et al., *High copy wildtype human 1N4R tau expression promotes early pathological tauopathy accompanied by cognitive deficits without progressive neurofibrillary degeneration.* Acta Neuropathol Commun, 2015. **3**: p. 33.
277. Kim, Y., et al., *Caspase-cleaved tau exhibits rapid memory impairment associated with tau oligomers in a transgenic mouse model.* Neurobiol Dis, 2016. **87**: p. 19-28.
278. Gumucio, A., L. Lannfelt, and L.N. Nilsson, *Lack of exon 10 in the murine tau gene results in mild sensorimotor defects with aging.* BMC Neurosci, 2013. **14**: p. 148.
279. Eckermann, K., et al., *The beta-propensity of Tau determines aggregation and synaptic loss in inducible mouse models of tauopathy.* J Biol Chem, 2007. **282**(43): p. 31755-65.
280. Terwel, D., et al., *Changed conformation of mutant Tau-P301L underlies the moribund tauopathy, absent in progressive, nonlethal axonopathy of Tau-4R/2N transgenic mice.* J Biol Chem, 2005. **280**(5): p. 3963-73.
281. Yoshiyama, Y., et al., *Synapse loss and microglial activation precede tangles in a P301S tauopathy mouse model.* Neuron, 2007. **53**(3): p. 337-51.
282. Grueninger, F., et al., *Phosphorylation of Tau at S422 is enhanced by Abeta in TauPS2APP triple transgenic mice.* Neurobiol Dis, 2010. **37**(2): p. 294-306.
283. Tatebayashi, Y., et al., *Tau filament formation and associative memory deficit in aged mice expressing mutant (R406W) human tau.* Proc Natl Acad Sci U S A, 2002. **99**(21): p. 13896-901.
284. Mocanu, M.M., et al., *The potential for beta-structure in the repeat domain of tau protein determines aggregation, synaptic decay, neuronal loss, and coassembly with endogenous Tau in inducible mouse models of tauopathy.* J Neurosci, 2008. **28**(3): p. 737-48.
285. Tanemura, K., et al., *Neurodegeneration with tau accumulation in a transgenic mouse expressing V337M human tau.* J Neurosci, 2002. **22**(1): p. 133-41.
286. Lewis, J., et al., *Enhanced neurofibrillary degeneration in transgenic mice expressing mutant tau and APP.* Science, 2001. **293**(5534): p. 1487-91.
287. Schindowski, K., et al., *Alzheimer's disease-like tau neuropathology leads to memory deficits and loss of functional synapses in a novel mutated tau transgenic mouse without any motor deficits.* Am J Pathol, 2006. **169**(2): p. 599-616.
288. Flunkert, S., et al., *Elevated levels of soluble total and hyperphosphorylated tau result in early behavioral deficits and distinct changes in brain pathology in a new tau transgenic mouse model.* Neurodegener Dis, 2013. **11**(4): p. 194-205.
289. Leyns, C.E.G., et al., *TREM2 deficiency attenuates neuroinflammation and protects against neurodegeneration in a mouse model of tauopathy.* Proc Natl Acad Sci U S A, 2017. **114**(43): p. 11524-11529.
290. Bemiller, S.M., et al., *TREM2 deficiency exacerbates tau pathology through dysregulated kinase signaling in a mouse model of tauopathy.* Mol Neurodegener, 2017. **12**(1): p. 74.
291. Colton, C.A., et al., *The effects of NOS2 gene deletion on mice expressing mutated human AbetaPP.* J Alzheimers Dis, 2008. **15**(4): p. 571-87.

292. Wilcock, D.M., et al., *Progression of amyloid pathology to Alzheimer's disease pathology in an amyloid precursor protein transgenic mouse model by removal of nitric oxide synthase 2.* J Neurosci, 2008. **28**(7): p. 1537-45.
293. Sagare, A.P., et al., *Pericyte loss influences Alzheimer-like neurodegeneration in mice.* Nat Commun, 2013. **4**: p. 2932.
294. Schneider, I., et al., *Mutant presenilins disturb neuronal calcium homeostasis in the brain of transgenic mice, decreasing the threshold for excitotoxicity and facilitating long-term potentiation.* J Biol Chem, 2001. **276**(15): p. 11539-44.
295. Wines-Samuelson, M., M. Handler, and J. Shen, *Role of presenilin-1 in cortical lamination and survival of Cajal-Retzius neurons.* Dev Biol, 2005. **277**(2): p. 332-46.
296. Hu, X., et al., *BACE1 deletion in the adult mouse reverses preformed amyloid deposition and improves cognitive functions.* J Exp Med, 2018. **215**(3): p. 927-940.
297. Willuweit, A., et al., *Early-onset and robust amyloid pathology in a new homozygous mouse model of Alzheimer's disease.* PLoS One, 2009. **4**(11): p. e7931.
298. Dewachter, I., et al., *Aging increased amyloid peptide and caused amyloid plaques in brain of old APP/V717I transgenic mice by a different mechanism than mutant presenilin1.* J Neurosci, 2000. **20**(17): p. 6452-8.
299. Savonenko, A., et al., *Episodic-like memory deficits in the APPswe/PS1dE9 mouse model of Alzheimer's disease: relationships to beta-amyloid deposition and neurotransmitter abnormalities.* Neurobiol Dis, 2005. **18**(3): p. 602-17.
300. Jankowsky, J.L., et al., *Co-expression of multiple transgenes in mouse CNS: a comparison of strategies.* Biomol Eng, 2001. **17**(6): p. 157-65.
301. Richards, J.G., et al., *PS2APP transgenic mice, coexpressing hPS2mut and hAPPswe, show age-related cognitive deficits associated with discrete brain amyloid deposition and inflammation.* J Neurosci, 2003. **23**(26): p. 8989-9003.
302. Saura, C.A., et al., *Loss of presenilin function causes impairments of memory and synaptic plasticity followed by age-dependent neurodegeneration.* Neuron, 2004. **42**(1): p. 23-36.
303. Herreman, A., et al., *Presenilin 2 deficiency causes a mild pulmonary phenotype and no changes in amyloid precursor protein processing but enhances the embryonic lethal phenotype of presenilin 1 deficiency.* Proc Natl Acad Sci U S A, 1999. **96**(21): p. 11872-7.
304. Arancio, O., et al., *RAGE potentiates Abeta-induced perturbation of neuronal function in transgenic mice.* Embo j, 2004. **23**(20): p. 4096-105.
305. Xiang, X., et al., *The Trem2 R47H Alzheimer's risk variant impairs splicing and reduces Trem2 mRNA and protein in mice but not in humans.* Mol Neurodegener, 2018. **13**(1): p. 49.
306. Kang, S.S., et al., *Behavioral and transcriptomic analysis of Trem2-null mice: not all knockout mice are created equal.* Hum Mol Genet, 2018. **27**(2): p. 211-223.
307. Wang, Y., et al., *TREM2 lipid sensing sustains the microglial response in an Alzheimer's disease model.* Cell, 2015. **160**(6): p. 1061-71.
308. Turnbull, I.R., et al., *Cutting edge: TREM-2 attenuates macrophage activation.* J Immunol, 2006. **177**(6): p. 3520-4.
309. Song, W.M., et al., *Humanized TREM2 mice reveal microglia-intrinsic and -extrinsic effects of R47H polymorphism.* J Exp Med, 2018. **215**(3): p. 745-760.
310. Lee, C.Y.D., et al., *Elevated TREM2 Gene Dosage Reprograms Microglia Responsivity and Ameliorates Pathological Phenotypes in Alzheimer's Disease Models.* Neuron, 2018. **97**(5): p. 1032-1048.e5.
311. Kim, H.Y., et al., *Intracerebroventricular Injection of Amyloid-beta Peptides in Normal Mice to Acutely Induce Alzheimer-like Cognitive Deficits.* J Vis Exp, 2016(109).

312. Schmid, S., et al., *Intracerebroventricular injection of beta-amyloid in mice is associated with long-term cognitive impairment in the modified hole-board test.* Behav Brain Res, 2017. **324**: p. 15-20.
313. Faucher, P., et al., *Hippocampal Injections of Oligomeric Amyloid beta-peptide (1-42) Induce Selective Working Memory Deficits and Long-lasting Alterations of ERK Signaling Pathway.* Front Aging Neurosci, 2015. **7**: p. 245.
314. Cetin, F. and S. Dincer, *The effect of intrahippocampal beta amyloid (1-42) peptide injection on oxidant and antioxidant status in rat brain.* Ann N Y Acad Sci, 2007. **1100**: p. 510-7.
315. Burwinkel, M., et al., *Intravenous injection of beta-amyloid seeds promotes cerebral amyloid angiopathy (CAA).* Acta Neuropathol Commun, 2018. **6**(1): p. 23.
316. Nisbet, R.M., et al., *Tau aggregation and its interplay with amyloid-beta.* Acta Neuropathol, 2015. **129**(2): p. 207-20.
317. Ramsden, M., et al., *Age-dependent neurofibrillary tangle formation, neuron loss, and memory impairment in a mouse model of human tauopathy (P301L).* J Neurosci, 2005. **25**(46): p. 10637-47.
318. Tanemura, K., et al., *Formation of filamentous tau aggregations in transgenic mice expressing V337M human tau.* Neurobiol Dis, 2001. **8**(6): p. 1036-45.
319. Fowler, S.C., *Microbehavioral methods for measuring the motor and associative effects of dopamine receptor antagonists and related drugs in rodents.* Psychopharmacology (Berl), 1999. **147**(1): p. 8-10.
320. Fowler, S.C., et al., *A force-plate actometer for quantitating rodent behaviors: illustrative data on locomotion, rotation, spatial patterning, stereotypies, and tremor.* J Neurosci Methods, 2001. **107**(1-2): p. 107-24.
321. Christmas, A.J. and D.R. Maxwell, *A comparison of the effects of some benzodiazepines and other drugs on aggressive and exploratory behaviour in mice and rats.* Neuropharmacology, 1970. **9**(1): p. 17-29.
322. Prut, L. and C. Belzung, *The open field as a paradigm to measure the effects of drugs on anxiety-like behaviors: a review.* Eur J Pharmacol, 2003. **463**(1-3): p. 3-33.
323. Deacon, R., *Assessing burrowing, nest construction, and hoarding in mice.* J Vis Exp, 2012(59): p. e2607.
324. Deacon, R.M., *Assessing nest building in mice.* Nat Protoc, 2006. **1**(3): p. 1117-9.
325. Erika D Nolte, K.A.N., Shirley ShiDu Yan, *Anxiety and task performance changes in an aging mouse model.* Biochemical and Biophysical Research Communications, 2019.
326. Gaskill, B.N., et al., *Nest building as an indicator of health and welfare in laboratory mice.* J Vis Exp, 2013(82): p. 51012.
327. Baines, C.P., et al., *Loss of cyclophilin D reveals a critical role for mitochondrial permeability transition in cell death.* Nature, 2005. **434**(7033): p. 658-62.
328. Abou-Ismail, U.A. and H.D. Mahboub, *The effects of enriching laboratory cages using various physical structures on multiple measures of welfare in singly-housed rats.* Lab Anim, 2011. **45**(3): p. 145-53.
329. Andre, V., et al., *Laboratory mouse housing conditions can be improved using common environmental enrichment without compromising data.* PLoS Biol, 2018. **16**(4): p. e2005019.
330. Krishnankutty, A., et al., *In vivo regulation of glycogen synthase kinase 3beta activity in neurons and brains.* Sci Rep, 2017. **7**(1): p. 8602.
331. Beurel, E., S.F. Grieco, and R.S. Jope, *Glycogen synthase kinase-3 (GSK3): regulation, actions, and diseases.* Pharmacol Ther, 2015. **148**: p. 114-31.
332. Rockstein, M. and K.F. Brandt, *Enzyme changes in flight muscle correlated with aging and flight ability in the male housefly.* Science, 1963. **139**(3559): p. 1049-51.

333. Petersen, K.F., et al., *Mitochondrial dysfunction in the elderly: possible role in insulin resistance.* Science, 2003. **300**(5622): p. 1140-2.
334. Boveris, A. and A. Navarro, *Brain mitochondrial dysfunction in aging.* IUBMB Life, 2008. **60**(5): p. 308-14.
335. Cortopassi, G.A. and N. Arnheim, *Detection of a specific mitochondrial DNA deletion in tissues of older humans.* Nucleic Acids Res, 1990. **18**(23): p. 6927-33.
336. Piko, L., A.J. Hougham, and K.J. Bulpitt, *Studies of sequence heterogeneity of mitochondrial DNA from rat and mouse tissues: evidence for an increased frequency of deletions/additions with aging.* Mech Ageing Dev, 1988. **43**(3): p. 279-93.
337. Soong, N.W., et al., *Mosaicism for a specific somatic mitochondrial DNA mutation in adult human brain.* Nat Genet, 1992. **2**(4): p. 318-23.
338. Hepple, R.T., *Mitochondrial involvement and impact in aging skeletal muscle.* Front Aging Neurosci, 2014. **6**: p. 211.
339. Goodpaster, B.H., et al., *The loss of skeletal muscle strength, mass, and quality in older adults: the health, aging and body composition study.* J Gerontol A Biol Sci Med Sci, 2006. **61**(10): p. 1059-64.
340. Lanza, I.R., D.E. Befroy, and J.A. Kent-Braun, *Age-related changes in ATP-producing pathways in human skeletal muscle in vivo.* J Appl Physiol (1985), 2005. **99**(5): p. 1736-44.
341. Terman, A., et al., *Mitochondrial turnover and aging of long-lived postmitotic cells: the mitochondrial-lysosomal axis theory of aging.* Antioxid Redox Signal, 2010. **12**(4): p. 503-35.
342. He, Y. and J. Tombran-Tink, *Mitochondrial decay and impairment of antioxidant defenses in aging RPE cells.* Adv Exp Med Biol, 2010. **664**: p. 165-83.
343. Origlia, N., et al., *Receptor for advanced glycation end product-dependent activation of p38 mitogen-activated protein kinase contributes to amyloid-beta-mediated cortical synaptic dysfunction.* J Neurosci, 2008. **28**(13): p. 3521-30.
344. Origlia, N., et al., *MAPK, beta-amyloid and synaptic dysfunction: the role of RAGE.* Expert Rev Neurother, 2009. **9**(11): p. 1635-45.
345. Du, H., et al., *Early deficits in synaptic mitochondria in an Alzheimer's disease mouse model.* Proc Natl Acad Sci U S A, 2010. **107**(43): p. 18670-5.
346. Wang, Y., et al., *Synergistic exacerbation of mitochondrial and synaptic dysfunction and resultant learning and memory deficit in a mouse model of diabetic Alzheimer's disease.* J Alzheimers Dis, 2015. **43**(2): p. 451-63.
347. Griffin, R.J., et al., *Activation of Akt/PKB, increased phosphorylation of Akt substrates and loss and altered distribution of Akt and PTEN are features of Alzheimer's disease pathology.* J Neurochem, 2005. **93**(1): p. 105-17.
348. Franke, T.F., et al., *PI3K/Akt and apoptosis: size matters.* Oncogene, 2003. **22**(56): p. 8983-98.
349. Okabe, S., *Fluorescence imaging of synapse dynamics in normal circuit maturation and in developmental disorders.* Proc Jpn Acad Ser B Phys Biol Sci, 2017. **93**(7): p. 483-497.
350. Parasuraman, S., *Toxicological screening.* J Pharmacol Pharmacother, 2011. **2**(2): p. 74-9.
351. *A novel gene containing a trinucleotide repeat that is expanded and unstable on Huntington's disease chromosomes. The Huntington's Disease Collaborative Research Group.* Cell, 1993. **72**(6): p. 971-83.
352. McNeil, S.M., et al., *Reduced penetrance of the Huntington's disease mutation.* Hum Mol Genet, 1997. **6**(5): p. 775-9.
353. Zhao, T., et al., *Subcellular Clearance and Accumulation of Huntington Disease Protein: A Mini-Review.* Front Mol Neurosci, 2016. **9**: p. 27.
354. Vonsattel, J.P. and M. DiFiglia, *Huntington disease.* J Neuropathol Exp Neurol, 1998. **57**(5): p. 369-84.

355. Folstein, S.E., *Huntington's Disease: a Disorder of Families.* Johns Hopkins University Press, 1989.
356. DiFiglia, M., et al., *Huntingtin is a cytoplasmic protein associated with vesicles in human and rat brain neurons.* Neuron, 1995. **14**(5): p. 1075-81.
357. Trushina, E., et al., *Mutant huntingtin impairs axonal trafficking in mammalian neurons in vivo and in vitro.* Mol Cell Biol, 2004. **24**(18): p. 8195-209.
358. Nucifora, F.C., Jr., et al., *Interference by huntingtin and atrophin-1 with cbp-mediated transcription leading to cellular toxicity.* Science, 2001. **291**(5512): p. 2423-8.
359. Reddy, P.H., *Increased mitochondrial fission and neuronal dysfunction in Huntington's disease: implications for molecular inhibitors of excessive mitochondrial fission.* Drug Discov Today, 2014. **19**(7): p. 951-5.
360. Shirendeb, U.P., et al., *Mutant huntingtin's interaction with mitochondrial protein Drp1 impairs mitochondrial biogenesis and causes defective axonal transport and synaptic degeneration in Huntington's disease.* Hum Mol Genet, 2012. **21**(2): p. 406-20.
361. Shirendeb, U., et al., *Abnormal mitochondrial dynamics, mitochondrial loss and mutant huntingtin oligomers in Huntington's disease: implications for selective neuronal damage.* Hum Mol Genet, 2011. **20**(7): p. 1438-55.
362. Tang, T.S., et al., *Disturbed Ca2+ signaling and apoptosis of medium spiny neurons in Huntington's disease.* Proc Natl Acad Sci U S A, 2005. **102**(7): p. 2602-7.
363. Panov, A.V., et al., *Early mitochondrial calcium defects in Huntington's disease are a direct effect of polyglutamines.* Nat Neurosci, 2002. **5**(8): p. 731-6.
364. Oliveira, J.M., et al., *Mitochondrial dysfunction in Huntington's disease: the bioenergetics of isolated and in situ mitochondria from transgenic mice.* J Neurochem, 2007. **101**(1): p. 241-9.
365. Milakovic, T., R.A. Quintanilla, and G.V. Johnson, *Mutant huntingtin expression induces mitochondrial calcium handling defects in clonal striatal cells: functional consequences.* J Biol Chem, 2006. **281**(46): p. 34785-95.
366. Gizatullina, Z.Z., et al., *Low stability of Huntington muscle mitochondria against Ca2+ in R6/2 mice.* Ann Neurol, 2006. **59**(2): p. 407-11.
367. Gellerich, F.N., et al., *Impaired regulation of brain mitochondria by extramitochondrial Ca2+ in transgenic Huntington disease rats.* J Biol Chem, 2008. **283**(45): p. 30715-24.
368. Perry, G.M., et al., *Mitochondrial calcium uptake capacity as a therapeutic target in the R6/2 mouse model of Huntington's disease.* Hum Mol Genet, 2010. **19**(17): p. 3354-71.
369. Menalled, L., et al., *Systematic behavioral evaluation of Huntington's disease transgenic and knock-in mouse models.* Neurobiol Dis, 2009. **35**(3): p. 319-36.
370. Rowland, L.P. and N.A. Shneider, *Amyotrophic lateral sclerosis.* N Engl J Med, 2001. **344**(22): p. 1688-700.
371. Sathasivam, S., P.G. Ince, and P.J. Shaw, *Apoptosis in amyotrophic lateral sclerosis: a review of the evidence.* Neuropathol Appl Neurobiol, 2001. **27**(4): p. 257-74.
372. Schymick, J.C., K. Talbot, and B.J. Traynor, *Genetics of sporadic amyotrophic lateral sclerosis.* Hum Mol Genet, 2007. **16 Spec No. 2**: p. R233-42.
373. Sasaki, S. and M. Iwata, *Ultrastructural change of synapses of Betz cells in patients with amyotrophic lateral sclerosis.* Neurosci Lett, 1999. **268**(1): p. 29-32.
374. Siklos, L., et al., *Ultrastructural evidence for altered calcium in motor nerve terminals in amyotropic lateral sclerosis.* Ann Neurol, 1996. **39**(2): p. 203-16.
375. Soraru, G., et al., *Activities of mitochondrial complexes correlate with nNOS amount in muscle from ALS patients.* Neuropathol Appl Neurobiol, 2007. **33**(2): p. 204-11.
376. Xiao, Y., et al., *ROS-related mitochondrial dysfunction in skeletal muscle of an ALS mouse model during the disease progression.* Pharmacol Res, 2018. **138**: p. 25-36.

377. Corti, S., et al., *Amyotrophic lateral sclerosis linked to a novel SOD1 mutation with muscle mitochondrial dysfunction.* J Neurol Sci, 2009. **276**(1-2): p. 170-4.
378. Martin, L.J., *p53 is abnormally elevated and active in the CNS of patients with amyotrophic lateral sclerosis.* Neurobiol Dis, 2000. **7**(6 Pt B): p. 613-22.
379. Kirkinezos, I.G., et al., *An ALS mouse model with a permeable blood-brain barrier benefits from systemic cyclosporine A treatment.* J Neurochem, 2004. **88**(4): p. 821-6.
380. Keep, M., et al., *Intrathecal cyclosporin prolongs survival of late-stage ALS mice.* Brain Res, 2001. **894**(2): p. 327-31.
381. Martin, L.J., et al., *The mitochondrial permeability transition pore in motor neurons: involvement in the pathobiology of ALS mice.* Exp Neurol, 2009. **218**(2): p. 333-46.
382. Parone, P.A., et al., *Enhancing mitochondrial calcium buffering capacity reduces aggregation of misfolded SOD1 and motor neuron cell death without extending survival in mouse models of inherited amyotrophic lateral sclerosis.* J Neurosci, 2013. **33**(11): p. 4657-71.
383. Wirdefeldt, K., et al., *Epidemiology and etiology of Parkinson's disease: a review of the evidence.* Eur J Epidemiol, 2011. **26 Suppl 1**: p. S1-58.
384. Braak, H., et al., *Stages in the development of Parkinson's disease-related pathology.* Cell Tissue Res, 2004. **318**(1): p. 121-34.
385. Hindle, J.V., *Ageing, neurodegeneration and Parkinson's disease.* Age Ageing, 2010. **39**(2): p. 156-61.
386. Yasuda, T., Y. Nakata, and H. Mochizuki, *alpha-Synuclein and neuronal cell death.* Mol Neurobiol, 2013. **47**(2): p. 466-83.
387. Pham, C.L. and R. Cappai, *The interplay between lipids and dopamine on alpha-synuclein oligomerization and membrane binding.* Biosci Rep, 2013. **33**(5).
388. Bir, A., et al., *alpha-Synuclein-induced mitochondrial dysfunction in isolated preparation and intact cells: implications in the pathogenesis of Parkinson's disease.* J Neurochem, 2014. **131**(6): p. 868-77.
389. Martin, L.J., et al., *Mitochondrial permeability transition pore regulates Parkinson's disease development in mutant alpha-synuclein transgenic mice.* Neurobiol Aging, 2014. **35**(5): p. 1132-52.
390. Ideguchi, K., et al., *Cyclophilin D-dependent mitochondrial permeability transition is not involved in neurodegeneration in mnd2 mutant mice.* Biochem Biophys Res Commun, 2010. **393**(2): p. 264-7.